UNIWERSYTET ŚLĄSKI
INSTYTUT FIZYKI
IM. AUGUSTA CHEŁKOWSKIEGO

Institute of Physics

Faculty of Science and Technology

Doctoral Thesis

Impact of the High Electric Field on the Crystallization Behavior of a Molecular Liquid, Vinyl Ethylene Carbonate

Daniel Duarte

Supervisor:

dr hab. Karolina Adrjanowicz

Chorzów, 2021

ABSTRACT

Control of the crystallization process has great importance in material engineering and pharmaceutical industry. Using electric fields for this purpose shows strong potential. However, the effect of electric field on crystallization is rather poorly recognized. In this Ph.D. Thesis, using dielectric spectroscopy, the effect of the alternating (ac) and direct current (dc) high-electric field on the crystallization of a molecular system with field-induced polymorphism, vinyl ethylene carbonate (VEC) is explored.

Among research that was performed, the importance of the sinewave properties of the applied alternating signal on crystallization kinetics was investigated. As it turned out, it is possible to control the crystallization rate or the morphology of the growing crystal by changing the amplitude or frequency of the applied electric field. The crystallization rate increases when the amplitude of the electric field increases or its frequency decreases. Moreover, by changing the properties of the applied time-dependent electric field, we can control the polymorph outcome. To be more specific, a high electric field can suppress the ordinary polymorphic form and induce the appearance of a new one.

Additionally, this study was extended to a broad temperature range to examine how the presence of a high electric field influences the temperature dependence of the crystallization rate. It was observed that the position of the maximum of the overall crystallization rate is not affected by the external electric field. However, the rate of crystallization increases when the field magnitude is increased or either the frequency of the ac field is decreased. Applying high amplitude time-dependent electric fields from a specific low-frequency region is responsible for generating an additional low-temperature maximum in the overall crystallization rate-temperature dependence. Interestingly, it is not observed in the absence of a high electric field.

As a final point, the stability of the field-induced VEC polymorph was investigated. It happens that if the field-induced polymorph is created along with the regular polymorph, it is unstable and will transform with time into a stable form. At this stage, applying a high-electric field does not affect the time transformation. On the other hand, if only the high-field polymorph is generated, the polymorphic transformation does not take place. The high-field polymorph does not convert with time into the regular form.

The research work that constitutes the basis of this doctoral thesis has been published in the following series of publications:

1. Daniel M. Duarte, Ranko Richert, and Karolina Adrjanowicz, *Frequency of the AC Electric Field Determines How a Molecular Liquid Crystallizes*, J. Phys. Chem. Lett. 2020, 11, 10, 3975–3979

2. Daniel M. Duarte, Ranko Richert, and Karolina Adrjanowicz, *Watching the Polymorphic Transition from a Field-Induced to a Stable Crystal by Dielectric Techniques*, Cryst. Growth Des. 2020,20, 5406-5412

3. Daniel M. Duarte, Ranko Richert, and Karolina Adrjanowicz, *AC versus DC field effects on the crystallization behavior of a molecular liquid, vinyl ethylene carbonate (VEC)*, Phys. Chem. Chem. Phys., 2021, 23, 498

4. Daniel M. Duarte, Ranko Richert, and Karolina Adrjanowicz, *Bimodal Crystallization Rate Curves of a Molecular Liquid with Field-Induced Polymorphism*, J. Molecular Liquids, 2021, 342, 117419

STRESZCZENIE

Kontrola procesu krystalizacji ma ogromne znaczenie w inżynierii materiałowej i przemyśle farmaceutycznym. Wykorzystanie do tego celu silnego pola elektrycznego może mieć ogromny potencjał aplikacyjny. Jednakże, wiele fundamentalnych aspektów związanych z wpływem zewnętrznego pola elektrycznego na krystalizację materiałów molekularnych jest bardzo słabo poznane. W niniejszej pracy doktorskiej, zbadano, za pomocą spektroskopii dielektrycznej, wpływ stałego i zmiennego pola elektrycznego o dużym natężeniu na krystalizację ze stanu cieczy przechłodzonej 4-winylo-1,3-dioxolan2-on-u (VEC). VEC jest silnie polarną pochodną węglanu propylenu zawierającą w swojej strukturze podstawnik winylowy.

W pracy zbadano wpływ właściwości przyłożonego pola elektrycznego na kinetykę krystalizacji. Okazuje się, że możliwe jest kontrolowanie szybkości krystalizacji lub morfologii wzrastających kryształów poprzez zmianę amplitudy lub częstotliwości przyłożonego pola elektrycznego. Szybkość krystalizacji wzrasta wraz ze wzrostem amplitudy pola lub spadkiem częstotliwości. Ponadto, poprzez zmianę charakterystyki przyłożonego pola elektrycznego a także protokołów pomiarowych można selektywnie uzyskiwać konkretne odmiany polimorficzne badanej substancji. W przypadku VEC krystalizacja w obecności silnego pola elektrycznego prowadzi do wygenerowania zupełnie nowej odmiany polimorficznej. Jak do tej pory, formy tej nie udało się nam uzyskać w żaden inny sposób, jak tylko w przypadku obecności zewnętrznego pola elektrycznego.

Badania poświęcone kinetyce krystalizacji zostały przeprowadzone w szerokim zakresie temperatur, tak aby zrozumieć jaki jest wpływ zewnętrznego pola elektrycznego na temperaturowe zależności szybkości krystalizacji. Zaobserwowano, że w obecności silnego pola elektrycznego położenie maksimum krystalizacji nie ulega zmianie. Jednak wraz ze wzrostem amplitudy czy też zmniejszeniem częstotliwości przyłożonego pola elektrycznego wzrasta ogólna szybkość procesu krystalizacji.

Co ciekawe, w obecności zmiennego pola elektrycznego z zakresu niskich częstotliwości pojawia się dodatkowe maksimum zlokalizowane w obszarze niższych temperatur. Jest ono związane z obecnością odmiany polimorficznej indukowanej polem o niższej temperaturze topnienia niż ta uzyskiwana zazwyczaj w trakcie ochładzania cieczy. Efektu tego nie obserwuje się gdy krystalizacja prowadzana jest bez udziału

zewnętrznego pola elektrycznego. W tym przypadku obserwuje się bowiem wyłącznie wzrost stabilnej formy I.

Ostatni aspekt rozprawy dotyczył stabilności nowej odmiany polimorficznej indukowanej w trakcie procesu krystalizacji w warunkach silnego pola elektrycznego. Wyniki uzyskanych badań wskazują, że w obecności krystalitów formy I indukowana polem odmiana polimorficzna VEC z czasem ulega transformacji do znacznie bardziej stabilnej formy I. Natomiast, jeśli protokół pomiarowy zostanie tak skonstruowany aby zapobiec równoczesnemu wzrostowi obu form, indukowana polem odmiana polimorficzna VEC nie ulega konwersji do formy I.

Wyniki badań stanowiące podstawę niniejszej rozprawy doktorskiej zostały opublikowane w postaci czterech spójnych tematycznie artykułów naukowych:

1. Daniel M. Duarte, Ranko Richert, and Karolina Adrjanowicz, *Frequency of the AC Electric Field Determines How a Molecular Liquid Crystallizes*, J. Phys. Chem. Lett. 2020, 11, 10, 3975–3979

2. Daniel M. Duarte, Ranko Richert, and Karolina Adrjanowicz, *Watching the Polymorphic Transition from a Field-Induced to a Stable Crystal by Dielectric Techniques*, Cryst. Growth Des. 2020,20, 5406-5412

3. Daniel M. Duarte, Ranko Richert, and Karolina Adrjanowicz, *AC versus DC field effects on the crystallization behavior of a molecular liquid, vinyl ethylene carbonate (VEC),* Phys. Chem Chem. Phys., 2021, 23, 498

4. Daniel M. Duarte, Ranko Richert, and Karolina Adrjanowicz, *Bimodal Crystallization Rate Curves of a Molecular Liquid with Field-Induced Polymorphism*, J. Molecular Liquids, 2021, 342, 117419

CONTENTS

MOTIVATION

Crystallization has a great significance in pharmaceutical applications, material chemistry, petrochemistry, food industry, and biotechnology, among others.[1–3] The ability to control crystallization or predict crystallization habits is crucial in numerous technology sectors. This is because crystallization behavior determines the most critical physical, chemical, or even biological properties of the final product. The outcome properties of the crystalline material will depend on the extent of crystallinity, polymorphism, the size and quality of obtained crystals.[4,5]

One way to promote crystallization and control the properties of acquired crystalline material is by using an external electric field. This method emerges as a topic that deserves considerable recognition due to its potential in numerous practical environments, such as inducing the crystallization and controlling the polymorphic outcome, and improving the quality of protein crystals. However, predicting how the electric field affects crystallization remains unclear.[6]

Recently, Adrjanowicz *et al.*[7] reported for the first time that under high static electric fields, one can induce crystallization of simple molecular liquid. The sample used was vinyl ethylene carbonate (VEC), a glass-forming liquid with a relatively large value of permanent dipole moment and a lack of directional bonding. Field-induced crystallization of VEC is an astonishing finding because for most molecular materials subjected to high electric fields, the potential energy for aligning a dipole in a field direction is always much smaller compared to the thermal energy, i.e., $\mu E \ll k_B T$. As a result, electric fields should have, in principle, a very little impact on the molecular orientation and thermodynamic potentials of the polar molecular glass-formers. Nevertheless, experimental evidence has demonstrated that electric fields in the range of 40-200 kV/cm promote crystallization of VEC. In addition to that, a new crystal polymorph is generated in the presence of an external electric field. Interestingly, it is not observed if crystallization occurs in a non-field environment.

This pioneering finding opens new routes to generate materials with interesting crystal structures and properties that can be potentially used in organic memory devices, molecular switches, sensors, and so on. However, before that, some fundamental aspects related to the field-induced crystallization of molecular materials need to be explored

more. For example, it is unknown if and how the alternating electric field can influence the crystallization process. Can we expect that the effects seen in the presence of ac fields are the same as for the static dc fields? What will be the effect of the frequency and the field magnitude of the time-dependent electric field on crystallization? How does the external electric field modify the position of the crystallization rate maximum concerning the non-field case? It is also essential to understand if the external electric field primarily affects the nucleation step or either the crystal growth? And finally, how stable is the field-induced polymorph (for example, will it disappear with time once the electric field is switched off)? The stability of the polymorph is crucial in the pharmaceutical industry since the material can transform into a more stable phase[8] which can affect the solubility and bioavailability of the drug substance.[9,10]

The motivation for this work was to face some of these open questions and provide a more in-depth characterization of how the high-electric field can influence the crystallization of simple molecular materials. The research work included in this doctoral thesis provides a comprehensive guide that can stimulate future experiments on how the high-electric field can be applied to control the crystallization of molecular materials.

This thesis is based on experimental work. It is focused on providing a better understanding of how the electric field can influence the crystallization outcome for a neat, simple liquid such as VEC. Since the melting temperatures of VEC polymorphs are much lower than the room temperature, *ex-situ* studies of the obtained crystals are not possible in this case. Nevertheless, the knowledge gained from this study serves as a solid ground for future work with a target to use high ac or dc electric fields to control the crystallization behavior of various molecular systems. As a next step, it is highly desirable to look for other polar materials, preferably with melting temperatures located above room temperature, for which the crystallization tendency can be affected by applying an external electric field.

THE AIM OF THE THESIS

The general objective of this doctoral thesis was to understand how external alternating current (ac) or direct current (dc) electric fields influence the crystallization of a supercooled molecular liquid, vinyl ethylene carbonate (VEC).

The following target points were set in:

i.   Characterize the influence of high electric ac field, including the field frequency and amplitude, on the crystallization of VEC;

ii. Compare how dc and ac electric fields affect the crystallization kinetics of VEC at different temperatures;

iii. Explore the influence of high electric field on the temperature evolution of the crystallization rate, particularly the location and maxima value of crystallization rate curve, as well as on the melting behavior;

iv. Verify the stability of the field-induced polymorph.

LIST OF PUBLICATIONS CONSTITUTING THE THESIS

This doctoral dissertation is based on research work published in the following peer-reviewed journals:

[A1] Duarte, D.M.; Richert, R.; Adrjanowicz, K. Frequency of the AC Electric Field Determines How a Molecular Liquid Crystallizes, *J. Phys. Chem. Lett.* 2020, 11, 10, 3975–3979

Impact Factor (year publication): 6.710

Number of points from MNiSW list (2021): 200

[A2] Duarte, D.M.; Richert, R.; Adrjanowicz, K. Watching the Polymorphic Transition from a Field-Induced to a Stable Crystal by Dielectric Techniques, *Cryst. Growth Des.* 2020,20, 5406-5412

Impact Factor (year publication): 4.089

Number of points from MNiSW list (2021): 100

[A3] Duarte, D.M.; Richert, R.; Adrjanowicz, K. AC versus DC field effects on the crystallization behavior of a molecular liquid, vinyl ethylene carbonate (VEC), *Phys. Chem Chem. Phys.*, 2021, 23, 498

Impact Factor (year publication): 3.430

Number of points from MNiSW list (2021): 100

[A4] Duarte, D.M.; Richert, R.; Adrjanowicz, K. Bimadal Crystallization Rate Curves of a Molecular Liquid with Field-Induced Polymorphism, *J. Molecular Liquid,* 2021, 342, 117419

Impact Factor (year publication): 6.165

Number of points from MNiSW list (2021): 100

The publications mentioned above, along with the statements of the co-authors, are available in Appendix.

OTHER SCIENTIFIC ACTIVITY DURING DOCTORAL STUDIES

Besides publications which consist the basis of this doctoral dissertation, I have also actively participated in some other research whose results were published in the scientific journals listed below:

B1. Adrjanowicz, K.; Winkler, R.; Chat, K.; Duarte, D.M.; Tu, W.; Unni, A.B.; Paluch, M.; Ngai, K.L., Study of Increasing Pressure and Nanopores Confinement Effect on the Segmental, Chain, and Secondary Dynamics of Poly(methylphenylsiloxane), *Macromolecules*, 2019, 52,10, 3763-3774
Impact Factor (year publication): 5.918
Number of points from MNiSW list (2021): 100

B2. Duarte, D.M.; Tu, W.; Dzienia, A.; Adrjanowicz, K., Study on the effect of side-chain group on the segmental dynamics of selected methacrylate polymers at ambient and high pressure, *Polymer*, 2019, 183, 121860
Impact Factor (year publication): 4.213
Number of points from MNiSW list (2021): 100

B3. Unni, A.B., Chat, K.; Duarte, D.M.; Wojtyniak, M.; Geppert-Rybczynska, M.; Kubacki, J.; Wrzalik, R.; Richert, R.; Adrjanowicz, K., Experimental evidence on the effect of substrate roughness on segmental dynamics of confined polymer films, *Polymer*, 2020, 199, 122501
Impact Factor (year publication): 4.430
Number of points from MNiSW list (2021): 100

The results of my research were presented during online conferences:

"Control Crystallization of Molecular Liquid Using AC Electric Field" – YOUNG MULTIS – Multiscale Phenomena in Condensed Matter - Conference for Young Researchers, Krakow, Poland, 5-7 July 2021 – oral presentation (Via Zoom) awarded with Best Oral Presentation;

"How AC Electric Field Frequency Influences the Crystallization of a Molecular Liquid" – Online IDS 2021 Workshop – 6-9 September 2021 – Poster (Via Zoom).

1. INTRODUCTION

Glass has been used by humankind since prehistoric times, when our ancestors used obsidian, a volcanic glass, to forge knives and arrows tips. In Egypt, around 1500 BC, it appears the first glass vessel.[11]

Recently, due to material engineering, new types of glasses, such as metallics, polymers, simple liquids, etc., made it a versatile and vital material. Besides all the advances in manufacturing glass, the nature of the glass transition is still an unsolved problem in solid-state theory. The glassy system shows some unique and distinguishes relaxation processes that reflect different aspects of molecular mobility. The structural, or α-relaxation, is associated with the cooperative motion of the molecules. The molecular movements slow down when the liquid is cooled. Eventually, a viscous liquid kinetically freezes, forming a glass. In the glassy state, the secondary processes can be observed clearly. They are labeled as β-, γ-, δ-relaxations, and so on. Secondary dynamics occur on a shorter time scale, and it is associated with more local dynamics of either inter or intramolecular origin.

1.1. Glass Transition

A liquid, when cooled from the high temperature, may crystallize at crystallization temperature, T_c. However, if the cooling rate is fast enough, the material can avoid crystallization and reach a glassy state. A liquid that does not crystallize below melting temperature, T_m, is termed a supercooled liquid. The supercooled liquid is in metastable equilibrium, and its physical properties change as decreasing the temperature. This includes, for example, a decrease in free energy and entropy.[12] Figure 1 demonstrates the typical evolution of the volume and enthalpy of a supercooled liquid in the function of temperature. The volume and enthalpy in the crystal state are smaller compared with the glassy state. This higher value in enthalpy and volume is due to the lack of long-range arrangement of the molecules. The glass transition temperature, T_g, is estimated by intercepting the extrapolated lines of the glass volume with that of the supercooled liquid. Below T_g, the enthalpy and volume decrease, but such changes are significantly lower than in the liquid state. T_g depends on the cooling rate.[13] For a faster cooling rate, T_g will be slightly higher than for slower rates.
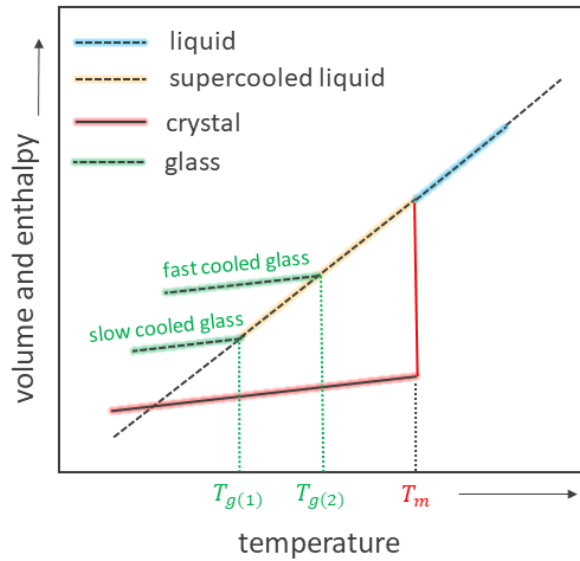
Figure 1. Temperature dependence of the volume or either enthalpy for a typical glass-forming liquid. T_m represents the melting temperature, while T_g is the glass transition temperature. T_g is defined as the temperature at which the lines corresponding to the liquid and glassy states intersect. Based on [12].

As the supercooled liquid is cooled to lower temperatures, it becomes more viscous. Simultaneously, the time scale of the molecular motion drastically increases. The equilibration of the system requires more and more time. As the supercooled liquid approaches T_g, the cooperative movements become more significant. This results in an increase in the structural relaxation time from picoseconds, close to T_m, to a scale of hundred seconds. At some temperature, T_g, the molecules will move so slow that the rate to rearrange exceeds the experimental timescale. In dielectric relaxation measurements, T_g is defined as the temperature where the α-relaxation time reaches 100 s. The system falls out of its thermodynamics equilibrium, turning into a glass.[13] The dynamics associated with glass transition can be studied using different experimental techniques, such as broadband dielectric spectroscopy (BDS), light scattering, mechanical spectroscopy, among others.

The glass prepared by cooling a liquid is an amorphous solid. This means a lack of long-range order, not having translational periodicity, and no defined atomic structure. By contrast, a crystalline state, obtained through a crystallization process, is defined as having atoms or molecules arranged in a pattern that repeats periodically in three dimensions. The glass transition and crystallization are mutually connected; only by avoiding one - you can get the other one. The glass can only be obtained if the

crystallization is avoided, while the crystallization is acquired if the glassy state is not reached.

1.2. Crystallization

The crystallization process involves two consecutive steps: the congregation of several molecules, forming an embryonic nucleus, named nucleation, followed by the growth of these clusters, referred to as crystal growth. If the nucleation occurs spontaneously, it is classified as homogeneous. Heterogeneous nucleation is when it is induced by foreign particles. The process of nucleation only begins when the activation energy ΔG (Gibbs energy) is overcome. The activation energy barrier for the nucleation process depends on the energy necessary to start a new interface and the Gibbs energy difference between the amorphous and crystalline phases.

The overall crystallization is the result of nucleation and crystal growth processes. Close to T_g, the crystallization is favored by the thermodynamics factors, while close to T_m, the mobility increases and facilitates it. Figure 2 illustrates the nucleation and crystal growth rates changes with temperature. Generally, the overall crystallization behavior depends on the balance between thermodynamics and kinetic factor, reaching a maximum value somewhere in between the glass-transition temperatures and the melting point.
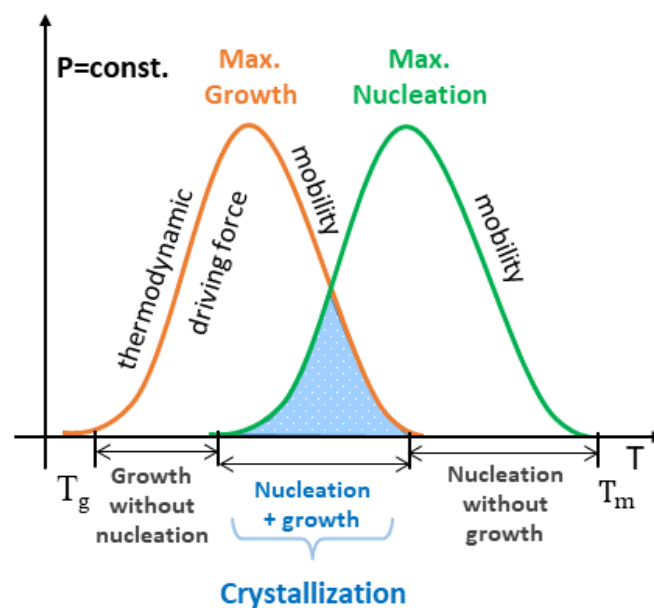

Figure 2. Temperature dependence of the nucleation rate and crystal growth rate. Based on [14].

The crystallization can be affected by various physical factors, such as pressure, temperature, geometrical confinement, purity of the sample, among others. An important factor that can potentially affect crystallization is the electric field. However, it is challenging to provide an appropriate description of how the electric field can influence crystallization. Applying an external electric field, E, will undoubtedly affect the Gibbs free energy and the difference in chemical potentials between melt and crystal phases, $\Delta\mu$. These changes will affect both nucleation rate, J, and crystal growth rate, u: [15]

$$J \propto D \exp\left(\frac{-\Delta G_c(E)}{k_B T}\right) \tag{1}$$

$$u \propto D \left[1 - \exp\left(\frac{-\Delta\mu(E)}{k_B T}\right)\right] \tag{2}$$

where D is the diffusion constant. Additionally, the crystallization from the supercooled liquid state is strongly affected by the kinetic factor.[16] The molecular mobility in liquids includes motions, like bending, rotation, or translation of molecules. Generally, the crystallization speeds up if the molecular motions are enhanced. Applying an electric field will create a field-induced orientation of the molecular material. Besides some supposition that the crystallization of supercooled liquids will be definitely affected by the electric field, there is no information about the extent or magnitude of such effect.

The study on the effect of the electric field on crystallization started in 1999, primarily for protein systems characterized by large values of the dipole moments. Taleb *et al.*[17] investigated the crystallization of proteins in solutions under a direct current (DC) electric field of 2 kV/cm magnitude. They have detected that the field affects both the size and quality of the produced crystals. The final crystallization product had fewer crystals with larger sizes compared with the crystallization carried out in the absence of field. In the succeeding work, Taleb *et al.*[18] showed that an electric field influences the protein concentration resulting in a concentration gradient between the electrodes. Following Taleb's experiment, Nanev and co-workers[18,19] confirmed these results. They found that at a relatively low temperature, the presence of an electric field has more impact on the induction time and nucleation time. This encouraged a scientific community to study how to control nucleation using dc fields.[1,17,18,20] However, the use of an alternating current field was only accomplished in 2009 by Koizumi *et al.*[21] They found that it is possible to control the nucleation rate successfully by changing the

9

frequency of the applied ac electric field. However, it is important to mention that these studies were done only in protein solutions under a uniform external electric field of not more than 10 kV/cm. Proteins are very complex large systems, in contrast to simple molecular liquids.

In 2018, Adrjanowicz *et al.*[7] reported, for the first time, that the high static (dc) electric field can also affect the crystallization of a very simple molecular glass-former. Field-induced crystallization of VEC is an astonishing finding because for most molecular materials subjected to high electric fields, the potential energy for aligning a dipole in a field direction is always much smaller compared to the thermal energy, i.e., $\mu E = k_B T$. The pioneering finding was the inspiration and foundation for the research work being the scope of this thesis.

Applying electric fields upon crystallization might have different practical applications, for example, in the food industry or material engineering. Jha *et al.*[3] reported that dc electric fields could enhance mass and heat transfer during the crystallization process. So, having a freezing process under a strong dc field can promote nucleation, decreases the nucleation and induction time. The advantage of this process is reducing the disruption of the cell and protein denaturing and improving the preservation qualities of fresh food. Another example is piezoelectric polymers, which can exhibit various crystalline properties when synthesized under an electric field.[22] The external electric field will affect the orientation of the polymer chain, forcing the monomer to orientate accordingly, resulting in a crystalline phase instead of an amorphous one. Another important application of electric field during crystallization is controlling the polymorphism of the final product.[1,2,7,20]

Changing the physical parameters, such as the temperature, pressure, applying an electric field, etc., can also induce polymorphic transformation.[4,5,7,23] Polymorphs are distinct crystal structures that can be formed by the same chemical compound.[24,25] Each polymorph has different thermodynamics properties, such as Gibbs energy, enthalpy, and entropy. At a given temperature and pressure, the polymorph with the lowest free energy is considered stable, while all others will be regarded as metastable. The representative potential energy in the function of the mean intermolecular distance is shown in Figure 3. The polymorph with the lowest free energy is the most stable. This form is called the thermodynamic form (polymorph C), and it differs from the kinetic form which is

characterized by a local minimum of energy (polymorph B). From a thermodynamical point of view, this metastable polymorph is unstable. It has a finite lifetime, which depends on its transformation rate into a more stable form and the activation energy required. The polymorphic transition can be explained by Ostwald's rules of stages, which describe a step-wise transformation of an unstable system into a more stable one with the closest energy level from the original one before finally reaching the thermodynamically stable state.[26,27]
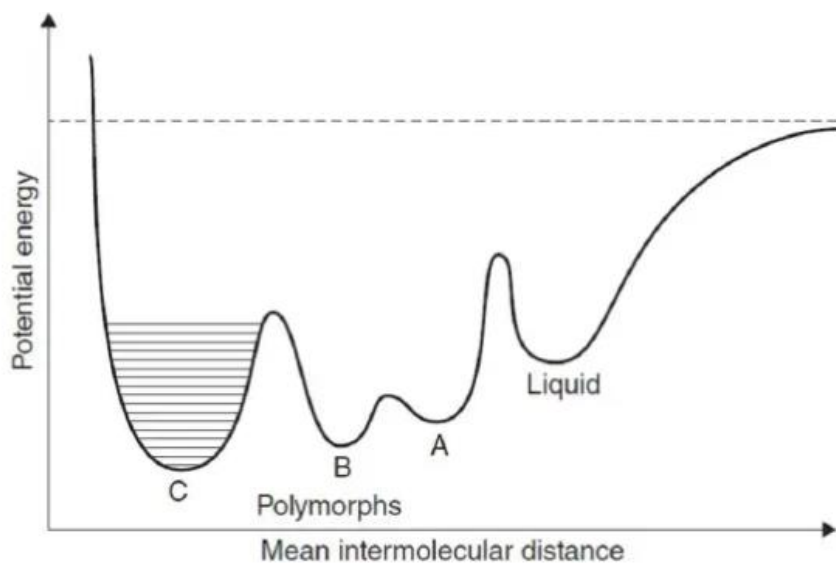

Figure 3. Comparison of the potential energy of various solid forms. Based on [28].

1.3. Dielectric Spectroscopy

The dynamics of glass-forming materials and crystallization kinetics can be studied using different experimental techniques, for example, neutron scattering, infrared spectroscopy, differential scanning calorimetry, among others. However, one of the most versatile and powerful is broadband dielectric spectroscopy (BDS). This technique is based on the interaction of an applied electric field with the sample, which needs to have a dipole moment. It analyzes the cooperative reorientation movements of molecules in the supercooled liquid phase in a range of frequencies between 10^{-3} Hz to 10^{12} Hz, as well as a wide range of temperature 433 K to 673 K.[29–31]

In the absence of an applied electric field, polar molecules are randomly oriented. When an electric field is applied, the dipolar molecules will begin to align themselves in

accordance with the field direction. This process is known as the dielectric polarization, P, which can be related to the electric field, E, through $P = \chi\varepsilon_0 E$, where χ is the susceptibility of the material, and ε_0 is the permittivity of vacuum. Figure 4 demonstrates an orientational polarization in a dielectric material when an external electric field is applied.
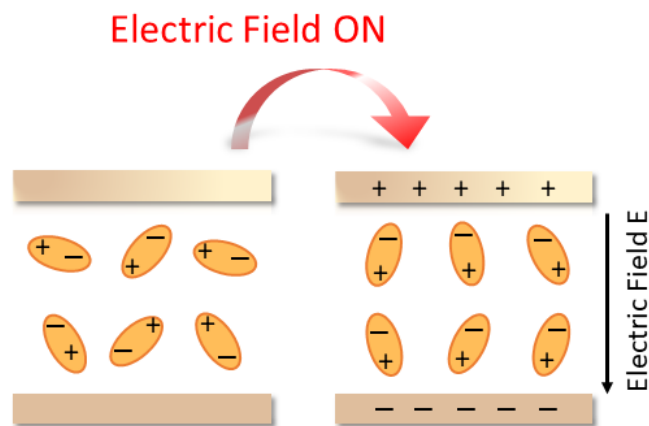
Figure 4. Diagram showing polarization of the dielectric material in the presence of the external electric field.

In the presence of the alternating electric field, with sinusoidally varying magnitude and direction, the dipoles try to arrange one way and the other. The total polarization of the material will depend on the ability of dipoles to orient themselves along the field lines. The different types of polarization, such as electronic polarization, atomic polarization, orientational polarization, etc., will depend on the frequency of the applied alternating electric field. At very high frequencies, only the electronic polarization is able to follow the rapid change in the alternate field. In contrast, at low frequencies (static case), the dominant contribution comes from dipole orientation. In this range, atomic and electronic mechanisms are less important. In addition to that, the interfacial polarization and electrode polarization effects can occur at low frequencies. There are related to the separation of charges (including free mobile charges) and their accumulation at the interface between two materials or close to the electrodes. When the external electric field is removed, the polarization function decays exponentially. In this way, the relaxation time can be understood as the average time needed by the dipoles to return to their original states.

To get a dielectric response of the studied sample over a wide range of frequencies/characteristic relaxation times, it is subjected to an alternating electrical field. The external electric field causes the orientation of the localized dipoles or ionic conduction (if any charged species are present in the sample). In most cases, it all happens within a linear response regime, i.e., when root-mean-square (rms) amplitudes are $E_{rms} <$ 1 kV/cm. When on top of the low measuring ac field, one adds electric fields with RMS amplitudes much higher than 1 kV/cm, the structure and dynamics might drastically change as the material enters the point at which the non-linear responses are seen.
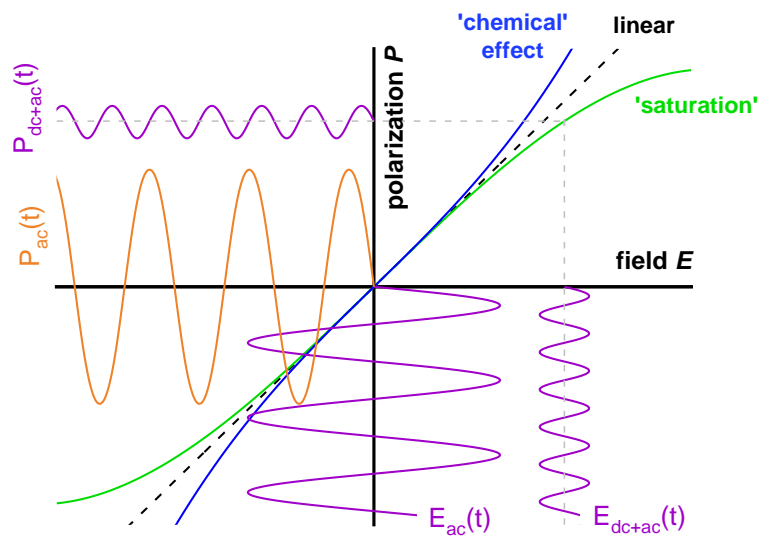
Figure 5. Schematic representation of linear (dashed) and non-linear P(E) behavior. Based on [32].

In the case of a typical dielectric experiment, that is, within the low field limit, polarization P changes linearly with the external electric field E. When the external electric field is sufficiently high, the relationship between P and E deviates from the linear behavior, $P = \varepsilon_0 \chi E + \varepsilon_0 \chi^{(2)} E^2 + \varepsilon_0 \chi^{(3)} E^3 + \cdots$, where $\chi^{(n)}$ represents higher-order susceptibilities. Deviations from linearity also give rise to higher-order Fourier components in the polarization response to a harmonic ac field. When the permittivity of the material is reduced in the presence of a high electric field, the process is known as saturation.[33] This is considered the most fundamental non-linear dielectric effect (NDE). A non-linear dielectric effect can be defined as the deflection of χ from its low field value, which overpasses the resolution of a certain experiment.[34] Another known NDE is the

chemical effects. In this case, an increase of the dielectric constant with the electric field is observed, in contrast with what is observed in dielectric saturation. The increase of permittivity can be due to a rise in density that will increase the number of dipoles being pulled into the capacitor volume or the shifting of protons in hydrogen bonding liquids, among others. This effect has not been resolved for many liquids, and the small increase of the dielectric amplitude can be covered by saturation effects. Another NDE is energy absorption, where the main principle is that any material under an ac electric field will absorb energy and eventually convert it into heat. This rise in heat will fill the phonon modes resulting in an accelerated dynamic, which leads to a distortion in the final spectra. Lastly, applying an electric field at constant temperature can change the thermodynamic entropy of the simple molecular liquid leading to a spectral shift of the loss peak towards lower frequencies (slowing down of the molecular mobility).

It is worth emphasizing that all four non-linear dielectric effects mentioned above are, in principle, reversible, meaning that when an electric field is switched off, the system recovers its stationary state. In addition to that, they all contribute to deviation from the linear response behavior in molecular materials subjected to high electric fields. Since various non-linear effects might occur simultaneously, in some of the cases, it might be very difficult to resolve the impact of the particular non-linear effect just by looking at the dielectric data.

In theory, entering into a high-field regime should be possible for a large variety of glass-forming systems having a non-zero molecular dipole moment. It is only a matter of field intensity which should be high enough to produce a pronounced non-linear response. However, in reality, we are limited to electric fields as high as several hundreds of kV/cm. Therefore, simple-structure highly polar molecular liquids with large values of the permanent dipole moments are preferred more among the others. While we know a lot about the effect of high electric fields on the dynamics of glass-forming systems, the effect of electric fields on crystallization is practically unknown.

The typical value to be considered as the high-electric field is much beyond 1 kV/cm. The high field, based on $E = V/d$, can be achieved either by applying high voltages, V, across the electrodes or reducing the sample thickness, d. As illustrated in Figure 5, there are two experimental approaches to achieve high-electric fields: imposing high ac field amplitudes or either a large dc bias. A small ac measuring field (voltages $\leq 1\ V_{rms}$) should

be superposed on a large electric field if one wishes to follow the ongoing changes in the dielectric response of the sample exposed to a high electric field. The ac voltage is expressed as V_{RMS}, which signifies the root mean square voltage value, and it is calculated using $V_{RMS}=V_P/\sqrt{2}$, where V_P is the amplitude of the voltage applied.

To achieve high electric fields in the dielectric experiment, a high-voltage amplifier is needed, which will boost the output voltage of the BDS analyzer. In the case of ac voltage, amplifiers with high slew rates are required. However, such amplifiers are usually the factor that restricts the highest usable frequency. In the case of the configuration that has been employed in this study, the dielectric response of the sample and the ac field applied were limited to kHz frequencies. To ensure a uniform electric field, a special high-electric field capacitor cell was utilized. The schematic draw of the high field capacitor cell – made of brass - is demonstrated in Figure 6. It consists of two spring-loaded polished stainless-steel disks (17 mm and 20 mm in diameter) separated by a Teflon (or either Kapton) spacer of 25 μm thickness, but the actual thickness of the sample is typically slightly different. The inner area of 14 mm diameter is left for the sample material. The top electrode is centered using the hole in the sapphire disk, which is tightened against a plastic o-ring using a steel frame. The surface of the electrode disks needs to be flat and highly polished to maintain a homogeneous field across the sample. The spring is used to assure temperature-invariant stress on the ring during the experiment. So in this way, a fixed distance between the electrodes is maintained all the time.
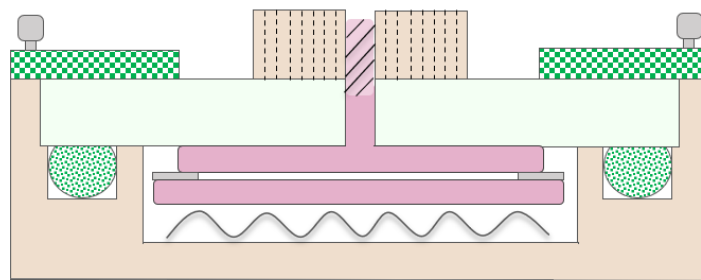

Figure 6. The schematic draw of the dielectric cell used for the high-electric field.

Attempting to reach a high electric field can bring a lot of difficulties. When the electrode separations are reduced, it helps increase the electric field. However, decreasing

15

the volume of the sample facilitates the creation of airborne particles, which can lead to failure via dielectric breakdown unless the samples are prepared in a cleanroom environment. Another aspect to consider is the dielectric strength of the spacer material used. To avoid the breakdown from the spacer, the applied fields should be lower than the dielectric strength material. Moreover, this property is affected by the thickness of the spacer and can degrade with increasing temperature. Besides the dielectric breakdown, it is possible to observe electrostriction during high field measurements. This problem is due to the attractive force generated by the application of a voltage that will compress the electrode distance d and can result in an apparent increase of the dielectric constant. However, the impact on the dielectric constant of the attractive forces will usually be much smaller than those originating from the non-linear effects seen in the presence of high fields.

The analysis of the crystallization kinetics of glass-forming materials by BDS is possible due to the fact that during the crystallization, the dipolar molecules from the supercooled liquid are frozen in the crystalline phase and, from now on, will not contribute to the total dielectric response of the liquid volume fraction. Consequently, the number of actively reorienting dipoles decreases with increasing the crystalline fraction in the system. The dielectric permittivity is the property that relates to polarization and electric field via $P = \varepsilon_0(\varepsilon^* - 1)E$. In the real and imaginary parts of the dielectric permittivity, the α-relaxation process (the primary relaxation process in supercooled liquid regime) is seen as dispersion of the dielectric permittivity and dielectric loss, as shown in Figure 7. The dielectric permittivity value decreases with increasing the degree of crystallinity of the system. Thus, the crystallization can be followed via a dielectric relaxation study. Typically, the crystallization process finishes when there are no traces of the α-relaxation process in the dielectric permittivity's real and imaginary components. This is also demonstrated in Figure 7.
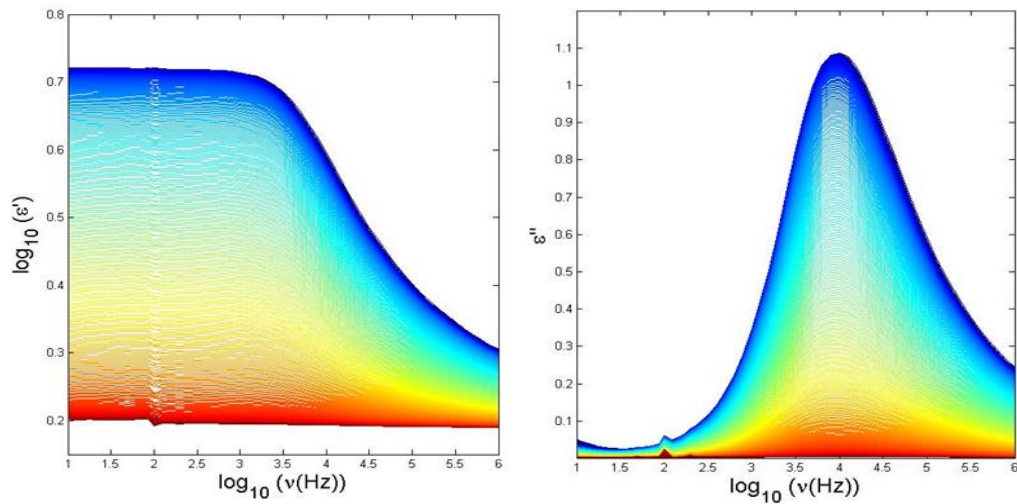
Figure 7. Typical changes in the real (on the left) and imaginary (on the right) parts of the dielectric permittivity for a typical glass-forming liquid upon crystallization under isothermal conditions.

In turn, upon melting process followed by dielectric spectroscopy, the opposite effect takes place. When the crystallized sample is subsequently heated up to the melting temperature, we observe a jump in the dielectric response due to the increased number of actively reorienting dipoles. The melting event can be detected as the point at which a sharp rise of the dielectric permittivity is observed (as shown in Figure 8). Knowing the melting temperature of the generated crystalline material is essential because it allows verifying the polymorphs content obtained upon the crystallization process.
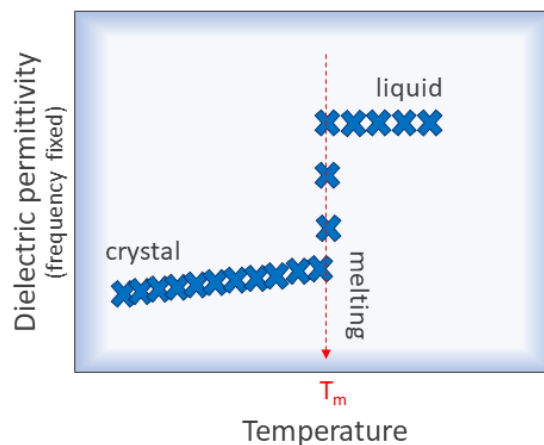

Figure 8. Representative changes in the real part of the dielectric permittivity (at a fixed frequency) are measured upon heating with a constant rate of the crystalline material.

2. RESULTS AND DISCUSSION

2.1. Effect of High AC Field on Crystallization

This section demonstrates how the properties of the external electric field can influence the crystallization of a polar molecular system. Tested material is a glass-forming liquid with a relatively high value of the permanent dipole moment, μ= 4.76 D,[35] vinyl ethylene carbonate (VEC), a vinyl derivate of propylene carbonate (PC). The chemical structure of VEC is presented in Figure 9. The glass transition temperature of VEC is T_g=171 K,[35] while the melting temperature of the ordinary crystal (formed in the absence of electric field) is 227 K.[7] The crystallization behavior of VEC depends on the frequency and the amplitude of the applied alternating electric field. These attributes of the time-dependent electric field can affect the kinetics of crystallization and the polymorph outcome. It is important to note that the field-induced effects on crystallization are not seen within the entire investigated frequency range. They are observed only below a specific frequency threshold. The following results were presented and discussed in more detail in papers **A1** and **A3**.

(a) VEC   (b) PC
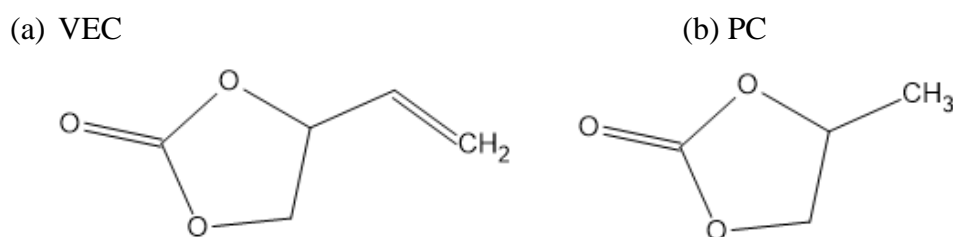
Figure 9. The chemical structure of VEC and PC.

The optimal temperature region for nucleation of the ordinary VEC crystals is located in the vicinity of the T_g, while the crystal growth is favored around 30 K above the glass transition temperature.[7,36] To understand how the electric field influences crystallization, two different thermal protocols were used. They are presented in Figure 10. In Protocol A, the sample goes straight to the crystallization temperature, which is 198 K (=T_g + 27 K). Immediately after reaching 198 K, an external electric field with different field amplitudes or frequencies was applied to the sample. In this case, the nucleation of the

ordinary (also termed here as "low-field") polymorph is greatly impeded, so it is expected that the liquid sample will not crystallize in the absence of an external electric field. However, in the presence of high alternating fields at 198 K the crystallization of a new field-induced polymorph of VEC is promoted. Crystallization progress with time was monitored by using dielectric spectroscopy (DS). When crystallization is completed, the ac field is switched off, and the crystalline material is heated up with a constant rate to 243 K, while the melting temperature is detected by DS (low-field permittivity measurements). Identical experiments performed in the absence of an external electric field serve as a reference.

In protocol B, the main objective was to study the effect of the high ac fields on nucleation. For that, in the absence of an external electric field, the liquid sample was cooled down to 173 K (i.e., T_g +2 K), from 243 K. Here, we wish to favor nucleation of the low-field polymorph and see how different field amplitudes and field frequencies affect the results. We waited at this temperature for 1 hour with the high ac field switched on, keeping different field magnitudes or field frequencies. Then, the external high electric field was switched off. The temperature was increased to 198 K. At selected crystallization temperature, in the absence of a high electric field, we followed the crystallization progress of VEC via DS. After completing crystallization, the melting behavior is analyzed upon heating, also using DS.
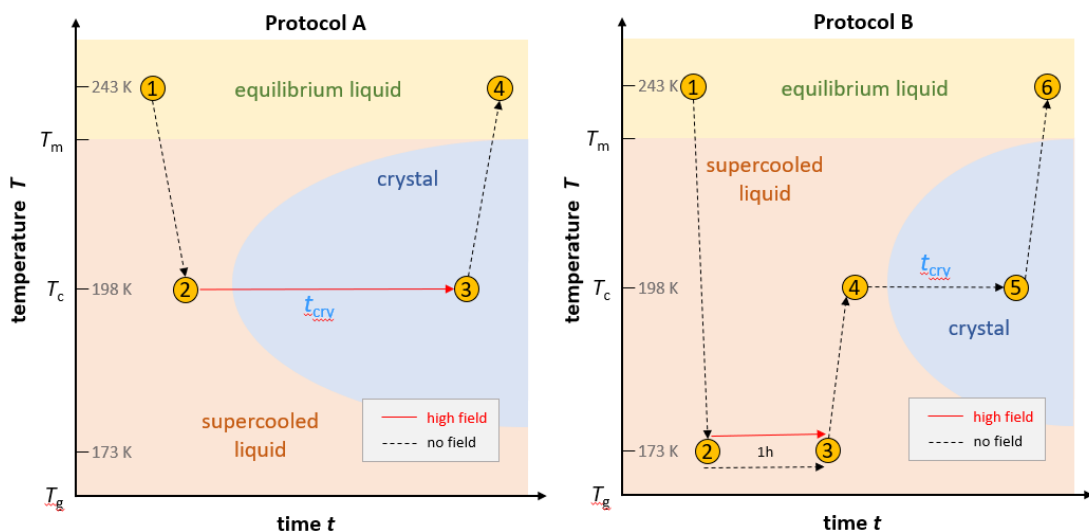

Figure 10. Overview of the experimental protocols used to study the effect of frequency and magnitude of the ac field on the crystallization behavior of VEC. Protocol A was followed to favor the formation of only the high-field polymorph. Protocol B was designed to study in detail the effect of the high-field on the nucleation process.

In polar liquids, like VEC, the rotational motion of permanent dipoles will dominate the dielectric constant values. For a crystalline material, these motions are suppressed. Therefore, it is possible to investigate the crystallization progress in glass-forming systems via dielectric spectroscopy by analyzing changes in the complex dielectric permittivity with time. The ratio between the crystal volume with the total volume of the sample can be estimated through [7,37,38]

$$\frac{V_{cry}}{V_{total}} = \frac{(\varepsilon_s - \varepsilon')}{(\varepsilon_s - \varepsilon_\infty)} \tag{3}$$

where ε_s is the static dielectric permittivity, while ε_∞ is the high-frequency permittivity limit of the liquid, i.e., in the absence of orientational contributions from permanent dipoles. The molecular electronic polarizability values in both the crystalline and the liquid states are very similar. Hence, ε_∞ can be considered as the permittivity of the crystalline state. The dielectric relaxation amplitude, $(\varepsilon_s - \varepsilon_\infty)$, is governed by dipole reorientation found in the liquid state. Thus, lowering the amplitude of the structural relaxation with time signifies a decrease of the liquid volume fraction as crystallization proceeds. The two limiting values of V_{cry}/V_{total}, 0 and 1, denote pure liquid and completely crystallized material, respectively.

Changes in the crystallization behavior of VEC at 198 K, described in terms of the crystal volume fraction, are presented as a function of the field frequency and field magnitude in Figure 11. These data were recorded when following thermal protocol A from Figure 10. The left panel (a) shows the case where the magnitude of the ac field was fixed, 80 kV/cm, while the frequency of the high ac field varies. The right panel (b) shows the opposite situation. The frequency is remained fixed, at 56.2 Hz, while the magnitude of the ac field is changed. For frequencies $\nu \geq 100$ Hz, no crystallization is observed during the first 14 hours. On the other hand, when a certain frequency threshold is reached, which is around ~18 Hz for VEC, crystallization is induced in the presence of the altered field. Then, below that characteristic frequency threshold, crystallization times dramatically decrease. At $\nu = 56$ mHz, the crystallization process is completed within half an hour. Consistent with the frequency effect on crystallization, the crystallization times can be reduced within the same order of magnitude by increasing the ac field amplitude to 180 kV/cm.
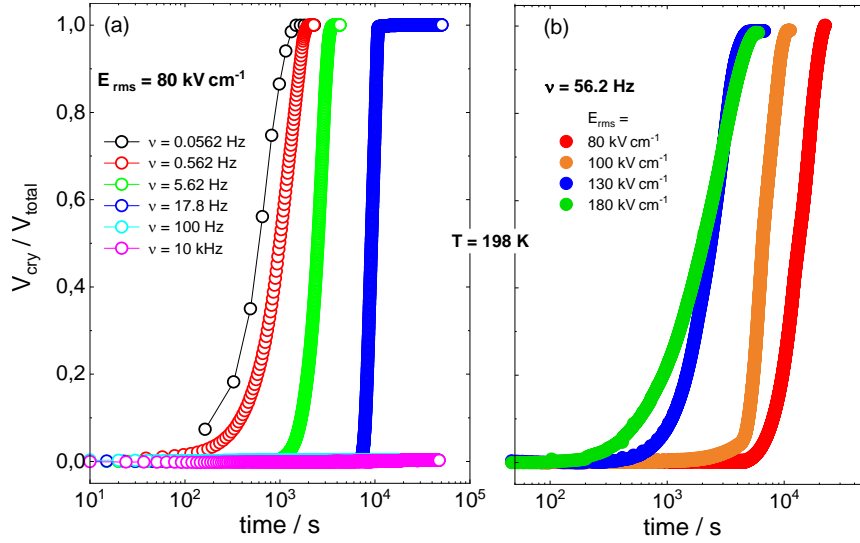
Figure 11. Isothermal crystallization of VEC reported as the volume fraction of crystalline material, V_{cry}/V_{total}. After reaching $T = 198$ K, the sample is exposed to an ac electric field of (a) $E_{rms} = 80$ kV/cm at different frequencies v as indicated; (b) frequency $v = 56.2$ Hz using different fields amplitude E_{rms} as indicated. Results from paper **A1**.

The volume fraction of the crystalline material, V_{cry}/V_{total}, can be related to the rate of crystallization, k, and the Avrami parameter, n, through the Avrami relation[39,40]

$$\frac{V_{cry}}{V_{total}} = 1 - \exp[- (k \cdot t)^n] = 1 - \exp\left[- \left(t/\tau_{cry}\right)^n\right] \tag{4}$$

where t is the time after the onset of crystallization, in other words, excluding the incubation time of the process. The Avrami parameter depends on the dimensionality and geometry of the growing crystals. Thus, the crystallization rate provides combined information about the rate of nucleation (N) as well as the crystal growth (G), where $k = NG^{n-1}$. It is important to note that the rate of crystallization k is the inverse of the characteristic crystallization time, τ_{cry}. Among the others, Equation 4 is frequently employed to analyze the crystallization kinetics of various materials. Hence, the crystallization curves shown in Figure 11 were fitted using the Avrami equation. Obtained in this way evolution of τ_{cry} as a function of the frequency and the magnitude of the applied ac field is demonstrated in Figure 12a and Figure 12b, respectively. When the ac field magnitude is fixed, the crystallization times decrease with decreasing the field
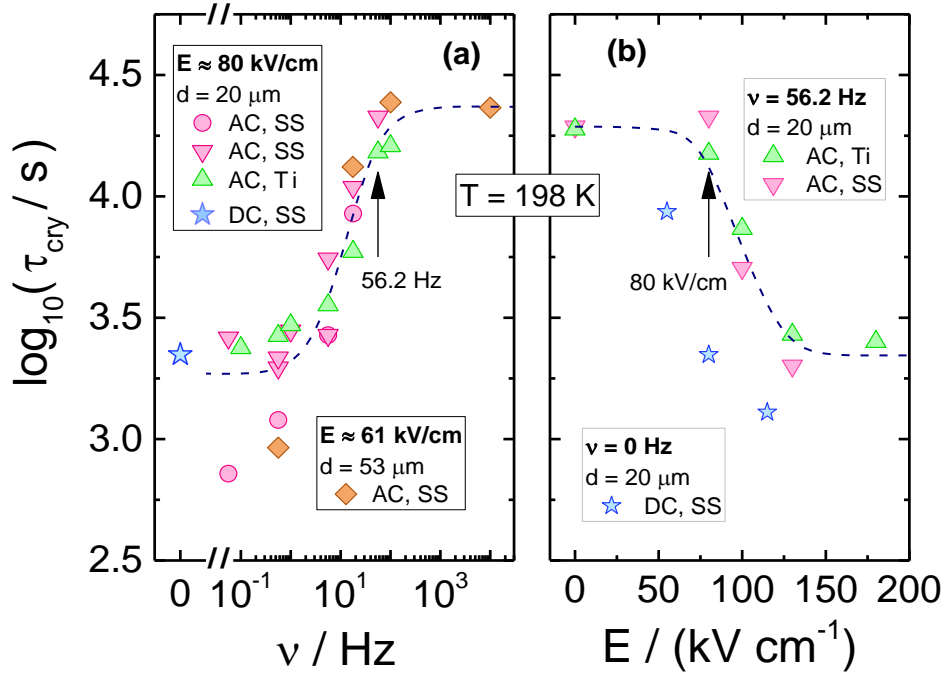
Figure 12. Time constants τ_{cry} characterizing the crystallization of VEC at T = 198 K. (a) Frequency dependence of τ_{cry} at a practically constant field of E_{rms} = 80 kV/cm. (b). Field amplitude dependence of τ_{cry} at a constant frequency of ν = 56.2 Hz. The E_{rms} = 80 kV/cm data point of the panel (b) is reproduced in panel (a) to show consistency. Different electrode materials (SS vs Ti) and different spacings d between the electrodes were used to discriminate possible electrode effects. The corresponding dc bias data were added for comparison. Results from paper **A3**.

frequency. The most pronounced changes are observed at the frequency range of 20 to 50 Hz. For frequencies below that threshold, the crystallization time constants eventually saturate and approach that characteristic for the static dc-field (ν = 0 Hz). Thus, the resulting $\tau_{cry}(\nu)$ is a sigmoidal-shaped curve with two plateaus at high and low-frequency limits. In turn, when the ac field frequency is fixed, the crystallization times analyzed as a function of the field magnitude, $\tau_{cry}(E)$, also follow an S-shaped dependence. With increasing the magnitude of the applied ac field, the crystallization rate will increase. However, at some point, it also saturates. Thus, the two limiting values of τ_{cry} for VEC are $E = 0\,\text{kV/cm}$ and $E = 150\,\text{kV/cm}$. Within that field magnitude range, the crystallization is accelerated by a factor of ten. Ideally, is when S-shaped $\tau_{cry}(E)$ obtained when applying high alternating electric and dc-bias fields of the same magnitude collapse. The discrepancy, seen in Figure 12b, comes from the fact that the frequency of ν = 56.2

Hz is relatively too high compared to the low-frequency limit (≤5.62 Hz) established based on the results described above (Figure 12a).

Different electrode materials, titanium and stainless steel were used to discriminate the possible effect of surface roughness (stainless steel electrodes were highly polished while titanium electrodes were rougher). In addition to that, the distance between the electrodes was increased from 20 to 53 mm to verify the role of the increased sample volume/reduce the electrode polarization. It can be seen that the electrode effects, in general, do not influence the ac field-induced changes in the crystallization of VEC. The very similar crystallization behavior seen when using different electrode materials suggests that the nucleation in the presence of ac electric field proceeds via homogeneous rather than heterogeneous mechanisms.

The crystallization time is not the only parameter affected by the presence of a high alternating field. On the condition that the crystal nuclei are polar, the electric field can force a particular orientation of the crystallites. The Avrami parameter captures the information on the arrangement of the molecular systems in crystalline structures. Figure 13 demonstrates the dependence of the Avrami parameter for VEC as a function of (a) frequency and (b) amplitude of the ac electric field. The results show that the morphology of the growing crystals is very sensitive to the frequency and amplitude of the ac field. At low amplitude or high frequencies, the value $n \approx 3.6$ indicates spherical growth of the crystallites with sporadic nucleation events. While, at low frequencies or high field magnitude, the Avrami parameter drops down to approximately $n \approx 1.5$, which suggests that the crystallites adopt a more rod-like morphology and grow from instantaneously formed nuclei. After adding to Figure 13 the values of the Avrami parameter determined from the dc bias fields, a remarkable agreement was found.
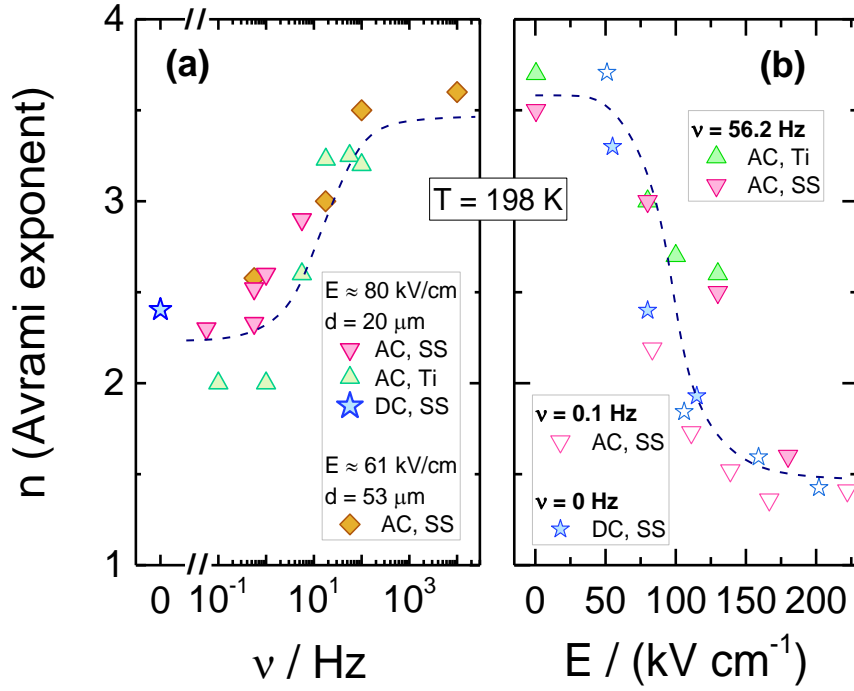
Figure 13. Dependence of the Avrami parameter *n* for VEC as a function of (a) frequency at $E = 80$ kV/cm and $E = 61$ kV/cm; (b) amplitude of the ac-field at fixed frequency $v = 56.2$ Hz and $v = 0.1$ Hz. The corresponding dc data were added for comparison. Results from paper **A3**.

To understand the ac-frequency threshold needed to observe crystallization from the supercooled liquid state of VEC, we have considered the possibility that the field-induced orientation of particles larger than the molecules may be involved in this process. For that purpose, we have made use of Stokes-Einstein-Debye (SED) equation which relates the viscosity of liquid, η, with the rotation time for given particle size, τ_{rot},

$$\tau_{rot} = \frac{4\pi\eta r^3}{k_B T} \tag{5}$$

At T=198 K, the viscosity of VEC is 70 Pa s, with the onset ac field frequency of ~18 Hz, the estimated particle radius is 3 nm. From that, we can suppose that an electric field is able to align or move around the crystal nuclei of radii r < 3 nm, provided that these crystallites possess a net permanent dipole moment μ. Another requirement is that these crystallites are able to rotate to lower their free energy via an external field, namely, the angular term μE cos θ in the potential energy.

24

The presence of a high ac field affects not only the crystallization kinetics of VEC but also the polymorph outcome. This was demonstrated by analyzing the melting behavior of the investigated samples via dielectric spectroscopy (in a low-field limit). The results obtained for crystalline material generated using high electric ac fields with different field frequencies and magnitudes are shown in Figure 14a and Figure 14b, respectively. The dielectric response was measured at low fields for a fixed frequency of 10 kHz upon continuous heating with 1 K/min from the crystallization temperature of T = 198 K to a value of T = 243 K, where the liquid state of VEC is completely recovered. The melting event is seen in the dielectric response of the sample as a characteristic rise of ε' until reaching the value characteristic for a liquid state. It can be seen that depending on the frequency and field amplitude used to induce crystallization of VEC at 198 K; the two melting events can be seen upon heating. Generally, low frequencies or high fields promote the polymorph formation, which melts at $T_{m,2}$ = 208.5 K. More specifically, the lower the frequency or the higher the magnitude of the ac field, the large the volume fraction of this polymorph is found in the total crystalline material. At $v \approx 0.56$ Hz, the melting scan shows that the final product is only the field-induced polymorph. It will be termed in this way because - in the absence of an electric field - it is impossible to achieve, irrespectively of the protocol which is used. The polymorph with the melting temperature, $T_{m,1}$ =227 K, can be routinely obtained without high fields just after supercooling VEC close to T_g region. Therefore, it is termed in this thesis as the ordinary or low-field polymorph. At 198 K, the high-temperature polymorph grows alone when using the frequency of $v \approx 56$ Hz at a fixed field amplitude of 80 kV/cm, or lower. At $v \approx 18$ Hz (Figure 14a) and 100 kV cm^{-1} (Figure 14b) the final product is a mixture of the low-melting polymorph and the ordinary one. The recrystallization seen as a drop-in ε' for T > $T_{m,2}$ is a matter of some trace amounts of nuclei or crystallites that leads to the formation of the polymorph that melts at $T_{m,1}$.
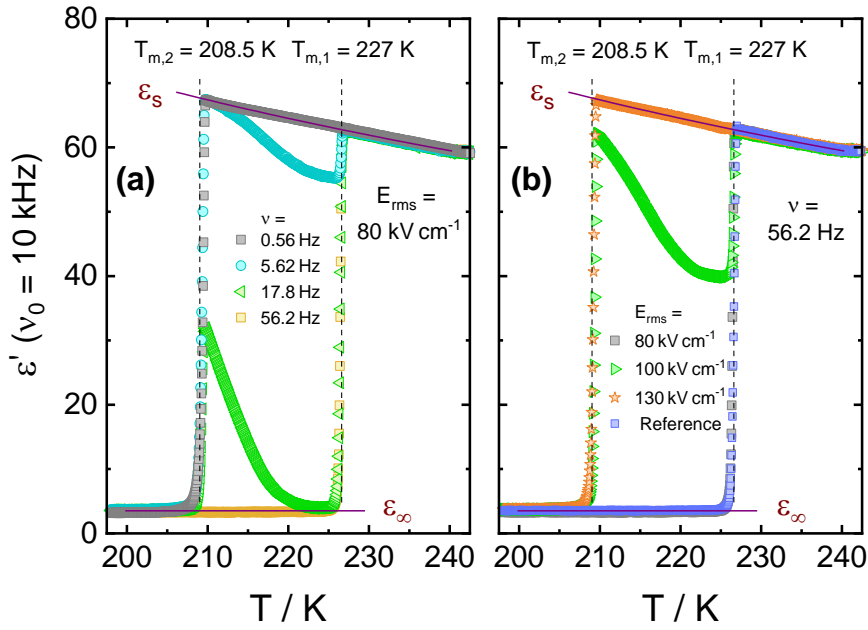
Figure 14. Melting curves of previously crystallized VEC analyzed in terms of the real part of dielectric permittivity measured at 10 kHz, recorded on heating from 198 K to 243 K with 1 K/min. Crystalline materials were obtained at 198 K by applying an external electric field of (a) fixed field for a range of frequencies and (b) fixed frequency for a range of fields, as indicated in the legends. The blue square represents the melting curve for the regular polymorph. Results from paper **A1.**

In the next step, the effect of a high ac field on the nucleation of VEC will be analyzed. For that, protocol B - shown in Figure 10 - was employed. As a reference, we have also included the crystallization data recorded in the absence of a high field. The results indicate that crystallization speeds up when the ac field is applied during the nucleation period. Comparing the zero-field reference data with that collected when the nucleation takes place in the presence of 130 kV/cm at $\nu=0.03$ Hz, we see only small differences in the time evolution of dielectric permittivity at 10 kHz upon crystallization of VEC at $T_c = 198$ K. The increase of the field amplitude from 130 kV/cm up to 180 kV/cm (at a fixed frequency $\nu=0.03$ Hz) also has very little effect on the crystallization rate. However, a relevant difference was noticed when the frequency of ac electric field was decreased to 0.01 Hz. For this frequency, using the field magnitude E=130 kV/cm, the crystallization process speeds up considerably. The results are shown in Figure 15. Based on the analysis of the α-loss maximum at 173 K ($\nu_{max}\approx60$ mHz), we conclude that crystallization progress is more effective when the ac field frequency $\nu \ll \nu_{max}$. This

supports our hypothesis that the high ac field affects the crystallization of VEC only when it matches with the time scale of reorientation of much bigger structures like crystal nuclei. Once this frequency condition is met, the increase in the field amplitude is able to accelerate the crystallization.
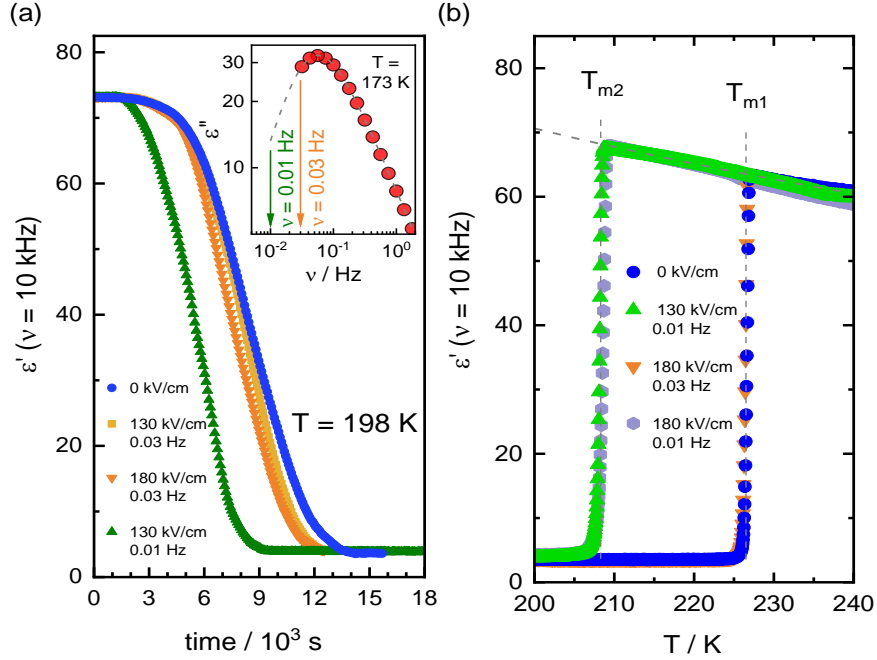
Figure 15. (a) Changes in the dielectric permittivity ε' at a fixed frequency of 10 kHz at T = 198 K for VEC after being exposed for 1 h at T = 173 K to the high-electric field: E = 130 kV/cm (v = 0.03 Hz and v = 0.01 Hz), E = 180 kV/cm (v = 0.03 Hz) and E = 0 kV/cm. The inset shows the α-loss maximum at T = 173 K measured within the linear response regime. The arrows identify the frequencies used for high-field experiments. (b) Melting curves recorded upon heating of VEC crystals generated in the previous step, following protocol B. Results from paper **A3.**

After the crystallization was completed, the melting behavior of obtained crystalline material was identified by scanning from 198 K to 245 K with a constant heating rate of 1 K/min. Obtained results are presented in Figure 15b. As can be seen, the ac field frequency modifies the rate of crystallization and changes the final crystallization product.

In addition to that, when studying the effect of the high ac field on VEC crystallization, we found another very interesting finding. It is described in more detail in paper **A3**. In short, the aim was to verify the influence of the high ac field on the ongoing crystallization of the ordinary crystal. For that purpose, a completely different protocol was created. Namely, in the absence of a high ac field, the liquid sample was cooled down

close to 163 K (i.e., T_g - 8 K), from 243 K. Cooling close to T_g (with no field) will induce the nucleation of a regular polymorph which grows afterward at higher temperatures. Without additional waiting time, the supercooled liquid was heated from 163 K to 198 K. The sample at this temperature was allowed to crystallize spontaneously for some time, and only once the liquid volume fraction dropped down to around 20%, the high-field was switched on. Then, when the liquid volume fraction was around 50%, the high-field was switched off. From the collected dielectric data, it is possible to observe an increase in the crystallization rate when the ac field is switched on. In turn, when the high electric field is switched off, the observed trend does not change. From that study, it was concluded that the nucleation rather than the crystal growth rate is mainly affected at high electric fields.

In summary, in this section, it was demonstrated how the time-dependent electric fields could affect the crystallization rate and the morphology of the growing crystals. The amplitude and frequency of the applied ac field can affect not only the kinetics of the crystallization but also the outcome product. Subjecting a tested material to high ac fields with a specific amplitude or frequency value not only induces the crystallization but also prevents the formation of the low-field polymorph in favor of a completely new form.
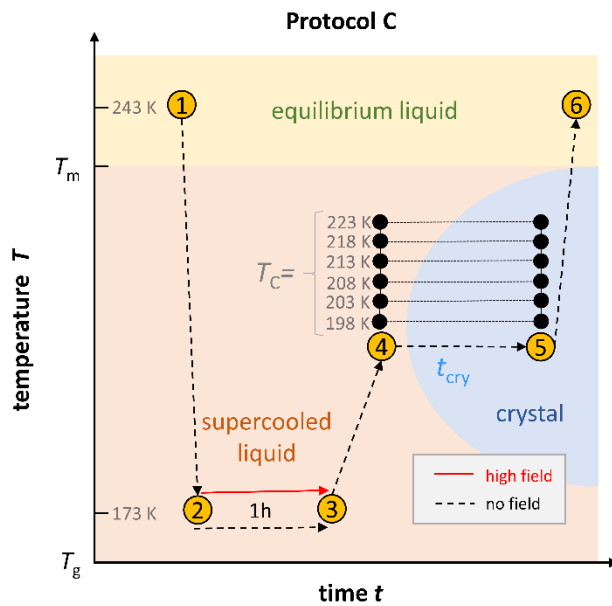
2.2. Effect of Electric Field on Crystallization Rate Curves

Currently, there is no theoretical or practical information that explains the impact of the high electric field on the temperature evolution of the crystallization rate. In this part, for the first time, it will be demonstrated how the electric field affects the maximum of the overall crystallization rate curve for a simple polar liquid, VEC. For that, different magnitude or frequencies of the ac or dc field were applied close to T_g, while the crystallization will occur at different temperatures. The following results were presented and discussed in paper **A4**.

As explained previously, the best temperature range to nucleate the ordinary VEC crystals is close to T_g. Using this knowledge, we have designed and followed the thermal protocol C illustrated in Figure 16. Here, starting from T = 243 K, the liquid sample was cooled down until 173 K to nucleate the regular polymorph. At this temperature, the high electric field was applied using either different field magnitudes or frequencies for 1 hour. After 1 hour in the absence of high-field, the sample was heated up to the desired crystallization temperature. Once the crystallization temperature was reached, we have

allowed the sample to crystallize in a non-field environment. When the crystallization was completed, the crystalline material was heated up back to T = 243 K to recover the liquid state. Both crystallization and melting processes were followed using DS in the linear response regime.

At this point, it is essential to explain why we have not used the protocol A shown in Figure 10a to study the field-induced changes in the crystallization behavior of VEC in a wide temperature range. For higher crystallization temperatures, such as T = 218 K, the conductivity of the sample is increased. When the high electric field is applied at such conditions, it generates excessive heating that, in most cases, burns the sample, making it impossible to measure the field effect on the ongoing crystallization. From this point of view, applying high electric fields is "more safe" when carried out in a very viscous liquid regime, close to T_g. On the other hand, following protocol C, in most cases, allow also nucleation of the ordinary crystals. Therefore, upon heating of the crystallized samples, two melting events will be detected.


Figure 16. Overview of the experimental protocol used to study the effect of the magnitude and frequency of the high electric field on the crystallization of VEC at different crystallization temperatures, T_c.

In a similar way, as demonstrated in the previous section, the crystallization data were analyzed using the Avrami approach (Eq. 4). The obtained temperature dependence of crystallization rate, k, after exposing VEC to high ac fields of different frequencies and

magnitudes (please remember that the field was applied only for 1 hour close to T_g while the ongoing crystallization was followed at different temperatures within 193 K and 223 K in the absence of electric field) are presented in Figures 17a and 17b, respectively. For the reference experiments, that is, upon which the sample was not exposed to an electric field at 173K, the crystallization rate maximum happens at around 213 K with $\log_{10}(k_{max}/s^{-1}) \approx$ -3.3. This maximum is obviously associated with the low-field polymorph of VEC. Using high ac fields of 160 kV/cm at 173 K does not affect the position of the maximum crystallization rate. However, with decreasing the frequency of the applied ac electric field, a small (but systematic) increment in the crystallization rate is observed. Interestingly, the evolution of $k(T_c)$ for ac fields of 160 kV/cm and ν=0.1 Hz shows a quantitative difference at low temperatures compared with 1 Hz situation. As can be seen in Figure 17a, applying a high electric field from the low-frequency range, $v = 10^{-1}$ or 10^{-2} Hz, will create a new crystallization rate maximum located at low temperatures, ~198 K. This new maximum is due to the field-induced polymorph which can be promoted by high amplitude ac fields only when using frequencies below a specific threshold. The effect of dc bias fields (ν=0 Hz) was also tested, as shown in Figure 17a. Just as expected, it produces a very similar behavior as when using low frequencies of the ac fields. As known from the results discussed in the previous section, a high ac field is able to induce the formation of a new polymorph only when the field frequency matches with the time scale of the reorientation corresponding to a particular polar structure/crystal nuclei. When the ac field frequency is incompatible with such motions, it results only in a slight increase in the magnitude of the overall crystallization rate.

Figure 17b demonstrates the dependence of the crystallization rate curves as a function of the field magnitude. For high ac fields, a fixed frequency of $v = 10^{-1}$ Hz was used. At this frequency, it is possible to generate the field-induced polymorph. Thus, we observe two crystallization rate maxima when using field magnitudes of 100 and 160 kV/cm. The crystallization rates increase when the amplitude of the ac field increases, analogous to the case when the ac field frequency is decreased while the high ac field magnitude remains unchanged. In this case, the temperature positions of both maxima is also invariant to the field magnitude. Likewise, for the dc bias fields, we also observe two crystallization rate maxima associated with the field-induced and ordinary polymorphs. When the static field magnitude increases from 100 and 200 kV/cm, the crystallization rates increases, but the positions of both maxima remain the same.
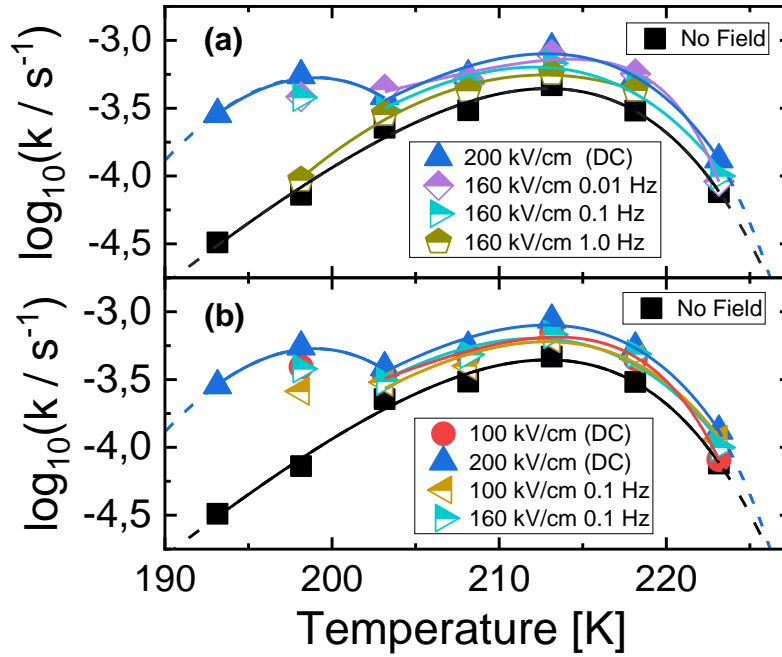
Figure 17. The characteristic time of crystallization for VEC plotted as a function of crystallization temperature using different field magnitudes (a) E = 200 kV/cm for a dc field and E = 160 kV/cm for an ac field with different frequencies; (b) E = 200 and 100 kV/cm for a dc field and E = 160 and 100 kV/cm for an ac field at a fixed frequency, $\nu = 10^{-1}$ Hz. Solid lines are fits to the experimental data using an exponential function plus a linear term. Results from paper **A4**.

Exposing VEC to a high electric field affects not only the crystallization rate but also the dimensionality of growing crystals. These changes can be captured by the Avrami parameter, n (Eq. 4). The evolution of n as a function of temperature is plotted in Figure 18a and 18b for the different ac field amplitudes and frequencies, respectively. In the absence of a high electric field, the Avrami parameter increases with increasing the temperature, from $n \approx 2$ to $n \approx 3.5$. At lower temperatures, there are no significant differences between values of the Avrami parameter for high-field and non-field cases. On the other hand, as the temperature increases, there is a pronounced influence of both alternating and static electric fields on the values of the Avrami parameter. Namely, with increasing the field magnitude, the value of the Avrami parameter increases. Within the studied temperature range, the frequency of the applied ac field does not change the dimensionality of growing crystals significantly. Thus, the temperature and the magnitude of the high electric field seem to have a more impact on the values of the Avrami

31

parameter in comparison with the field frequency. As a matter of fact, the ac field frequency is more important when it comes to the crystallization rate, as demonstrated earlier. Nevertheless, it should be remembered that the crystallization progress is studied in accordance with experimental protocol C (Figure 16). So, it takes place in the absence of a high electric field. Thus, the crystallizing particles are not explicitly forced to be oriented by the high electric field. This is contrary to the situation when the high electric field is applied directly at the crystallization temperature.
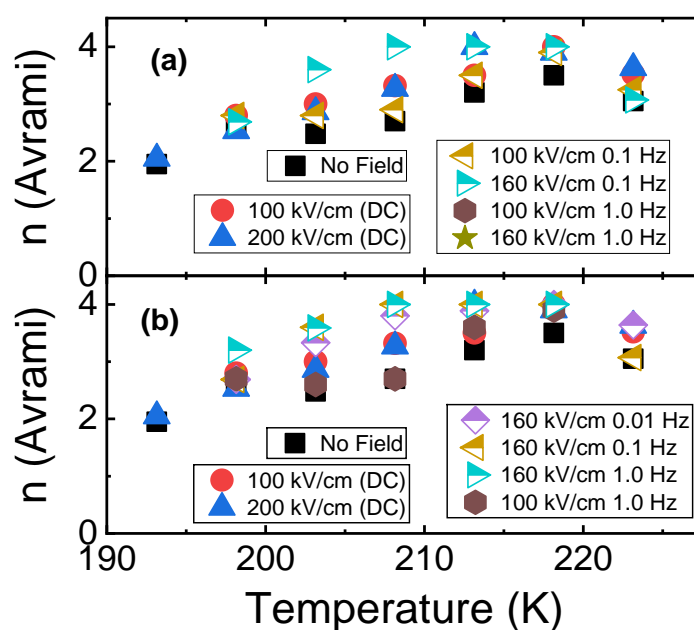
Figure 18. The Avrami parameter for VEC plotted as a function of crystallization temperature at (a) $E = 200$ kV/cm for dc field and $E = 160$ kV/cm for ac field with different frequencies; (b) $E = 200$ kV/cm and 100 kV/cm for dc field and $E = 160$ and 100 kV/cm for ac field for different frequencies. The values obtained in the absence of high-field and for dc cases were added for reference. Results from paper **A4**.

When the crystallization was completed, the final product was analyzed upon heating scan to recognize the melting behavior. The melting curves were measured in the absence of a high electric field at a frequency of $v = 10$ kHz, keeping a constant heating rate of 1 K/min. The collected results for all crystallization temperatures are gathered together in Figure 19. For the non-field case, in all crystallization temperatures covered by this study, there is only one melting event located at $T_{m1} \approx 227$ K. As mentioned before, it is associated with the ordinary polymorph. Likewise, for high ac fields (100 or 160 kV/cm) using frequency $v = 1$ Hz, only one melting process is detected.
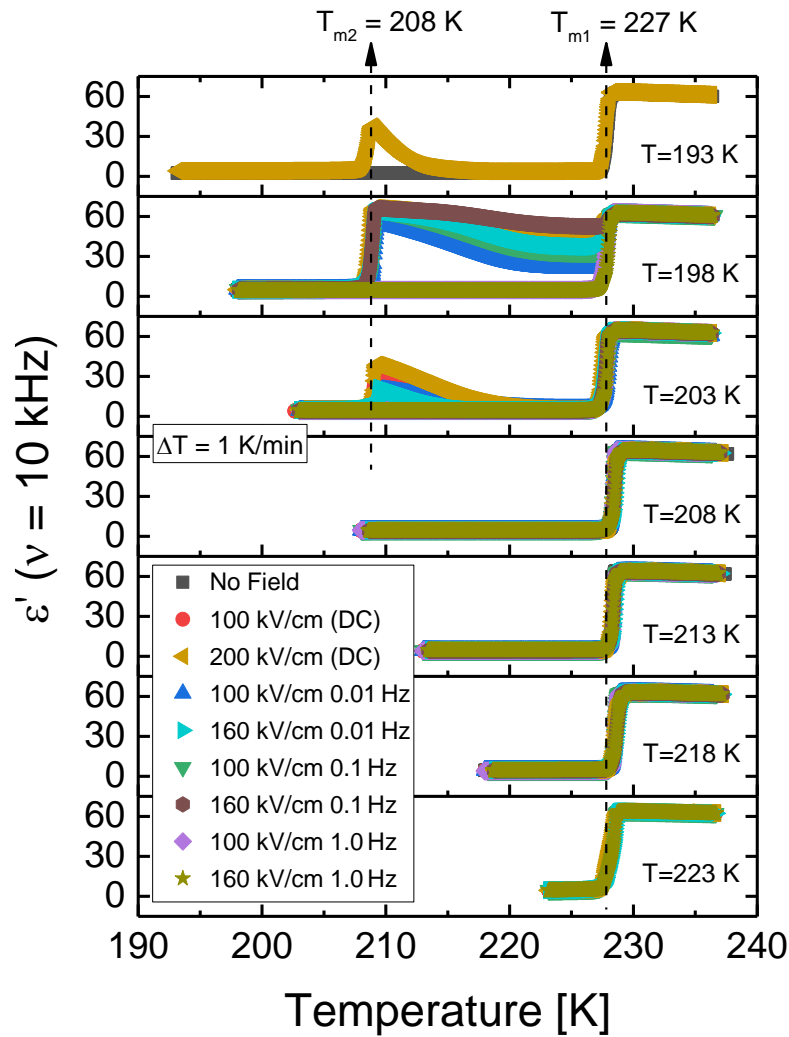
Figure 19. Melting curves of previously crystallized VEC analyzed in terms of the permittivity ε' measured at a frequency $v = 10$ kHz upon scanning temperature from the crystallization temperature to 245 K at a rate of 1 K min^{-1}. Crystallization has been field-induced using different magnitudes and frequencies of the field, as indicated in the legends. The zero-field crystallization counterpart is added for reference. Results from paper **A4**.

As the crystallization temperature is decreased to $T_c = 198$ K, and with the frequency of the ac field decreased from 1 Hz to $v = 10^{-1}$ or 10^{-2} Hz, there is an additional melting process seen at $T_{m2} \approx 208$ K, and related with the field-induced polymorph. Because of some residual fraction of the ordinary form nuclei in the crystallized product, the subsequent heating also shows the melting process at $T_{m1} \approx 227$ K. Since the values of ε' near T_{m2} can be associated with the volume fraction of the high-field polymorph; it can be seen that using ac field frequency of 10^{-2} Hz instead of 10^{-1} Hz results in obtaining

a larger fraction of the field-induced polymorph. For the dc fields, the magnitude of the high electric fields affects the quantity of the polymorphs in the crystalline material obtained at temperatures below 208 K; the melting scans taken for these samples also show two melting events related to the field-induced and ordinary polymorphs. All other melting curves associated with crystallization temperatures between 208 K and 223 K follow the same behavior as the non-field case, indicating a melting process of the ordinary polymorph (T_{m1}).

In summary, this section demonstrates the effect of a high electric field on the overall crystallization kinetics of VEC in a wide temperature range. It was explored how the frequency and amplitude of an applied ac electric field affect the temperature evolution of the crystallization rate and Avrami parameter. Changing the magnitude and frequency of the high ac fields allows generating at lower temperatures additional crystallization rate maximum associated with the formation of the field-induced polymorph. In general, the location of the overall crystallization rate maximum corresponding to the ordinary VEC polymorph remains unaffected by the electric field. Nevertheless, the crystallization rates were observed to increase slightly with increasing the field magnitude. Static electric fields influence the crystallization of VEC in the same manner as high alternating electric fields of very low frequency.

2.3. Stability of the Field-Induced Polymorph

The stability of the field-induced polymorph of VEC is studied in this section. The field-induced polymorph reveals to be unstable at certain conditions. So, using dielectric spectroscopy, we have monitored the potential polymorphic transition of the field-induced polymorph into the stable state. These results are discussed in paper **A2**.

Two different thermal protocols were utilized to investigate the stability of the field-induced polymorph, as demonstrated in Figure 20. The first protocol, protocol D, aims to induce the nucleation of the regular polymorph via decreasing the temperature to 173 K. Then, the supercooled sample is heated to the crystallization temperature $T_c = 198$ K, where the high-electric field, with amplitude $E_{cry} \approx 80$ kV/cm at a frequency of $v = 5.62$ Hz, will be applied. This should result in obtaining a crystalline material containing both field-induced and ordinary polymorphs. Once crystallization is completed, we had added some waiting time, t_w, up to 72h, before the heating scan from 198 K to 245 K was performed. The waiting time was carried out with either the electric field to be switched

on or off. In the second protocol, protocol E, the plan was to avoid the formation of the regular polymorph. Therefore, the liquid sample was cooled down straight to the crystallization temperature, 198 K, without any further cooling to the temperature region close to T_g. In this way, using sufficiently high ac field magnitudes matched with the ac field frequencies below a characteristic threshold, the crystallized sample should contain only the field-induced polymorph. After completing the crystallization, the crystalline material was kept at 198 K for up to 72h, with the field switched on or off. After the waiting time, the temperature was increased, and the melting behavior of obtained crystalline products was analyzed.
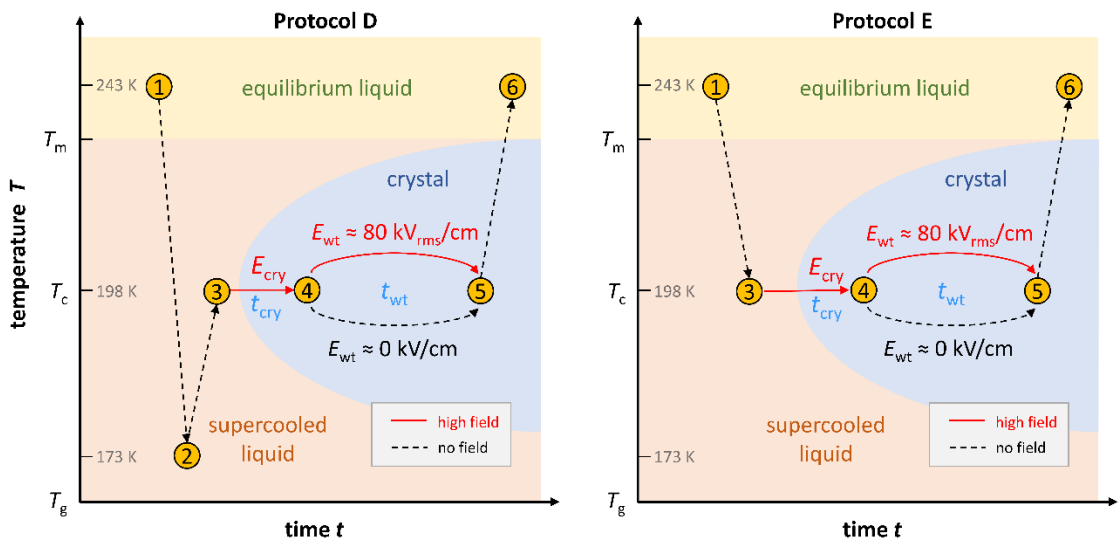
Figure 20. Schematic representation of the two different protocols used to prepare samples and test the stability of the field-induced polymorph. Protocol 'D' inserts additional cooling to T = 173 K, whereas the temperature in protocol 'E' was never lower than T_c = 198 K.

The results of the dielectric study collected by following protocol D are demonstrated in Figure 21a. The evolution of the dielectric permittivity ε' at v = 5.62 Hz was monitored upon crystallization of VEC in the presence of a high ac field. As a reference, the same experiment was also performed in the absence of a high electric field. Since these data are the basepoint for further consideration, the analysis will start from the changes in ε' at a fixed frequency (5.62 Hz) with time as measured at low fields (~ 0 kV/cm). In this case, a final drop of ε' values as due to crystallization takes place from ε' ~73 to a level close to 3.6. And this value remains unchanged with time. In turn, when

the high field is applied during crystallization (~80 kV/cm), the dielectric permittivity terminates the rapid descent near a level of $\varepsilon' = 6.0$. But then, interestingly, the value of the ε' decreases linearly with waiting time and reaches the value of $\varepsilon' = 3.6$ after 14 h. This situation is seen much better in the inset of Figure 21a.
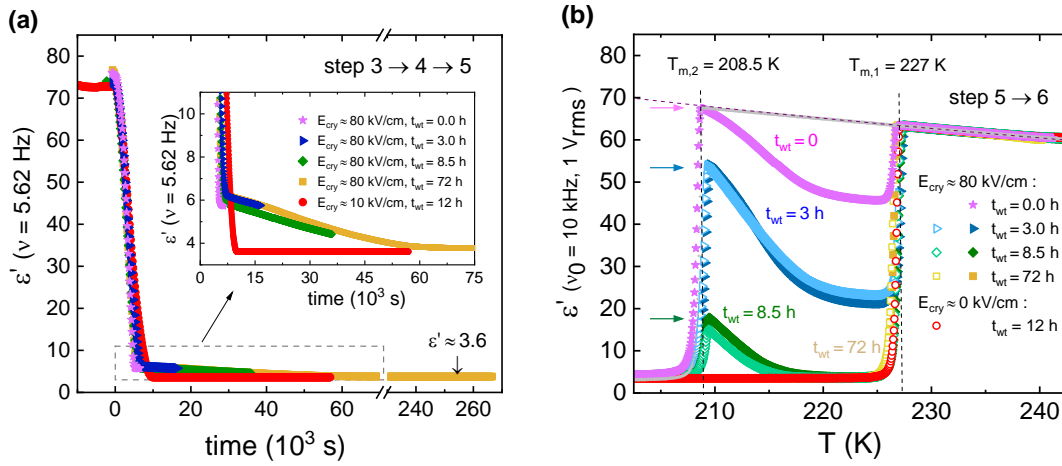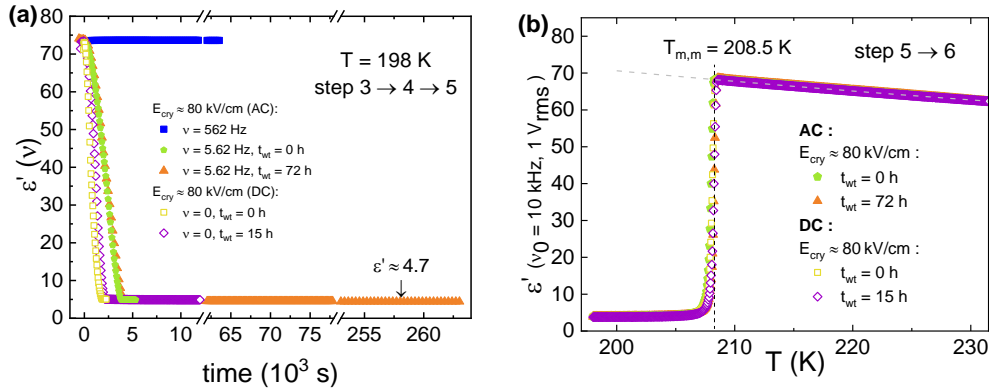

Figure 21. (a) Time-dependent changes in dielectric permittivity ε' at a frequency $v = 5.62$ Hz recorded for VEC in the presence of an ac-field E_{cry} as indicated in the legend for protocol D. After completing crystallization, there is an additional waiting time t_{wt}, during which the ac field with $E_{wt} = E_{cry}$ is still applied. The time dependence of ε' in the range 6 to 3.6 is shown on an enlarged scale in the inset; (b) Temperature dependence of the dielectric permittivity ε' (at $v_0 = 10$ kHz) measured on heating of the crystalline material obtained in the previous step. Results from paper **A2**.

After completing crystallization and additional waiting time at 198 K, the melting behavior of the crystallized material was analyzed. The results presented in Figure 21b show changes of ε' ($v_0 = 10$ kHz) during a temperature scan from 198 to 243 K at a heating rate of about 1 K/min. The dielectric data were recorded within a linear response regime. For the non-field case, only one melting event located at $T_{m1} \approx 227$ K was detected. When the high-field is applied with $t_w = 0$ h, we observe two melting events, one associated with routinely obtained low-field polymorph and the other one, at $T_{m2} \approx 208$ K, related with the field-induced polymorph. The dielectric permittivity of the first melting event is close to 73. However, this value decreases when t_w is increased. For example, after $t_w = 3$ h ε' goes up to around 54, while for $t_w = 8.5$ h it decreases to ~18. The field-induced polymorph melting event eventually disappears for the case when the waiting time is very long, $t_w = 72$ h. Combining together the crystallization and melting behavior results it was concluded that a transformation of the field-induced metastable polymorph to the stable

form takes place with time. It proceeds almost linearly with time. Moreover, the results presented in Figure 21 indicates that the presence of an electric field switched on or off during the waiting time has no impact on the polymorph transformation progress (open symbols refers to t_w in a non-field environment while filled symbols refer to t_w in the presence of high electric field).

With that, we move on to protocol E, shown in Figure 20. As noted before, using this protocol, the growth of ordinary VEC crystals should not be induced. This can be indeed seen by looking at the dielectric data presented in Figure 22a. Only certain frequencies below a characteristic threshold can cause the formation of the new polymorph. For ac field magnitudes of 80 kV/cm and with v = 562 Hz, the crystallization was not observed for up to 22 h. The level of ε' remains the same as for the liquid sample. The same results are observed for VEC sample when following protocol E at no high electric field. However, for lower field frequencies, like v = 5.62 Hz, the crystallization takes place, and the dielectric permittivity decreases from ~73 to 4.7. The same results are observed when dc fields are used. In contrast to the previous protocol, the value of the permittivity is not affected by the additional waiting time.

Figure 22. (a) Time-dependent changes in dielectric permittivity ε' for various frequencies recorded for VEC in the presence of an ac-field E_{cry} as indicated in the legend for protocol E. After crystallization is completed, there is an additional waiting time t_{wt}, during which the ac field amplitude $E_{wt} = E_{cry}$ remains applied; (b) Temperature dependence of the dielectric permittivity ε' (at v_0 = 10 kHz) measured on heating of the crystalline material obtained in the previous crystallization. Results from paper **A2**.

Figure 22b shows the corresponding melting curves for the samples crystallized in the previous step. For both ac and dc cases, there is only one melting event at $T_{m2} \approx$

208 K, related to the field-induced polymorph. This remains unchanged even after a prolonged waiting time. By looking at the crystallization and melting behavior of VEC when following protocol E, it was concluded that the field-induced polymorph, if prepared in the absence of the nuclei of the stable polymorph, does not suffer from a polymorphic transformation with time.

In summary, it was observed, for the first time, using dielectric spectroscopy, that the field-induced polymorph can transform into a stable ordinary VEC crystal with time. Depending on the temperature protocol introduced before crystallization, the field-induced crystals of VEC can be obtained either with high polymorphic purity or mixed with seed crystals of the ordinary stable polymorph. In such as case, polymorphic transition takes place. In contrast, no sign of such transformations is observed when the field-induced crystal structure is obtained in the absence of the ordinary form. Switching the field on/on after crystallization does not have any other impact on the transformation kinetics/stability of the polymorph.

3. CONCLUSIONS AND SUMMARY

This thesis focuses on the effect of a high electric field on the crystallization behavior of the polar molecular liquid, VEC. The aim was to understand better how the external electric field can affect the crystallization tendency of glass-forming systems and control the polymorph formation. This study covers the impact of static electric fields and high alternating fields of different field magnitudes and frequencies.

It was demonstrated that the high electric field favors the formation of a new polymorph with lower melting temperature while at the same time it impedes the growth of the ordinary crystals. The high amplitude of the ac field matched with a certain frequency – from the low-frequency limit - allows the reorientation of crystallites so that their free energy can be lowered by the field. Additionally, changing these parameters facilitates the control over the crystallization time and the morphology of the growing crystals. The analysis of the crystallization kinetics via Avrami equation shows that the crystallization time and Avrami parameter depend on the frequency and ac field amplitude. The sigmoidal shape of obtained dependences indicates limiting behavior for high amplitudes/low frequencies and for low amplitudes/high frequencies. In general, the crystallization results obtained using a high alternating electric field from the established low-frequency limit are consistent with the dc bias fields, where the frequency can be considered as 0 Hz.

The field-induced changes in crystallization will occur only for polar molecules systems that form crystal nuclei with lowered free energy due to the presence of the electrical field. For VEC, this is consistent with the homogeneous nucleation of polar crystals with radii below 3 nm. Faster crystallization observed via dielectric study correlates strongly with the selective formation of the field-induced lower melting polymorph, indicating that electric field promotes a distinct polymorph rather than modifies the crystallization that results in the ordinary and probably nonpolar crystal structure.

This study also provides key experimental data on the impact of the external electric field on the temperature dependence of the crystallization rate. It was observed that when using some frequencies below a certain threshold and higher amplitudes of the applied ac electric field, an additional crystallization rate maximum is formed at lower temperatures. It is associated with the formation of the field-induced polymorph with a distinct melting

temperature. Likewise, high dc fields result in seeing the same effect as when the alternating electric field of very low frequencies is applied. For the crystallization rate maximum located at higher temperatures, the electric field parameters, such as frequency and amplitude, do not affect its location. Nevertheless, they are responsible for a slight increase in the overall crystallization rate. The morphology of the growing crystal was found to not be affected by the frequency of the ac field. In turn, it depends on the magnitude of the electric field as well as the crystallization temperature. From the melting curves, it is possible to conclude that the quantity of the field-induced polymorph can be controlled by changing the magnitude and the frequency of the applied field.

As a final point, this thesis covers the problem of the field-induced polymorph stability and transformation from the field-induced metastable to the stable ordinary polymorph. The field-induced metastable polymorph can be formed at 198 K. On the condition that there are no ordinary crystal nuclei in the crystallizing material, the field-induced polymorph can be obtained with high polymorphic purity and stability. However, this can change dramatically when the nuclei of the stable polymorph are present in the system. In such a case, a polymorphic transformation from the field-induced metastable polymorph to the stable polymorph is observed. Such transformation takes place almost linearly with time. It cannot be affected in any other way by the high electric field, switched on or off. The use of dielectric spectroscopy to monitor such polymorphic transformation in real-time was reported for the first time.

The most important scientific achievements of this thesis can be summarized as

1. Characterizing how the magnitude and frequency of high ac electric field affect the crystallization behavior of a simple molecular liquid. This happens only under certain conditions, i.e., when using sufficiently high field amplitudes matched with the specific frequency that allow aligning crystal nuclei with sizes much larger than the molecules.

2. Demonstrating that the use of a high alternating electric field of very low frequencies results in seeing a similar effect on crystallization as when high dc bias fields are applied. Confirm that the nucleation rather than the crystal growth rate is mainly affected at high electric fields.

3. Showing that the dielectric spectroscopy can be successfully used in the real-time of the experiment to follow the polymorphic transition from the field-induced metastable

to the stable crystal structure. Interestingly, such transformation was found to take place in the presence of the nuclei of the stable polymorph.

4. Providing first experimental data which demonstrate the effect of high electric field on the overall crystallization kinetics in a wide temperature range for a molecular system with the field-induced polymorphism.

The information that a high electric field can suppress the formation of one polymorph in favor of a completely different one opens new paths in pharmaceutical science and material engineering, constantly looking for better strategies to control and tune the crystallization propensity of molecular systems.

Regrettably, it is not able to provide a more in-depth molecular understanding of the interplay between the effect of the external field and crystallization temperature. The specific frequency threshold seen when using high ac fields pointed toward the field-induced crystal nuclei being macroscopically polarized. Such conjecture requires, however, the analysis of the crystal structure. However, the final crystallization product of VEC melts at sub-ambient temperatures, which practically limits the options of in-situ studies of the structure. Nevertheless, the original results gained from this study provide an essential experimental piece of work that can guide future reach aimed to utilize high electric fields to control the crystallization behavior of different polar materials. The upcoming research will involve looking for some other polar molecular materials with higher values of the melting points and various crystal structures that can be potentially oriented by the electric field.

Finally, it should be noted here that the field-induced changes in the crystallization behavior of VEC are completely reversible. Heating the field-induced polymorph above its melting temperature results in recovering the pure liquid state of the same properties as before applying the electric field. Therefore, each time after the melting process, the static dielectric constant of the initial liquid sample was recovered. The same applies to glass transition dynamics. In addition to that, whenever needed, the ordinary polymorph - that melts at T_{m1}- can be obtained in the absence of a high electric field. For that, one needs to cool down a liquid sample close to T_g to promote nucleation of the ordinary form. Switching the high electric field will immediately favor the growth of the field-induced polymorphic form of VEC.

REFERENCES

(1)   Aber, J. E.; Arnold, S.; Garetz, B. A.; Myerson, A. S. Strong Dc Electric Field Applied to Supersaturated Aqueous Glycine Solution Induces Nucleation of the γ Polymorph. *Phys. Rev. Lett.* **2005**, *94* (14), 145503.

(2)   Di Profio, G.; Reijonen, M. T.; Caliandro, R.; Guagliardi, A.; Curcio, E.; Drioli, E. Insights into the Polymorphism of Glycine: Membrane Crystallization in an Electric Field. *Phys. Chem. Chem. Phys.* **2013**, *15* (23), 9271.

(3)   Jha, P. K.; Sadot, M.; Vino, S. A.; Jury, V.; Curet-Ploquin, S.; Rouaud, O.; Havet, M.; Le-Bail, A. A Review on Effect of DC Voltage on Crystallization Process in Food Systems. *Innov. Food Sci. Emerg. Technol.* **2017**, *42*, 204–219.

(4)   Haleblian, J.; McCrone, W. Pharmaceutical Applications of Polymorphism. *J. Pharm. Sci.* **1969**, *58* (8), 911–929.

(5)   Lendlein, A.; Kelch, S. Shape-Memory Effect. *Angew. Chemie Int. Ed* **2002**, *41*, 2034–2057.

(6)   Gutzow, I. S.; Schmelzer, J. W. P. *The Vitreous State*, 2nd ed.; Springer Berlin Heidelberg: Berlin, Heidelberg, 2013.

(7)   Adrjanowicz, K.; Paluch, M.; Richert, R. Formation of New Polymorphs and Control of Crystallization in Molecular Glass-Formers by Electric Field. *Phys. Chem. Chem. Phys.* **2018**, *20* (2), 925–931.

(8)   Anwar, J.; Zahn, D. Polymorphic Phase Transitions: Macroscopic Theory and Molecular Simulation. *Adv. Drug Deliv. Rev.* **2017**, *117*, 47–70.

(9)   Bauer, J.; Spanton, S.; Henry, R.; Quick, J.; Dziki, W.; Porter, W.; Morris, J. Ritonavir: An Extraordinary Example of Conformational Polymorphism. *Pharm. Res. 2001 186* **2001**, *18* (6), 859–866.

(10)   Morissette, S. L.; Soukasene, S.; Levinson, D.; Cima, M. J.; Almarsson, O. Elucidation of Crystal Form Diversity of the HIV Protease Inhibitor Ritonavir by High-Throughput Crystallization. *Proc. Natl. Acad. Sci.* **2003**, *100* (5), 2180–2184.

(11)   Rasmussen, S. C. *How Glass Changed the World*; SpringerBriefs in Molecular Science; Springer Berlin Heidelberg: Berlin, Heidelberg, 2012; Vol. 3.

(12)   Debenedetti, P. G.; Stillinger, F. H. Supercooled Liquids and the Glass Transition. *Nature* **2001**, *410* (6825), 259–267.

(13)   Ediger, M. D.; Angell, C. A.; Nagel, S. R. Supercooled Liquids and Glasses. *J. Phys. Chem.* **1996**, *100* (31), 13200–13212.

(14) Taylor, L. S. Physical Stability and Crystallization Inhibition. In *Pharmaceutical Sciences Encyclopedia*; John Wiley & Sons, Inc.: Hoboken, NJ, USA, 2015; pp 1–39.

(15) Schmelzer, J. W. P. Crystal Nucleation and Growth in Glass-Forming Melts: Experiment and Theory. *J. Non. Cryst. Solids* **2008**, *354* (2–9), 269–278.

(16) Bhugra, C.; Pikal, M. J. Role of Thermodynamic, Molecular, and Kinetic Factors in Crystallization from the Amorphous State. *J. Pharm. Sci.* **2008**, *97* (4), 1329–1349.

(17) Taleb, M.; Didierjean, C.; Jelsch, C.; Mangeot, J. . P.; Capelle, B.; Aubry, A. Crystallization of Proteins under an External Electric Field. *J. Cryst. Growth* **1999**, *200* (3–4), 575–582.

(18) Taleb, M.; Didierjean, C.; Jelsch, C.; Mangeot, J. .; Aubry, A. Equilibrium Kinetics of Lysozyme Crystallization under an External Electric Field. *J. Cryst. Growth* **2001**, *232* (1–4), 250–255.

(19) Nanev, C. N.; Penkova, A. Nucleation of Lysozyme Crystals under External Electric and Ultrasonic Fields. *J. Cryst. Growth* **2001**, *232* (1–4), 285–293.

(20) Parks, C.; Koswara, A.; Tung, H.-H.; Nere, N.; Bordawekar, S.; Nagy, Z. K.; Ramkrishna, D. Molecular Dynamics Electric Field Crystallization Simulations of Paracetamol Produce a New Polymorph. *Cryst. Growth Des.* **2017**, *17* (7), 3751–3765.

(21) Koizumi, H.; Fujiwara, K.; Uda, S. Control of Nucleation Rate for Tetragonal Hen-Egg White Lysozyme Crystals by Application of an Electric Field with Variable Frequencies. *Cryst. Growth Des.* **2009**, *9* (5), 2420–2424.

(22) Ganguly, R.; Bandyopadhyay, S.; Miriyala, K.; Gunasekaran, V.; Bhattacharya, S.; Acharyya, A.; Ramadurai, R. Tunable Polarization Components and Electric Field Induced Crystallization in Polyvinylidenefluoride: A Piezo Polymer. *Polym. Cryst.* **2019**, *2* (1), e10027.

(23) Rodríguez-Hornedo, N.; Murphy, D. Significance of Controlling Crystallization Mechanisms and Kinetics in Pharmaceutical Systems. *Journal of Pharmaceutical Sciences*. American Chemical Society July 1, 1999, pp 651–660.

(24) Bernstein, J. Polymorphism - A Perspective. *Cryst. Growth Des.* **2011**, *11* (3), 632–650.

(25) Cruz-Cabeza, A. J.; Bernstein, J. Conformational Polymorphism. *Chem. Rev.* **2014**, *114* (4), 2170–2191.

(26) Ostwald, W. Studien Über Die Bildung Und Umwandlung Fester Körper. *Zeitschrift für Phys. Chemie* **1897**, *22U* (1).

(27) Threlfall, T. Structural and Thermodynamic Explanations of Ostwald's Rule. *Org. Process Res. Dev.* **2003**, *7* (6), 1017–1027.

(28) Byrn, S.; Zografi, G.; Chen, X. *Solid-State Properties of Pharmaceutical Materials*; Wiley, 2017.

(29) Kremer, F.; Schönhals, A. *Broadband Dielectric Spectroscopy*; Kremer, F., Schönhals, A., Eds.; Springer Berlin Heidelberg, 2003.

(30) Lunkenheimer, P.; Schneider, U.; Brand, R.; Loid, A. Glassy Dynamics. *Contemp. Phys.* **2000**, *41* (1), 15–36.

(31) Lunkenheimer, P.; Loidl, A. Dielectric Spectroscopy of Glass-Forming Materials: α-Relaxation and Excess Wing. *Chem. Phys.* **2002**, *284* (1–2), 205–219.

(32) Richert, R. Frequency Dependence of Dielectric Saturation. *Phys. Rev. E* **2013**, *88* (6), 062313.

(33) Herweg, J. Die Elektrischen Dipole in Flüssigen Dielektricis. *Zeitschrift für Phys.* **1920**, *3* (1), 36–47.

(34) Richert, R. Nonlinear Dielectric Effects in Liquids: A Guided Tour. *J. Phys. Condens. Matter* **2017**, *29* (36), 363001.

(35) Jedrzejowska, A.; Wojnarowska, Z.; Adrjanowicz, K.; Ngai, K. L.; Paluch, M. Toward a Better Understanding of Dielectric Responses of van Der Waals Liquids: The Role of Chemical Structures. *J. Chem. Phys.* **2017**, *146* (9), 094512.

(36) Adrjanowicz, K.; Richert, R. Control of Crystallization Pathways by Electric Fields. In *Dielectrics and crystallization*; Springer, 2020; pp 149–167.

(37) Jensen, M. H.; Alba-Simionesco, C.; Niss, K.; Hecksher, T. A Systematic Study of the Isothermal Crystallization of the Mono-Alcohol n-Butanol Monitored by Dielectric Spectroscopy. *J. Chem. Phys.* **2015**, *143* (13), 134501.

(38) Mijovic, J.; Sy, J.-W.; Kwei, T. K. Reorientational Dynamics of Dipoles in Poly(Vinylidene Fluoride)/Poly(Methyl Methacrylate) (PVDF/PMMA) Blends by Dielectric Spectroscopy. *Macromolecules* **1997**, *30* (10), 3042–3050.

(39) Avrami, M. Kinetics of Phase Change. I General Theory. *J. Chem. Phys.* **1939**, *7* (12), 1103–1112.

(40) Avrami, M. Kinetics of Phase Change. II Transformation-Time Relations for Random Distribution of Nuclei. *J. Chem. Phys.* **1940**, *8* (2), 212–224.

FULL TEXT OF PUBLICATIONS CONSTITUTING THE THESIS

Letter

Frequency of the AC Electric Field Determines How a Molecular Liquid Crystallizes

Daniel M. Duarte, Ranko Richert, and Karolina Adrjanowicz*

Read Online

ACCESS | | Metrics & More | | Article Recommendations

ABSTRACT: The ability to control crystallization is of central importance to many technologies and pharmaceutical materials. Electric fields have been shown to impact crystallization, but little is known about the mechanism of such effects. Here we report on our observations of how the frequency of an external electric (ac) field changes the crystallization rate and the partitioning into distinct polymorphs of vinylethylene carbonate. We find that the field effects are pronounced only for frequencies below a certain threshold, which is orders of magnitude below that characterizing molecular orientation but consistent with the reorientation of polar crystal nuclei of radius $r < 3$ nm. We conclude that the electric field opens an additional nucleation pathway by lowering the free-energy barrier to form a polymorph that melts at a temperature ∼20 K below that of the ordinary crystal. This lower melting polymorph is not obtained at zero electrical field.
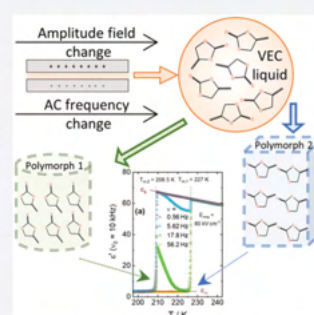
Crystallization is an important aspect of materials science, numerous technologies, and pharmaceutical applications. Understanding the parameters that affect crystallization is critical either to enhance crystallization rates or to avoid this phase transition to an ordered solid when a supercooled or glassy material is desired. In case a compound can crystallize into two or more distinct crystal structures, that is, in the case of polymorphic solids, it is important to understand how the crystallization process can be tuned toward or away from a certain polymorph. In general, distinct polymorphs of the same molecular compound differ with respect to their solubility, bioavailability, and shelf life, with implications for medicinal use.

A number of experimental as well as theoretical studies have revealed that a sufficiently high electric field affects crystallization.[1−9] The mechanisms considered for the origin of these field effects include contributions from field-dependent thermodynamic potentials[10−12] and from field-induced orientations.[13,14] Whereas the existence of the impact of electric fields on the crystallization rate and the polymorph outcome is well established, there is little experimental evidence that helps one decide which mechanism is at the origin of this field effect.

Recently, the field-induced crystallization of a pure dipolar liquid, vinyl ethylene carbonate (VEC), has been studied using static electric fields in the 40−210 kV cm^{-1} amplitude range. That study demonstrated a field-induced increase in the crystallization rate of VEC by more than a factor of 10, and it showed that static fields give rise to a previously unknown polymorph that melts at a temperature located ∼20 K below the ordinary melting temperature.[15] However, the path by which the electric field promoted this new polymorph of VEC remained unclear.

In the present work, we address the origin of such field effects by studying the dependence of crystallization outcomes on the frequency of the alternating (ac) electric fields that the sample is subjected to. Our main observation is that the field-induced change in crystallization behavior sets in only for frequencies that are at least 5 decades below the peak frequency, ν_{max}, of the dielectric loss that characterizes the molecular reorientation time, τ_α. From this unexpected frequency dependence, we conclude that the most likely source of this effect is the field-assisted orientation of small ($r < 3$ nm) crystallites, whose free-energy reduction in the presence of a field assists the nucleation process of that lower melting polymorph by virtue of their polar structure.

The low-field (linear response regime) dielectric spectra, $\varepsilon'(\nu)$ and $\varepsilon''(\nu)$, for VEC at the crystallization temperature $T = 198$ K are depicted in Figure 1. At this temperature, the primary (α) structural relaxation process is characterized by a peak at $\nu_{max} = 2 \times 10^5$ Hz, equivalent to a peak relaxation time of $\tau_{max} = 8 \times 10^{-7}$ s. The signature of dc conductivity is the increase in ε'' for $\nu < 10^3$ Hz, and the increase in ε' below $\nu \approx 1$ Hz indicates electrode polarization.
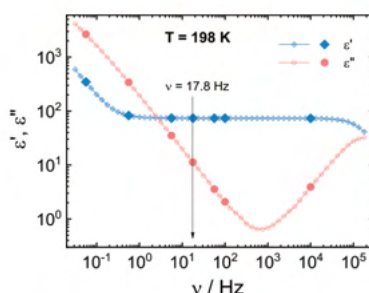
Figure 1. Linear response ($E_{rms} < 10$ kV cm^{-1}) dielectric susceptibility of VEC at $T = 198$ K. The ε'' peak near $\nu = 2 \times 10^5$ Hz originates from the primary (α) structural relaxation. The increase in ε'' for $\nu < 10^3$ Hz is the result of dc conductivity. The increase in ε' below $\nu \approx 1$ Hz indicates electrode polarization. Solid symbols identify frequencies used for high electric field experiments shown later.
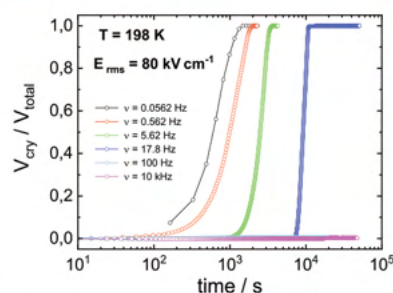
Figure 2. Isothermal crystallization of VEC after cooling the melt, reported as the volume fraction of crystalline material, V_{cry}/V_{total}. After reaching $T = 198$ K, the sample is exposed to an ac electrical field of $E_{rms} = 80$ kV cm^{-1} at different frequencies ν, as indicated. For frequencies $\nu \geq 100$ Hz, no crystallization is observed during the first 50 000 s.

In the absence of a high electric field, the crystallization progress is monitored via the real part of permittivity, $\varepsilon'(\nu_0)$, with the fixed frequency $\nu_0 = 10$ kHz, selected such that $\varepsilon'(\nu_0)$ represents the static dielectric constant, ε_s, of the liquid. The basis for assessing crystallization via dielectric techniques is that the dielectric constant, ε_s, of polar liquids is governed by the rotational motion of permanent dipoles, which is suppressed in the crystalline state. Thus, as a good approximation,[16−18] this value of ε' gauges the crystal (V_{cry}/V_{total}) or liquid (V_{liq}/V_{total}) volume fraction according to

$$V_{cry}/V_{total} = (\varepsilon_s - \varepsilon')/(\varepsilon_s - \varepsilon_\infty) \tag{1a}$$

$$V_{liq}/V_{total} = (\varepsilon' - \varepsilon_\infty)/(\varepsilon_s - \varepsilon_\infty) \tag{1b}$$

Here the value of ε_∞ is understood as the permittivity of the crystalline state. In the liquid state, ε_∞ represents the high frequency limit of permittivity, that is, in the absence of orientational contributions from permanent dipoles. Its magnitude is thus governed by the molecular electronic polarizability and density, values that are very similar in both the crystalline and the liquid states. To monitor the progress of crystallization of a sample subjected to a high field, sinusoidal fields with frequencies 50 mHz $\leq \nu \leq 10$ kHz and root-mean-square (rms) amplitudes between 60 and 180 kV cm^{-1} were used. All crystallization curves were recorded isothermally at $T = 198$ K, a temperature situated between the glass-transition temperature $T_g = 171$ K and the regular melting temperature at $T_m = 227$ K.[15] Prior to cooling to $T = 198$ K, the sample had been melted by holding it at $T = 243$ K ($= T_m + 16$ K) for at least 30 min.

The effect of the frequency of an ac field with amplitude $E_{rms} = 80$ kV cm^{-1} on the crystallization rate is depicted as V_{cry}/V_{total} versus log t curves in Figure 2. At a frequency $\nu = 100$ Hz or higher, no significant crystallization is observed for times up to 50 000 s ($\sim$14 h). However, at the somewhat lower frequency of $\nu = 18$ Hz, crystallization is practically complete after 10 000 s, and at $\nu = 56$ mHz, the crystallization rate has increased by another factor of 10. Consistent with the frequency dependence at a field of $E_{rms} = 80$ kV cm^{-1} outlined in Figure 2, the crystallization curve at the same field for $\nu = 56$ Hz shown in Figure 3 indicates completion at $\sim$20 000 s, that is, twice as long as the 18 Hz case. Moreover, Figure 3 indicates that the crystallization rate at a fixed frequency of $\nu = $
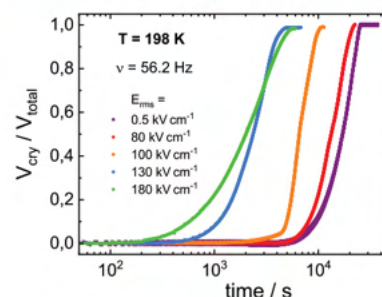
Figure 3. Isothermal crystallization of VEC after cooling the melt, reported as the volume fraction of crystalline material, V_{cry}/V_{total}. After reaching $T = 198$ K, the sample is exposed to an ac electrical field of frequency $\nu = 56.2$ Hz at different field amplitudes E_{rms}, as indicated.

56 Hz can be tuned a factor of about ten by changing the field amplitude from 80 to 180 kV cm^{-1}.

Among others, the crystallization curves of Figures 2 and 3 have been analyzed in terms of the Avrami relation[19,20]

$$V_{cry}/V_{total} = 1 - \exp[-(t/\tau_{cry})^n] \tag{2}$$

Here τ_{cry} is the characteristic crystallization time and n is the exponent that depends on the dimensionality and geometry of crystal growth. The time t is taken to start at the onset of crystallization, thus disregarding the incubation time of the process. The resulting respective dependencies of τ_{cry} on frequency ν and on field amplitude E_{rms} are compiled in Figure 4, with all data referring to crystallization at $T = 198$ K after cooling the liquid from $T > T_m$. Note that τ_{cry} is associated with an effective rate that includes the zero-field and the field-induced paths to the crystal state.

The field amplitude and frequency impact not only the rate of crystallization but also the polymorph obtained by crystallization. This is demonstrated in Figure 5 by melting curves measured at a very low field ($E_{rms} = 0.5$ kV cm^{-1}) at a fixed frequency of $\nu_0 = 10$ kHz by scanning the temperature from the crystallization temperature of $T = 198$ K to a value of $T = 243$ K, where the liquid state of VEC is recovered. The curves for selected frequencies and field amplitudes indicate that low frequencies or a high field (where τ_{cry} is small) lead to a large volume fraction of the lower melting polymorph, with $T_{m,2} = 208.5$ K. This large amount of the field-induced crystal

47
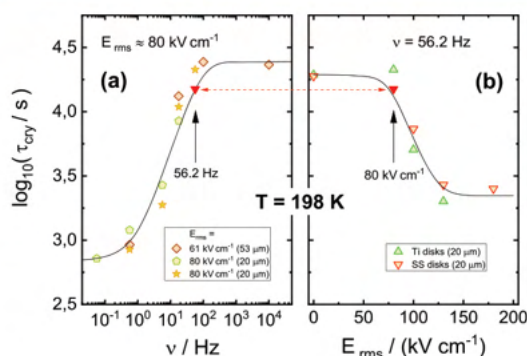
Figure 4. Time constants τ_{cry} characterizing the rate of the crystallization process of VEC at T = 198 K. (a) Frequency dependence of τ_{cry} at a practically constant field of $E_{rms} \approx 80$ kV cm^{-1}. (b). Field amplitude dependence of τ_{cry} at a constant frequency of ν = 56.2 Hz. The E_{rms} = 80 kV cm^{-1} data point of panel b is reproduced in panel a to show consistency.
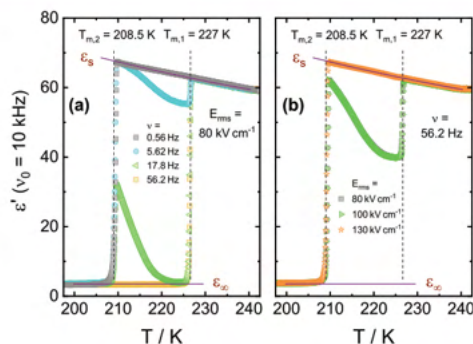
Figure 5. Melting curves of previously crystallized VEC in terms of the permittivity ε' measured at a frequency ν = 10 kHz upon scanning temperature from 198 to 245 K at a rate of 1 K min^{-1}. Crystallization at T = 198 K has been field-induced using various conditions: (a) at a fixed field of E_{rms} = 80 kV cm^{-1} for a range of frequencies and (b) at a fixed frequency of 56.2 Hz for a range of fields, as indicated in the legends. Lines labeled ε_s and ε_∞ refer to the dielectric constants in the limits of low and high frequencies, respectively. At each temperature, the liquid volume fraction is given by $V_{liq}/V_{total} = (\varepsilon' - \varepsilon_\infty)/(\varepsilon_s - \varepsilon_\infty)$.

shows in Figure 5 as ε' rising a significant fraction of the ε_∞ to ε_s interval, cf. eqs 1a and 1b. The recrystallization seen as a drop in ε' for $T > T_{m,2}$ is a matter of the amount of nuclei or crystallites leading to the higher melting polymorph with $T_{m,1}$ = 227 K (equal to the standard melting point T_m = 227 K). Only for the zero-field case in Figure 5a is the melting curve free of a signature of the low melting polymorph. On the contrary, a field of E_{rms} = 180 kV cm^{-1} at ν = 56 Hz yields only the low melting polymorph (see Figure 5b), with no recrystallization due to the lack of nuclei that could form the high melting polymorph.

The present polar and glass-forming material, VEC, has been characterized in detail regarding its low-field (linear response) dielectric properties and structural relaxation.[21,22] With respect to the crystallization behavior of VEC, it had already been shown that dc fields between 40 and 210 kV cm^{-1} accelerate the crystallization rate and lead to a polymorph whose melting point is ~20 K below that of the ordinary crystal, which is

formed at zero electric field.[15] As a result, it is not surprising that similar changes in crystallization outcomes can be achieved with alternating fields (at zero bias) of similar magnitudes, which is what the present results demonstrate. The novel information on this study lies in the unexpected frequency dependence of the field effect. At the crystallization temperature of T = 198 K, the molecular reorientation process of this polar liquid is characterized by a dielectric peak at ν_{max} = 2×10^5 Hz. Thus one may expect the absence of a considerable field effect for frequencies in excess of ν_{max} but field-assisted crystallization for $\nu < \nu_{max}$ that is similar to the dc field case previously reported.[15] Instead, Figure 4a reveals that the field effect (at E_{rms} = 80 kV cm^{-1}) becomes considerable at or below about 20−50 Hz, that is, five orders of magnitude below the loss peak at ν_{max} = 200 kHz; see Figure 1. The low frequency of 20 Hz is still a safe distance from electrode polarization with an onset frequency of ~1 Hz. Moreover, if space charge accumulation observed as electrode polarization was at the origin of this field effect, then the impact of a dc field should exceed that for ac fields, which is not observed.

To understand this frequency dependence shown in Figures 2 and 4a, we consider the possibility that the orientation of particles larger than the molecules is responsible for only low frequencies modifying the crystallization process. To clarify this idea, we use the Stokes−Einstein−Debye (SED) relation to establish a connection between the experimentally determined viscosity of VEC at the crystallization temperature and the rotation time for a given particle size

$$\tau_{rot} = \frac{4\pi\eta r^3}{k_B T} \tag{3}$$

With the parameters T = 198 K and η = 70 Pa s and translating the onset frequency of $\nu \approx 18$ Hz to $\omega = 2\pi\nu$ = 110 Hz and further to $\tau_{rot} = 1/\omega$ = 8.8 ms, a particle radius of r = 3 nm is estimated to match the frequency $\nu \approx 18$ Hz according to SED hydrodynamics. This onset frequency is determined from Figure 3a as the frequency below which the crystallization rate is systematically affected by the field, namely, data at ν = 17.8 Hz. This is consistent with aligning or agitating low-melting polymorph crystal nuclei of radii $r < 3$ nm, provided these crystallites possess a net permanent dipole moment μ. Another requirement is that these crystallites are able to rotate to lower their free energy via an external field, namely, the angular term $\mu E \cos \theta$ in the potential energy.[23] This would not be the case with heterogeneous nucleation. In the present case, homogeneous nucleation seems more likely, as the use of titanium (Ti) versus the more highly polished stainless-steel (SS) electrodes (majority of surface) shows very similar crystallization behavior, except for very long crystallization times. Moreover, increasing the sample volume by a factor of 2.65 by changing the electrode separation from d = 20 to 53 μm has little effect.

Apart from the onset frequency information ($\nu \approx 18$ Hz), Figure 4 suggests that frequency (at a given field of E_{rms} = 80 kV cm^{-1}) modifies the rate of crystallization by a factor of about 30 that separate the high and low frequency plateau values for τ_{cry}, 25 000 and 800 s, respectively. The low rate (high τ_{cry}) level is near the field free case, whereas the high rate (low τ_{cry}) is likely a matter of the crystal growth rate and its limitation due to transport coefficients at T = 198 K, such as viscosity. Within the transition frequency range, increasing the field amplitude can accelerate crystallization, as shown in

48

Figure 4b. Of course, these results on the rates of crystallization do not specify which fractions of the two distinct polymorphs are being formed. To answer this question, melting curves were recorded after crystallization had practically completed, that is, when $V_{cry} = V_{total}$.

Melting curves are recorded at a low field and fixed frequency $\nu_0 = 10$ kHz, so that $\varepsilon'(T)$ gauges the liquid volume fraction according to eq 1b. A set of $\varepsilon'(T)$ melting curves are compiled in Figure 5a, measured after the sample crystallized while exposed to a fixed field amplitude of $E_{rms} = 80$ kV cm^{-1} but with various frequencies ν. For a relatively high frequency of 56.2 Hz, where the crystallization rate is modified only marginally relative to the zero-field case, only the ordinary crystal that melts at $T_{m,1} = 227$ K is formed, as no melting event is observed for $T < T_{m,1}$. As the frequency is lowered toward values that result in significant elevations of the crystallization rate, an increase in the volume fraction that melts already at $T_{m,2} = 208.5$ K is seen in Figure 5a. In the case of $\nu = 17.8$ Hz, ~46% of the material melts at $T_{m,2}$, which then rapidly recrystallizes due to the large amount of ordinary crystals that melt at $T_{m,1}$. For the two lowest frequencies, $\nu = 5.62$ and 0.56 Hz, practically 100% of the sample melts at the lower temperature $T_{m,2}$. Still, the $\nu = 0.56$ Hz curve reveals a higher volume fraction of the lower melting crystal via the diminished recrystallization for $T > 208.5$ K, which is indicative of a smaller amount of ordinary crystallites. Analogous to this frequency dependence of Figure 5a, the melting curves for different field amplitudes in Figure 5b also point toward a larger fraction of the low-melting field-induced polymorph for situations in which the crystallization rate is faster. This suggests that the crystallization rate of the low-melting polymorph depends on the amplitude and frequency of the strong electric field, whereas the ordinary high-melting polymorph crystallization rate is largely field invariant. In turn, this implies that the field effect on the crystallization rate is matter of adding a further crystallization route leading to the low-melting polymorph rather than impacting the nucleation or crystallization of the ordinary polymorph that melts at $T_m = 227$ K.

In summary, we have observed the overall crystallization rate and the resulting volume fractions of the ordinary and field-induced polymorphs of vinylethylene carbonate while the sample is subjected to electric fields of varying amplitudes and frequencies. Only for sufficiently high field amplitudes and for frequencies below a certain threshold does the field modify the crystallization behavior toward faster rates and toward favoring a lower melting polymorph that is not observed in the absence of an external electric field. Compatible with calculations,[12] the results suggest that the field acts via lowering the free energy of formation of crystal nuclei by their orientation along the field, a picture consistent with the homogeneous nucleation of polar crystals with radii below ~3 nm. Situations of faster crystallization correlate strongly with the selective formation of the field-induced lower melting polymorph, indicating that the field opens a new path to a distinct polymorph rather than modifying the crystallization that results in the ordinary and probably nonpolar crystal structure. In conclusion, the amplitude and frequency of external electric fields may serve as new strategies for controlling and tuning crystallization outcomes in the context of materials engineering and pharmaceutical applications.

METHODS

The compound 4-vinyl-1,3-dioxolan-2-one or VEC was supplied by Sigma-Aldrich (purity 99%, CAS no. 4427-96-7) and used as received. VEC is a vinyl derivative of propylene carbonate (PC) and is sometimes referred to as "vinyl-PC". The liquid is loaded into a high-field capacitor cell described in detail in a previous publication.[15] The polished parallel disk pairs are made of SS or Ti and are separated by a Teflon ring of $d = 25$ or 50 μm nominal thickness, leaving an active inner electrode surface area of $r = 7$ mm radius. For the $d = 25$ μm spacer, the geometric capacitance is $C_{geo} = \varepsilon_0 \pi r^2/d = 54.5$ pF. By comparing the observed permittivity, $\varepsilon = \varepsilon' - i\varepsilon''$, with reference data, the actual electrode separations were determined to be 20 and 53 μm. The temperature regulation of the sample cell was achieved by a Novocontrol Quatro temperature control system.

For dielectric measurements using large ac electric fields, a Trek PZD-700 high-voltage amplifier boosts the output voltage of a Solartron SI-1260 gain-phase analyzer by a factor of 200. The current was determined from the voltage drop across a calibrated RC-shunt connected to the analyzer via a buffer amplifier that tolerates voltages of up to $500V_p$, employed to protect the system from sample failure. This setup facilitates dielectric response measurements within the frequency range from 30 mHz to 200 kHz at low fields and for frequencies of 30 mHz to 120 kHz for fields up to 240 kV cm^{-1}.

AUTHOR INFORMATION

Corresponding Author

Karolina Adrjanowicz — *Institute of Physics, University of Silesia, 41-500 Chorzow, Poland; Silesian Center for Education and Interdisciplinary Research (SMCEBI), 41-500 Chorzow, Poland;* orcid.org/0000-0003-0212-5010; Email: kadrjano@us.edu.pl

Authors

Daniel M. Duarte — *Institute of Physics, University of Silesia, 41-500 Chorzow, Poland; Silesian Center for Education and Interdisciplinary Research (SMCEBI), 41-500 Chorzow, Poland;* orcid.org/0000-0002-8230-0255

Ranko Richert — *School of Molecular Sciences, Arizona State University, Tempe, Arizona 85287, United States;* orcid.org/0000-0001-8503-3175

Complete contact information is available at:
https://pubs.acs.org/10.1021/acs.jpclett.0c01002

Notes

The authors declare no competing financial interest.

REFERENCES

(1) Evans, G. J. Crystal Growth in Electric Fields. *Mater. Lett.* **1984**, *2* (5), 420−423.

(2) Kotsuki, K.; Obata, S.; Saiki, K. Electric-Field-Assisted Position and Orientation Control of Organic Single Crystals. *Langmuir* **2014**, *30* (47), 14286−14291.

49

(3) Parks, C.; Koswara, A.; Tung, H.-H.; Nere, N.; Bordawekar, S.; Nagy, Z. K.; Ramkrishna, D. Molecular Dynamics Electric Field Crystallization Simulations of Paracetamol Produce a New Polymorph. *Cryst. Growth Des.* **2017**, *17* (7), 3751−3765.

(4) Taleb, M.; Didierjean, C.; Jelsch, C.; Mangeot, J.; Capelle, B.; Aubry, A. Crystallization of Proteins under an External Electric Field. *J. Cryst. Growth* **1999**, *200* (3−4), 575−582.

(5) Hammadi, Z.; Veesler, S. New Approaches on Crystallization under Electric Fields. *Prog. Biophys. Mol. Biol.* **2009**, *101* (1−3), 38−44.

(6) Nanev, C. N.; Penkova, A. Nucleation of Lysozyme Crystals under External Electric and Ultrasonic Fields. *J. Cryst. Growth* **2001**, *232* (1−4), 285−293.

(7) Aber, J. E.; Arnold, S.; Garetz, B. A.; Myerson, A. S. Strong Dc Electric Field Applied to Supersaturated Aqueous Glycine Solution Induces Nucleation of the γ Polymorph. *Phys. Rev. Lett.* **2005**, *94* (14), 145503.

(8) Di Profio, G.; Reijonen, M. T.; Caliandro, R.; Guagliardi, A.; Curcio, E.; Drioli, E. Insights into the Polymorphism of Glycine: Membrane Crystallization in an Electric Field. *Phys. Chem. Chem. Phys.* **2013**, *15* (23), 9271.

(9) Gutzow, I. S.; Schmelzer, J. W. P. *The Vitreous State - Thermodynamics, Structure, Rheology, and Crystallizationr*, 2nd ed.; Springer-Verlag, 2013.

(10) Kashchiev, D. Nucleation in External Electric Field. *J. Cryst. Growth* **1972**, *13−14* (C), 128−130.

(11) Kashchiev, D. On the Influence of the Electric Field on Nucleation Kinetics. *Philos. Mag.* **1972**, *25* (2), 459−470.

(12) Isard, J. O. Calculation of the Influence of an Electric Field on the Free Energy of Formation of a Nucleus. *Philos. Mag.* **1977**, *35* (3), 817−819.

(13) Gattef, E.; Dimitriev, Y. Reversible Monopolar Switching in Vanadium-Tellurite Glass Threshold Devices. *Philos. Mag. B* **1979**, *40* (3), 233−242.

(14) Gattef, E.; Dimitriev, Y. Nucleation Theory of Threshold Switching in Vanadate-Glass Devices. *Philos. Mag. B* **1981**, *43* (2), 333−343.

(15) Adrjanowicz, K.; Paluch, M.; Richert, R. Formation of New Polymorphs and Control of Crystallization in Molecular Glass-Formers by Electric Field. *Phys. Chem. Chem. Phys.* **2018**, *20* (2), 925−931.

(16) Mijovic, J.; Sy, J.-W.; Kwei, T. K. Reorientational Dynamics of Dipoles in Poly(Vinylidene Fluoride)/Poly(Methyl Methacrylate) (PVDF/PMMA) Blends by Dielectric Spectroscopy. *Macromolecules* **1997**, *30* (10), 3042−3050.

(17) Jensen, M. H.; Alba-Simionesco, C.; Niss, K.; Hecksher, T. A Systematic Study of the Isothermal Crystallization of the Mono-Alcohol n-Butanol Monitored by Dielectric Spectroscopy. *J. Chem. Phys.* **2015**, *143* (13), 134501.

(18) Adrjanowicz, K.; Richert, R. Control of Crystallization Pathways by Dielectric Fields. In *Dielectrics and Crystallization*; Springer, 2020.

(19) Avrami, M. Kinetics of Phase Change. I General Theory. *J. Chem. Phys.* **1939**, *7* (12), 1103−1112.

(20) Avrami, M. Kinetics of Phase Change. II Transformation-Time Relations for Random Distribution of Nuclei. *J. Chem. Phys.* **1940**, *8* (2), 212−224.

(21) Jedrzejowska, A.; Ngai, K. L.; Paluch, M. Modifications of Structure and Intermolecular Potential of a Canonical Glassformer: Dynamics Changing with Dipole-Dipole Interaction. *J. Phys. Chem. A* **2016**, *120* (44), 8781−8785.

(22) Young-Gonzales, A. R.; Adrjanowicz, K.; Paluch, M.; Richert, R. Nonlinear Dielectric Features of Highly Polar Glass Formers: Derivatives of Propylene Carbonate. *J. Chem. Phys.* **2017**, *147* (22), 224501.

(23) Böttcher, C. J. F. *Theory of Electric Polarization*; Elsevier, 1973.

50

Article

Watching the Polymorphic Transition from a Field-Induced to a Stable Crystal by Dielectric Techniques

Daniel M. Duarte, Ranko Richert, and Karolina Adrjanowicz*

ACCESS | Metrics & More | Article Recommendations

ABSTRACT: We prepared a metastable polymorph of vinyl ethylene carbonate by inducing crystallization of the supercooled liquid via an electric field of about 80 kV cm^{-1}. Electric fields with sufficiently low frequencies are required to observe polymorphism for this material. Depending on the temperature protocol prior to crystallization, the field-induced crystal structure can be obtained either with high polymorphic purity or mixed with seed crystals of the ordinary stable polymorph. At the crystallization temperature of T_c = 198 K, the pure field-induced polymorph shows no sign of a polymorphic transition, while at the same temperature, this crystal structure converts to the stable state in a matter of several hours if seeded by the stable polymorph. Interestingly, we find that the permittivity changes linearly with the volume fraction of the field-induced polymorph during the conversion, so that the polymorph transition can be followed in real time by dielectric techniques.
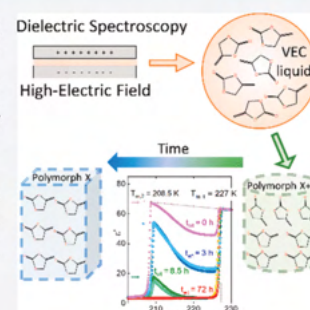
INTRODUCTION

Polymorphs are distinct crystal structures that can be formed by the same chemical compound.[1,2] Numerous examples of polymorphism exist for organic molecular materials.[3−5] For instance, a compound known as ROY for its red, orange, and yellow crystals has seven polymorphs whose structures have been determined,[6] while computational approaches to the structures of this organic molecule suggest the existence of many more.[7] Polymorphic transitions are conversions from one metastable polymorph to a more stable one,[8] while retaining the chemical identity of the material. In the case of enantiotropic polymorphism, temperature affects which structure is the more stable one,[9] i.e., the polymorph with lower free energy. One complication has been recognized already a long time ago by Ostwald,[10,11] namely, that a structural transition will not necessarily proceed to the lowest free energy state in a single step, but is likely to undergo a polymorphic transition that is associated with a smaller change in free energy.

Understanding the existence of polymorphs and the transitions among them is of great importance to materials science and relevant to societal issues in the case of pharmaceuticals. For example, the HIV protease inhibitor ritonavir was found to be subject to a polymorphic transition leading to a structure with highly compromised solubility and thus bioavailability.[12,13] Many other pharmaceuticals, as well as their precursors, are known to display polymorphism.[1,5,6,14,15] Although the molecular chemistry is the same, polymorphs of lower thermodynamic stability are usually associated with higher solubility and rate of dissolution, thus favoring

bioavailability, but the shelf life of that structure might be limited.

The feature that creates different polymorphs in the first place is the variety of thermodynamic paths that impact nucleation and growth kinetics. Commonly, these are the temperature and/or pressure histories that the sample has undergone before settling at ambient conditions, for instance. It may be speculated that every compound is associated with polymorphism, but for many systems the thermodynamic path required to create a novel polymorph has not yet been found.[1] A less common route to forming new polymorphs is by applying an electric field of sufficient magnitude.[16−21]

In the case of vinyl ethylene carbonate (VEC), it has been demonstrated that a field gives rise to a new polymorph that melts about 20 K below the ordinary one and that has not been formed in the absence of a field.[22] Unfortunately, the crystal structures of both polymorphs are not known, because both melt at temperatures far below ambient conditions. In order to discriminate these two structures unambiguously, we label the polymorphs as follows: The polymorph that is formed only in the presence of an electric field is named "field-induced metastable" or "metastable" (with melting temperature $T_{m,m}$ = 208.5 K), and the ordinary one is referred to as a "stable"
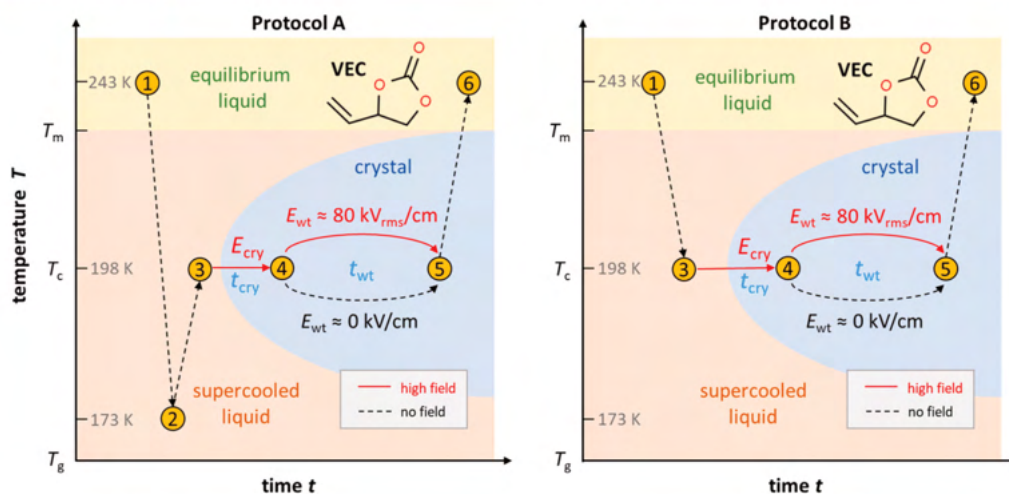
Figure 1. Schematic representation of the two different protocols used to prepare samples and record crystallization. Each case starts at the equilibrium liquid state (1) at $T = 243$ K $\approx T_m + 15$ K, and takes the sample to point (3), where the temperature is held at $T_c = 198$ K. Protocol A inserts cooling to point (2) at $T = 173$ K $\approx T_g + 2$ K, whereas the temperature in protocol B is never lower than $T_c = 198$ K. Crystallization occurs during the time interval t_{cry}, step 3 → 4, followed by a waiting time t_{wt}, step 4 → 5. Finally, the melting behavior is recorded during heating from $T_c = 198$ K back to $T = 243$ K, step 5 → 6. The yellow areas are for the equilibrium liquid (and include the molecular structure of VEC), beige is for the supercooled state, and blueish gray is for the crystal formation domain, analogous to a time−temperature transformation (TTT) diagram.

polymorph (with melting temperature $T_{m,s} = 227$ K). It is already established that a moderately high electric field accelerates the crystallization of VEC, leading to a field-induced metastable polymorph,[22] but only if the frequency of that field does not exceed a certain threshold.[23] Because the nucleation rate curves, $J(T)$, for the field-induced metastable and stable crystals have significantly different maxima positions on the temperature scale, the metastable or stable polymorph can be prepared in a targeted fashion.

This study focuses on the stability of the field-induced metastable polymorph, its potential polymorphic transition to the stable state, and the possibility of monitoring such a transition in real time by dielectric techniques. At a temperature of $T_c = 198$ K, the supercooled liquid crystallizes within less than 2 h into the metastable structure when subject to a field of $E \approx 80$ kV cm^{-1}. At the same temperature, we observe that this field-induced metastable polymorph transforms into the stable polymorph within a time frame of 15 h if seeded by the ordinary crystal. By contrast, no such transformation is observed in the absence of seed crystals. Interestingly, the dielectric constant changes along with the progress of the polymorphic transition, so that the composition of the polymorph mixture can be monitored in real time as the system changes the volume fraction of the more stable structure from practically zero to 100%.

■ EXPERIMENTAL SECTION

The compound 4-vinyl-1,3-dioxolan-2-one or vinyl ethylene carbonate (VEC, purity 99%) was obtained from Sigma-Aldrich and used as received. VEC is a vinyl derivative of propylene carbonate (PC) and has been referred to as "vinyl-PC". The liquid is loaded into a high-field capacitor cell described in detail in a previous publication (Figure S1, Supporting Information).[22] The polished parallel disks are made of stainless steel and are separated by a Teflon ring of $d = 25$ μm nominal thickness, leaving an active inner electrode surface area of $r = 7$ mm radius. The resulting geometric capacitance is $C_{geo} = (\varepsilon_0 \pi r^2)/(d = 54.5$ pF). By comparing the observed permittivity with reference

data, the actual electrode separation was determined to be closer to 20 μm. Temperature regulation of the sample cell was achieved by a Novocontrol Quatro temperature control system.

For dielectric measurements using large ac electric fields, a Trek PZD-700 high-voltage unit amplifies the output voltage of a Solartron SI-1260 gain−phase analyzer by a factor of 200. The current was measured via the voltage drop across a calibrated RC-shunt connected to the analyzer with a buffer amplifier that tolerates high voltages, employed to protect the system from sample failure. A schematic outline of the system is provided in Figure 1a of a previous publication.[24] This setup can generate dielectric permittivity data, $\varepsilon = \varepsilon' - i\varepsilon''$, within the frequency range from 30 mHz to 120 kHz for fields up to 240 kV cm^{-1}. All voltage and field amplitudes are reported as root-mean-square (RMS) values. All fields intended to affect crystallization were around $E \approx 80$ kV cm^{-1}, while amplitudes of the alternating fields used to measure dielectric permittivity only were kept below 16 kV cm^{-1}, which is a factor of 25 lower in terms of nonlinear ($\sim E^2$) effects. Fields much below 80 kV cm^{-1} that are used only to measure the permittivity (without affecting the crystallization) are designated as $E \approx 0$ kV cm^{-1}, regardless of their actual value.

Two distinct thermal protocols were used to generate VEC crystals at $T_c = 198$ K, both starting at the equilibrium liquid state at $T = 243$ K, which is approximately 15 K above the melting temperature of the stable (ordinary, low-field) polymorph. Schematic representations of these experimental protocols are provided in Figure 1. In the case of protocol A, the sample is cooled down to $T = 173$ K $\approx T_g + 2$ K a rate of approximately 10 K min^{-1}, i.e., to just above the glass-transition region. The aim of this step is to induce nucleation of the stable polymorph, as nucleation rate maxima are often located close to T_g. Except for a few minutes needed for temperature stabilization, there is no waiting time at $T = 173$ K. Subsequently, the temperature is increased to $T_c = 198$ K at a rate of approximately 5 K min^{-1}. No field is applied prior to reaching T_c at point 3 in Figure 1. After T_c is reached, the sample is exposed to an ac-field of $E \approx 80$ kV cm^{-1} at a frequency of $\nu = 5.62$ Hz. Via dielectric spectroscopy, the progress of crystallization of VEC at $T_c = 198$ K is measured in the presence of the ac-field. Once the crystallization is completed, we waited for some additional time ($t_{wt} = 0$, 3, 8.5, or 72 h) with or without the ac-field remaining on. Afterward, the sample was heated at a rate of 1 K min^{-1} to $T = 243$ K, while the changes in ε' at 10 kHz were monitored to

52

detect melting events and determine the volume fraction of the crystalline materials.

In the case of protocol B, the sample is cooled down from $T = 243$ K at a rate of approximately 5−10 K min^{-1} directly to the crystallization temperature at $T_c = 198$ K without applying an electric field. This was done in order to avoid nucleation of the stable polymorph, as its nucleation rate is negligible for temperatures $T \geq 198$ K. After T_c was reached, the sample was exposed to an ac-field of $E \approx 80$ kV cm^{-1} of various frequencies or to a dc-field of the same amplitude. The progress of crystallization was monitored via the dielectric permittivity in the presence of the high electric field. Once the transformation to the crystalline state was completed, i.e., after t_{cry} has elapsed, an additional time t_{wt} may be added with the ac-field remaining on. Finally, the temperature was increased at a rate of 1 K min^{-1} to $T = 243$ K, while ε' at 10 kHz detected melting events and volume fractions of the polymorphs.

RESULTS

The molecular liquid VEC belongs to the class of dipolar materials with negligible conductivity, such that electronic polarizability and orientational polarizability of the molecular dipoles are the main contributing features to the static dielectric constant, ε_s, which decreases mildly with increasing temperature. At the fields used here, the effect of the field magnitude on the permittivity ε is negligible. The high-frequency limit, ε_∞, of permittivity is governed by electronic polarizability and thus relatively independent of the structure, liquid or crystalline, and of temperature. Therefore, the progress of crystallization can be gauged by the real part of dielectric permittivity, ε', recognizing that only the volume fraction that is in the liquid state contributes to the orientational polarizability of permanent dipoles.[25] Thus, after ε_∞ is subtracted, the value of ε' relative to the static limit of the pure liquid, ε_s, is a good approximation of the volume fraction of the liquid in the sample:

$$V_{liq}/V_{total} = (\varepsilon' - \varepsilon_\infty)/(\varepsilon_s - \varepsilon_\infty) \tag{1}$$

Deviation from this relation due to dielectric mixing effects is sufficiently small to not interfere with the results of this study.[26,27] The frequency ν at which ε' is determined has to be sufficiently low such that the dipole orientation can follow the field with no time lag, which is the case for all frequencies used here. Various low frequencies (0.562 Hz $\leq \nu \leq$ 562 Hz) are employed to check the frequency dependence of the high field effect, $\nu = 10$ kHz is selected for all melting curves because it allows for more robust results at higher data acquisition rates.

The results are shown separately for each protocol used, A or B, the difference being that the stable polymorph is nucleated prior to crystallization in the A case, whereas protocol B is designed to avoid nucleation of the stable crystal form. For each protocol (A first, B second), one graph depicts the crystallization behavior for different field conditions, and another shows the melting behavior of these crystalline samples, generally measured at practically zero field.

We begin with results obtained by following protocol A of Figure 1, designed to nucleate the stable crystal via a temperature excursion to just above T_g before taking the sample to the crystallization temperature $T_c = 198$ K. For this protocol, the processes of crystallization at $T_c = 198$ K for different measurement conditions are shown in terms of ε' versus t in Figure 2, observed while the sample is subjected to a sinusoidal electric field of $E_{cry} \approx 80$ kV cm^{-1} at a frequency of $\nu = 5.62$ Hz. As a point of reference, one curve for $E_{cry} \approx 0$ kV cm^{-1} is also included in Figure 2, where only a very low field is
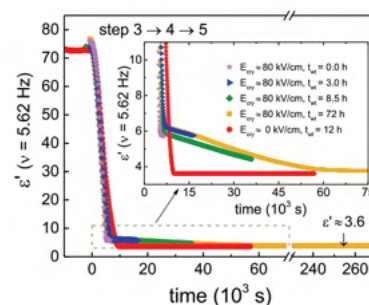

Figure 2. Time-dependent changes in dielectric permittivity ε' at a frequency $\nu = 5.62$ Hz recorded for VEC in the presence of an ac-field E_{cry} as indicated in the legend. Prior to this measurement, the sample followed steps $1 \rightarrow 2 \rightarrow 3$ of protocol A as illustrated in Figure 1. The drop of ε' signifies crystallization progress according to eq 1. After complete crystallization, there is an additional waiting time t_{wt} during which the ac field amplitude $E_{wt} = E_{cry}$ remains applied. The time dependence of ε' in the range 6−3.6 is shown on enlarged scales in the inset.

used to measure permittivity. For all curves in this figure, $t = 0$ has been defined as the onset of considerable crystallization, i.e., the extrapolated intersection between a more time-invariant ε' plateau and the practically linear steep decline toward $\varepsilon' = 3.6$. After the target of $T = 198$ K at stage 3 was reached, the induction times are about 10^4 s for the field-free case and typically less than 10^3 s for the application of 80 kV cm^{-1}; see the $t < 0$ range of Figure 2. Crystallization for the $E_{cry} \approx 0$ kV cm^{-1} case takes ε' rapidly to a level near 3.6, see inset of Figure 2, whereas all $E_{cry} \approx 80$ kV cm^{-1} curves terminate the rapid descent near a level of $\varepsilon' = 6.0$. Common to all $E_{cry} \approx 80$ kV cm^{-1} cases is the subsequent slow change from $\varepsilon' = 6.0$ to $\varepsilon' = 3.6$ in a near-linear fashion across about 14 h. However, these curves differ in the wait time ($t_{tw} = 0, 3, 8.5,$ or 72 h) during which the slow change has been recorded, which is relevant for the subsequent measurements, i.e., step $5 \rightarrow 6$ of protocol A. For clarity, Figure 2 shows only results for which the field during the wait time has remained that applied during the crystallization phase, i.e., $E_{wt} = E_{cry}$. However, another such set of $E_{cry} \approx 80$ kV cm^{-1} curves has been recorded, but with $E_{wt} \approx 0$ kV cm^{-1}, cf. Figure 3.

The results of Figure 3 are measured immediately following the end of the corresponding curves of Figure 2, all based upon a field that is within the linear response regime. The data represent ε' ($\nu_0 = 10$ kHz) recorded during a temperature scan from 198 to 243 K at a rate of about 1 K min^{-1}. Each curve starts at $T_c = 198$ K at a level that is equal to the end of the corresponding data set of Figure 2, indicative of practically complete crystallization. The main feature of Figure 3 is that an increase of the waiting time t_{wt} of step $4 \rightarrow 5$ leads to the amount of material melting already at $T_{m,m} = 208.5$ K decreasing systematically. The comparison between open ($E_{wt} \approx 0$ kV cm^{-1}) and closed ($E_{wt} \approx 80$ kV cm^{-1}) symbols demonstrates that the magnitude of the field during the wait time has no effect on the melting outcome of Figure 3. Only two cases do not show any signs of melting the field-induced metastable (low-melting) polymorph at $T_{m,m} = 208.5$ K, the case of crystallization in the absence of a high field ($E_{cry} \approx 0$ kV cm^{-1}), and the case of very long waiting periods ($t_{wt} = 72$ h).

The remaining results are all derived from applying protocol B, where a deliberate nucleation of the stable polymorph has

53
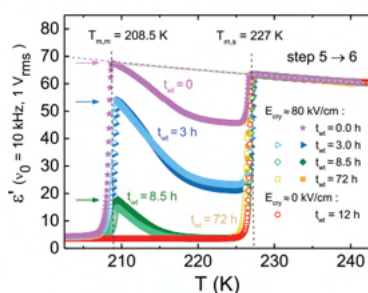
Figure 3. Temperature dependence of the dielectric permittivity ε' (at $\nu_0 = 10$ kHz) measured on heating of the crystalline material obtained by following protocol A and directly after the end of the traces of Figure 2. With increasing waiting time t_{wt} at $T_c = 198$ K (step 4 → 5), the volume fraction of the field-induced metastable polymorph melting at $T_{m,m} = 208.5$ K decreases, as it converts to a stable form during t_{wt}, which melts at $T_{m,s} = 227$ K. Open symbols represent cases with $E_{wt} \approx 0$, and solid symbols are for $E_{wt} \approx 80$ kV cm^{-1}, indicating the magnitude of E_{wt} has a minimal effect on the volume fractions. The dashed curve indicates $\varepsilon_s(T)$; the arrows are explained in the text.

been avoided by cooling directly from $T > T_m$ to T_c, cf. Figure 1. In contrast to the protocol A cases, protocol B can lead to situations in which the sample resists crystallization for extended periods of time, because the stable polymorph had not been nucleated. This can be observed in Figure 4 for two
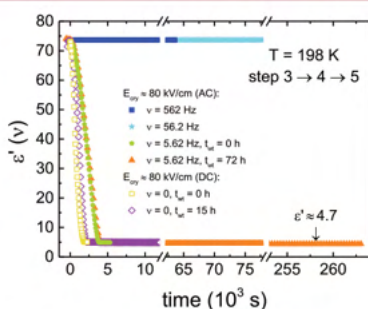

Figure 4. Time-dependent changes in dielectric permittivity ε' measured for various frequencies ν of the applied field of $E_{cry} = 80$ kV cm^{-1} for VEC at $T_c = 198$ K. Prior to this measurement, the sample followed step 1 → 3 of protocol B as illustrated in Figure 1. The drop of ε' signifies crystallization progress according to eq 1. After complete crystallization, there is an additional waiting time t_{wt}, during which the field amplitude $E_{wt} = E_{cry}$ remains applied. The type of field (ac or dc), frequency ν, and waiting time t_{wt} are given in the legend. Crystallization of VEC at $T_c = 198$ K occurs only for sufficiently low frequencies.

curves whose ε' levels remain at ε_s for up to 22 h. Consistent with previous results, this can occur even for fields of $E_{cry} = 80$ kV cm^{-1}, provided that the frequency exceeds $\nu \approx 18$ Hz at $T_c = 198$ K;[23] see the $\nu = 562$ and 56.2 Hz data in Figure 4. Note that VEC also resists crystallization with protocol B at zero field ($E_{cry} = 0$);[22,23] i.e., $E_{cry} = 80$ kV cm^{-1} at frequencies $\nu > 56.2$ Hz yields the same outcome as $E_{cry} = 0$. For all lower frequencies (including the dc cases, $\nu = 0$), crystallization leads to a rapid drop of permittivity values to around $\varepsilon' = 4.7$. Different wait times (with $E_{wt} = E_{cry} = 80$ kV cm^{-1}) have been applied to cases for which crystallization had occurred, i.e., for

$\nu = 5.62$ Hz and $\nu = 0$, but the ε' level remains constant at 4.7 for up to 72 h.

Analogous to Figure 3, melting curves have been recorded for samples crystallized using protocol B, again by ramping temperature from $T_c = 198$ K to $T = 243$ K at about 1 K min^{-1}, directly after the end of the measurements shown in Figure 4. These results are compiled in Figure 5, which reveals that only
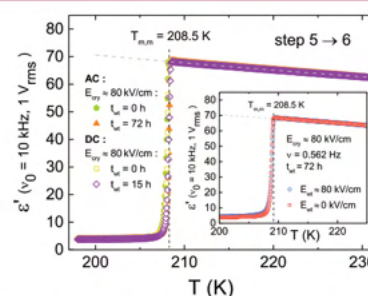
Figure 5. Temperature dependence of the dielectric permittivity ε' (at $\nu_0 = 10$ kHz) measured on heating of the crystalline material obtained by following protocol B and directly after the end of the traces of Figure 4. Melting occurs only at $T_{m,m} = 208.5$ K, indicating 100% volume fraction of field-induced metastable polymorph, regardless of waiting time t_{wt} and type of the high field, ac versus dc. The inset demonstrates that the magnitude of E_{wt}, 80 or 0 kV cm^{-1}, does not alter the stability of the field-induced metastable polymorph. The dashed curve indicates $\varepsilon_s(T)$.

one melting event is observed at $T_{m,m} = 208.5$ K, regardless of high field frequency ($\nu \approx 5.62$ Hz versus $\nu \approx 0$) and wait time ($t_{wt} = 0$ versus $t_{wt} \gg 0$). Furthermore, the inset of Figure 5 shows that whether the field is $E_{wt} = 80$ kV cm^{-1} or zero during the waiting time of $t_{wt} = 72$ h, it has no effect on melting for a sample crystallized at $E_{cry} = 80$ kV cm^{-1} with frequency $\nu = 0.562$ Hz.

■ DISCUSSION

To our knowledge, polymorphic transitions from a field-induced metastable polymorph to the stable crystal structure that forms under ordinary conditions have not been studied to date. In this case of VEC, no polymorphism had been reported prior to applying an electric field, which led to a crystal structure that melts at $T_{m,m} = 208.5$ K, located about 20 K below the regular melting point at $T_{m,s} = 227$ K.[22] On the basis of that observation, one might speculate that electric fields may widen the range of materials exhibiting polymorphism, particularly with polar substances. Electric fields can modify the free energies relevant for nucleation and growth rates,[28−31] but only for polar particles is the interaction with the field sufficiently strong to impact crystallization.

The questions addressed in the following are concerned with how to stabilize the metastable polymorph, what are the time scales of polymorphic transformations, and can dielectric techniques monitor these transitions in real time. Before focusing on the polymorph transition and stability, a discussion of the field-effect on crystallization outcome and the resulting polymorph selectivity appears in order. Although the field effects such as accelerated crystallization and formation of a metastable polymorph have been established earlier,[22,23] we confirm agreement with earlier observations for the present samples in the following subsection.

Field Effect. In order to clarify the impact of an electric field on the crystallization of VEC, we focus on the curves measured at low fields, $E_{cry} \approx 0$ kV cm^{-1}, and those obtained for $E_{cry} \approx 80$ kV cm^{-1} at zero wait time, $t_{wt} = 0$. According to Figure 2, both low and high field cases crystallize at about the same rate after the induction time ($t < 0$) has elapsed. The dominant field effect is revealed in Figure 3, where practically the entire volume fraction melts at $T_{m,s} = 227$ K for the $E_{cry} \approx 0$ case, whereas practically complete melting occurs at $T_{m,m} = 208.5$ K for the $E_{cry} \approx 80$ kV cm^{-1} and $t_{wt} = 0$ experiment. That these situations correspond to relatively high polymorphic purity in the crystalline state ($T < 205$ K in Figure 3) can be derived from the observation that the rise of ε' reaches ε_s (dashed curve in Figure 3) for each melting process, indicative of ~100% liquid volume fraction after melting. For the field-induced metastable crystal melting at $T_{m,m} = 208.5$ K, subsequent crystallization for $T > T_{m,m}$ is the result of having nucleated the stable crystal with protocol A. By comparison, the analogous set of curves obtained using protocol B ($E_{cry} \approx 80$ kV cm^{-1} and $t_{wt} = 0$ in Figure 4 and Figure 5) shows no such crystallization process above $T_{m,m} = 208.5$ K. That protocol B suppresses nucleation of the stable crystal very effectively is confirmed by the $E_{cry} \approx 0$ case in Figure 4, where the liquid resists crystallization for 22 h.

As a result of the measurements discussed above, two distinct crystalline states of VEC with considerable polymorphic purity can be prepared: (1) the stable crystal using protocol A without high electric fields, and (2) the field-induced metastable crystal using protocol B while subjecting the sample to a high electric field of sufficiently low frequency. In the former case, no indication of a melting event at $T_{m,m} = 208.5$ K is observed, while the latter case does not show any formation of the stable crystal when heating above $T_{m,m}$.

These results are consistent with the picture of an electric field inducing a high nucleation rate of the metastable polymorph at $T_c = 198$ K, a temperature at which the nucleation rate of the stable polymorph is negligible. Therefore, the high electric field appears to open a new parallel crystallization route, without affecting nucleation and crystal growth rates of the stable crystal.

Polymorph Transition. A subtle feature of the curves in Figure 2 is the variety of levels to which the ε' values fall in the course of crystallization if judged on the permittivity scale of the main figure, $0 \leq \varepsilon' \leq 85$. The inset of Figure 2 emphasizes these features and clearly shows that the level reached during the first ~2 h correlates strongly with the field E_{cry}: $\varepsilon' = 6.0$ for $E_{cry} \approx 80$ kV cm^{-1} and $\varepsilon' = 3.6$ for $E_{cry} \approx 0$. Therefore, according to Figure 2, the presence or absence of a considerable electric field during crystallization impacts the crystallization outcome in a qualitative fashion, with the zero-field case crystallizing only the stable polymorph (red filled circles in Figure 2). For this protocol, it has been established that the low-field case gives rise to the stable polymorph, while the high field cases yield the new field-induced metastable polymorph. The interesting feature is that the permittivity transitions from $\varepsilon' = 6.0$ to $\varepsilon' = 3.6$ across a time window of about 14 h.

Now, one could speculate that these values $\varepsilon' = 6.0$ and $\varepsilon' = 3.6$ are the permittivities of the two distinct crystal structures, the field-induced metastable and the stable polymorph, respectively. However, in the absence of orientational degrees of freedom, these permittivities should be governed by molecular electronic polarizability and density and thus be much more similar for the two polymorphs. Therefore, it is too early to conclude that the change in ε' from 6.0 to 3.6 can be translated into a time-dependent volume partitioning of the two polymorphs. However, an independent approach to linking ε' to the volume fractions is via the levels observed after different waiting times, i.e., at the end of the traces in Figure 2. In the order of $t_{wt} = 0$, 3, 8.5, and 72 h, the ε' values reached at the end of the $E_{cry} \approx 80$ kV cm^{-1} curves in Figure 2 are 6, 5.5, 4.2, and 3.6, corresponding to $x = 100$, 79, 26 and 0% height if normalized to the 6.0 and 3.6 limits. These percentages are indicated as arrows in Figure 3, with their positions on the permittivity scale calculated as $\varepsilon = \epsilon_\infty + x(\epsilon_s - \epsilon_\infty)$. These levels provide a very good match with the volume fraction of the field-induced metastable polymorph as derived from the peak height of the melting process at $T = T_{m,m}$ relative to the limits ε_∞ and ε_s, cf. eq 1. Therefore, it is justified to interpret the change of $\varepsilon'(t)$ from 6.0 to 3.6 (inset of Figure 2) as linearly related to the volume fraction of the field-induced metastable polymorph.

With the above reasoning, the statement of the waiting time dependence of Figure 2 is that the volume fraction $x_m = V_{polymorph\,m}/V_{total}$ of the field-induced metastable polymorph decreases approximately linearly with time. The dependence can be approximated by $x_m = 1 - t/14h$ and is reproduced for the runs differing in t_{wt}, where $t = 0$ is defined by the kink near $\varepsilon' = 6$ in Figure 2. Such a linear time dependence of volume fraction is compatible with a growth-front like transformation process with time-invariant front velocities.[32]

Comparing the open ($E_{wt} \approx 0$) and solid ($E_{wt} \approx 80$ kV cm^{-1}) symbols in Figure 3, it can be observed that the presence of an electric field during the wait time has no impact on the polymorph transformation dynamics. It may seem reasonable to assume that the field would stabilize the field-induced metastable over the stable polymorph, but the orientational degree of freedom necessary for the field to lower the free energy is absent in the solid state. Therefore, in contrast to the field being able to reduce the free energy of polar crystal nuclei suspended in the liquid,[23] the lack of crystallite orientation in a crystalline solid prevents such a field effect.

The feature responsible for the crystal type dependence of the dielectric constant, $\varepsilon' = 6.0$ versus $\varepsilon' = 3.6$, remains to be clarified. The level of $\varepsilon' = 6.0$ is hard to justify on the basis of reasonable values for electronic polarizability and density. A more likely cause for such high ε' numbers for a crystalline state is a residual amount of liquid or amorphous material between crystallites, the volume fraction of which may depend on the polymorph and crystallite sizes.

Polymorph Stability. The previous section has demonstrated that the field-induced metastable polymorph can transform to the stable polymorph, cf. Figure 2 and Figure 3. It is important to realize that these transformation curves were obtained employing protocol A, cf. Figure 1, where a deliberate nucleation of the stable polymorph preceded the crystallization process under a field. This initial cooling to near T_g has a considerable effect on the stability of the field-induced metastable polymorph. That nuclei of the stable polymorph are present in the system subject to protocol A even after field-induced crystallization and melting of the metastable polymorph is clearly seen by the crystallization that sets in for $T > T_{m,m}$ in Figure 3, even though their volume fraction is too small to show in the ε' data. A similar effect is absent in the case of protocol B, as no indication of crystallization for $T >$

55

$T_{m,m}$ is found in Figure 5. Therefore, the system is practically free of nuclei of the stable polymorph when the sample is prepared using protocol B.

Crystallization curves based on protocol B are depicted in Figure 4, where crystallization sets in only when an electric field of sufficiently high amplitude and low frequency is applied. The ε' values rapidly drop to 4.6 and remain at that level for at least 72 h, with no indication of a polymorph transformation as outlined in the previous section. This reveals the much-increased stability of field-induced metastable polymorph if prepared in the absence of nuclei of the stable polymorph. The conclusion is that the polymorph transition requires seed crystals of the more stable crystal structure, analogous to the case of ritonavir,[12] where specks of the more stable crystal were found responsible for inducing the polymorphic transition to a form that resulted in the market withdrawal of the drug.

■ SUMMARY AND CONCLUSIONS

In the absence of an electric field, vinyl ethylene carbonate (VEC) has thus far shown only one crystal structure (the stable one) that melts at $T_{m,s}$ = 227 K, with no indication of polymorphism. At fields in excess of about E = 40 kV cm^{-1},[22] and with a sufficiently low frequency,[23] VEC crystallizes into a field-induced metastable polymorph that melts at $T_{m,m}$ = 208.5 K. This study focuses on the polymorphic transition from the field-induced metastable to the stable crystal structure. It turns out that the field-induced metastable polymorph can be nucleated and grown efficiently at a temperature, T_c = 198 K, at which the nucleation rate of the stable polymorph is negligible (protocol B). As a result, this field-induced metastable crystal structure can be obtained with high polymorphic purity, and in this case the metastable crystal displays no indication of a transformation for 72 h at T_c = 198 K, where the crystal growth of the stable polymorph can be completed within about 2 h.

The situation regarding the stability of the field-induced metastable polymorph changes when protocol A is employed, where approaching T_g nucleates the stable polymorph, which remains as undetected volume fraction of seeds after an electric field turned practically the entire sample into the metastable polymorph. In this case, a polymorphic transition is observed, and the volume fraction of the stable structure increases linearly from ~0 to ~100% within a time window of 14 h at T_c = 198 K. This result is independent of the electric field remaining on or switched off for the duration of this transition, indicating that the field-induced metastable polymorph cannot be stabilized via the field that promoted its nucleation. Interestingly, the dielectric permittivity changes linearly with the volume fractions during this transformation process, which allows for a direct observation of the polymorphic transition in real time.

It seems reasonable to assume that polymorphic transitions can be monitored by dielectric techniques also for other materials, i.e., for polymorphs that have not been obtained by the application of high electric fields. Metastable crystal structures of pharmaceuticals may be advantageous with regard to bioavailability, but only if the shelf life is not cut short by a polymorphic transition. The present study underlines the importance of polymorphic purity for increasing the shelf life of metastable crystal structures.

■ AUTHOR INFORMATION

Corresponding Author

Karolina Adrjanowicz − *Institute of Physics, University of Silesia, 41-500 Chorzow, Poland; Silesian Center for Education and Interdisciplinary Research (SMCEBI), 41-500 Chorzow, Poland;* ◉ orcid.org/0000-0003-0212-5010; Email: kadrjano@us.edu.pl

Authors

Daniel M. Duarte − *Institute of Physics, University of Silesia, 41-500 Chorzow, Poland; Silesian Center for Education and Interdisciplinary Research (SMCEBI), 41-500 Chorzow, Poland;* ◉ orcid.org/0000-0002-8230-0255

Ranko Richert − *School of Molecular Sciences, Arizona State University, Tempe, Arizona 85287, United States;* ◉ orcid.org/0000-0001-8503-3175

Complete contact information is available at:
https://pubs.acs.org/10.1021/acs.cgd.0c00626

Notes

The authors declare no competing financial interest.

■ REFERENCES

(1) Bernstein, J. Polymorphism - A Perspective. Polymorphism - A Perspective. *Cryst. Growth Des.* **2011**, *11*, 632−650.

(2) Cruz-Cabeza, A. J.; Bernstein, J. Conformational Polymorphism. *Chem. Rev.* **2014**, *114*, 2170−2191.

(3) Svärd, M.; Nordström, F. L.; Hoffmann, E.-M.; Aziz, B.; Rasmuson, Å. C. Thermodynamics and Nucleation of the Enantiotropic Compound P-Aminobenzoic Acid. Thermodynamics and Nucleation of the Enantiotropic Compound p-Aminobenzoic Acid. *CrystEngComm* **2013**, *15*, 5020−5031.

(4) Heinrich, M. A.; Pflaum, J.; Tripathi, A. K.; Frey, W.; Steigerwald, M. L.; Siegrist, T. Enantiotropic Polymorphism in Di-Indenoperylene. Enantiotropic Polymorphism in Di-Indenoperylene. *J. Phys. Chem. C* **2007**, *111*, 18878−18881.

(5) Nogueira, B. A.; Castiglioni, C.; Fausto, R. Color Polymorphism in Organic Crystals. Color Polymorphism in Organic Crystals. *Comm. Chem.* **2020**, *3*, 34.

(6) Yu, L. Polymorphism in Molecular Solids: An Extraordinary System of Red, Orange, and Yellow Crystals. Polymorphism in molecular solids: An Extraordinary System of Red, Orange, and Yellow Crystals. *Acc. Chem. Res.* **2010**, *43*, 1257−1266.

(7) Habgood, M.; Sugden, I. J.; Kazantsev, A. V.; Adjiman, C. S.; Pantelides, C. C. Efficient Handling of Molecular Flexibility in Ab Initio Generation of Crystal Structures. Efficient Handling of Molecular Flexibility in Ab Initio Generation of Crystal Structures. *J. Chem. Theory Comput.* **2015**, *11*, 1957−1969.

(8) Anwar, J.; Zahn, D. Polymorphic Phase Transitions: Macroscopic Theory and Molecular Simulation. Polymorphic Phase Transitions: Macroscopic Theory and Molecular Simulation. *Adv. Drug Delivery Rev.* **2017**, *117*, 47−70.

(9) Vorländer, D. Die Erforschung Der Molekularen Gestalt Mit Hilfe Der Kristallinischen Flüssigkeiten. Die Erforschung der molekularen Gestalt mit Hilfe der kristallinischen Flüssigkeiten. *Z. Phys. Chem.* **1923**, *105U*, 211−254.

(10) Ostwald, W. Studien Über Die Bildung Und Umwandlung Fester Körper. Studien über die Bildung und Umwandlung fester Körper. *Z. Phys. Chem.* **1897**, *22U*, 289−330.

56

(11) Schmelzer, J.; Möller, J.; Gutzow, I. Ostwald's Rule of Stages: The Effect of Elastic Strains and External Pressure. Ostwald's rule of stages: The Effect of Elastic Strains and External Pressure. *Z. Phys. Chem.* **1998**, *204*, 171−181.

(12) Bauer, J.; Spanton, S.; Henry, R.; Quick, J.; Dziki, W.; Porter, W.; Morris, J. Ritonavir: An Extraordinary Example of Conformational Polymorphism. Ritonavir: An Extraordinary Example of Conformational Polymorphism. *Pharm. Res.* **2001**, *18*, 859−866.

(13) Morissette, S. L.; Soukasene, S.; Levinson, D.; Cima, M. J.; Almarsson, Ö. Elucidation of Crystal Form Diversity of the HIV Protease Inhibitor Ritonavir by High-Throughput Crystallization. Elucidation of Crystal Form Diversity of the HIV Protease Inhibitor Ritonavir by High-Throughput Crystallization. *Proc. Natl. Acad. Sci. U. S. A.* **2003**, *100*, 2180−2184.

(14) Clout, A. E.; Buanz, A. B. M.; Gaisford, S.; Williams, G. R. Polymorphic Phase Transitions in Carbamazepine and 10,11-Dihydrocarbamazepine. Polymorphic Phase Transitions in Carbamazepine and 10,11-Dihydrocarbamazepine. *Chem. - Eur. J.* **2018**, *24*, 13573−13581.

(15) Barbas, R.; Martí, F.; Prohens, R.; Puigjaner, C. Polymorphism of Norfloxacin: Evidence of the Enantiotropic Relationship between Polymorphs A and B. Polymorphism of Norfloxacin: Evidence of the Enantiotropic Relationship Between Polymorphs A and B. *Cryst. Growth Des.* **2006**, *6*, 1463−1467.

(16) Evans, G. J. Crystal Growth in Electric Fields. Crystal Growth in Electric Fields. *Mater. Lett.* **1984**, *2*, 420−423.

(17) Taleb, M.; Didierjean, C.; Jelsch, C.; Mangeot, J. P.; Capelle, B.; Aubry, A. Crystallization of Proteins under an External Electric Field. Crystallization of Proteins Under an External Electric Field. *J. Cryst. Growth* **1999**, *200*, 575−582.

(18) Hammadi, Z.; Veesler, S. New Approaches on Crystallization under Electric Fields. *Prog. Biophys.* New Approaches on Crystallization Under Electric Fields. *Prog. Biophys. Mol. Biol.* **2009**, *101*, 38−44.

(19) Nanev, C. N.; Penkova, A. Nucleation of Lysozyme Crystals under External Electric and Ultrasonic Fields. Nucleation of Lysozyme Crystals Under External Electric and Ultrasonic Fields. *J. Cryst. Growth* **2001**, *232*, 285−293.

(20) Aber, J. E.; Arnold, S.; Garetz, B. A.; Myerson, A. S. Strong Dc Electric Field Applied to Supersaturated Aqueous Glycine Solution Induces Nucleation of the γ Polymorph. Strong DC Electric Field Applied to Supersaturated Aqueous Glycine Solution Induces Nucleation of the Polymorph. *Phys. Rev. Lett.* **2005**, *94*, 145503.

(21) Di Profio, G.; Reijonen, M. T.; Caliandro, R.; Guagliardi, A.; Curcio, E.; Drioli, E. Insights into the Polymorphism of Glycine: Membrane Crystallization in an Electric Field. Insights Into the Polymorphism of Glycine: Membrane Crystallization in an Electric Field. *Phys. Chem. Chem. Phys.* **2013**, *15*, 9271−9280.

(22) Adrjanowicz, K.; Paluch, M.; Richert, R. Formation of New Polymorphs and Control of Crystallization in Molecular Glass-Formers by Electric Field. Formation of New Polymorphs and Control of Crystallization in Molecular Glass-formers by Electric Field. *Phys. Chem. Chem. Phys.* **2018**, *20*, 925−931.

(23) Duarte, D. M.; Richert, R.; Adrjanowicz, K. Frequency of the AC Electric Field Determines How a Molecular Liquid Crystallizes. Frequency of the AC Electric Field Determines how a Molecular Liquid Crystallizes. *J. Phys. Chem. Lett.* **2020**, *11*, 3975−3979.

(24) Pathak, U.; Richert, R. Dielectric loss of poly(vinylacetate) at electric fields of 400 kV/cm. Dielectric Loss of Poly(vinylacetate) at Electric Fields of 400 kV/cm. *Colloid Polym. Sci.* **2014**, *292*, 1905−1911.

(25) Böttcher, C. J. F. *Theory of Electric Polarization*; Elsevier: Amsterdam, 1973; Vol. 1.

(26) Jensen, M. H.; Alba-Simionesco, C.; Niss, K.; Hecksher, T. A Systematic Study of the Isothermal Crystallization of the Mono-Alcohol n-Butanol Monitored by Dielectric Spectroscopy. A Systematic Study of the Isothermal Crystallization of the Mono-Alcohol n-Butanol Monitored by Dielectric Spectroscopy. *J. Chem. Phys.* **2015**, *143*, 134501.

(27) Adrjanowicz, K.; Richert, R. Control of Crystallization Pathways by Electric Fields. In *Dielectrics and Crystallization*, Ezquerra, T. A.; Nogales, A., Eds., Springer: Cham, 2020.

(28) Gutzow, I.; Schmelzer, J. W. P. *The Vitreous State: Thermodynamics, Structure, Rheology, and Crystallization*; Springer: Berlin, 2013.

(29) Kashchiev, D. Nucleation in External Electric Field. Nucleation in External Electric Field. *J. Cryst. Growth* **1972**, *13/14*, 128−130.

(30) Kashchiev, D. On the Influence of the Electric Field on Nucleation Kinetics. On the Influence of the Electric Field on Nucleation Kinetics. *Philos. Mag.* **1972**, *25*, 459−470.

(31) Isard, J. O. Calculation of the Influence of an Electric Field on the Free Energy of Formation of a Nucleus. Calculation of the Influence of an Electric Field on the Free Energy of Formation of a Nucleus. *Philos. Mag.* **1977**, *35*, 817−819.

(32) Swallen, S. F.; Traynor, K.; McMahon, R. J.; Ediger, M. D.; Mates, T. E. Stable glass transformation to supercooled liquid via surface-initiated growth front. Stable Glass Transformation to Supercooled Liquid via Surface-Initiated Growth Front. *Phys. Rev. Lett.* **2009**, *102*, 065503.
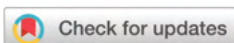
57

Check for updates

AC *versus* DC field effects on the crystallization behavior of a molecular liquid, vinyl ethylene carbonate (VEC)

Daniel M. Duarte, [ID] [ab] Ranko Richert [ID] [c] and Karolina Adrjanowicz [ID] *[ab]

Using electric fields to control crystallization processes shows a strong potential for improving pharmaceuticals, but these field effects are not yet fully explored nor understood. This study investigates how the application of alternating high electric fields can influence the crystallization kinetics as well as the final crystal product, with a focus on the possible difference between alternating (ac) and static (dc) type fields applied to vinyl ethylene carbonate (VEC), a molecular system with field-induced polymorphism. Relative to ac fields, static electric fields lead to more severe accumulation of impurity ions near the electrodes, possibly affecting the crystallization behavior. By tuning the amplitude and frequency of the electric field, the crystallization rate can be modified, and the crystallization outcome can be guided to form one or the other polymorph with high purity, analogous to the findings derived from dc field experiments. Additionally, it is found that low-frequency ac fields reduce the induction time, promote nucleation near T_g, and affect crystallization rates as in the dc case. Consistency is also observed for the Avrami parameters n derived from ac and dc field experiments. Therefore, it appears safe to conclude that ac fields can replicate the effects seen using dc fields, which is advantageous for samples with mobile charges and the resulting conductivity.

Introduction

The study of crystallization plays an essential role in materials science and technology. The reason is that numerous physico-chemical or mechanical properties of various materials depend on the degree of crystallinity, polymorphism, grain size, or crystal quality.[1,2] Furthermore, understanding how to control the promotion or suppression of certain crystallization outcomes is essential for numerous applications. Applying an electric field is one of the methods to achieve this,[3] and understanding the crystallization process of samples subjected to electric fields can lead to improved control of the crystalline product.

There are several interesting effects that have been observed when applying an electric field during crystallization. Examples are a reduced nucleation time,[4–12] increased nucleation rate,[8,12] enlarged crystal size,[4,10,12,13] and controlled polymorphic outcome.[11,14–17] Guiding the crystallization behavior with the use of an external electric field might affect the nucleation and crystal growth process, thus leading to a completely different crystalline structure. Such

phenomena are relevant for a wide range of compounds, such as pharmaceuticals, food products, and other chemicals. Recently,[11] for the first time, it has been studied the crystallization behavior of a single component glass-forming liquid, vinyl ethylene carbonate (VEC), under high static (DC) electric field. This study has demonstrated that the dc field might affect the crystallization of a neat low-molecular-weight van der Waals liquid in a qualitative fashion. For example, the crystallization time is shortened and/or a completely new polymorphic form of the tested material can be obtained. The use of high fields in polar liquids results in field-induced orientations of the constituents[18,19] as well as the modification of thermodynamics potentials,[20–22] *e.g.*, free energy and entropy. It was also suggested that high electric fields could be used targeted crystallization into different polymorphs. Therefore, field-induced crystallization is a powerful tool for materials engineering and pharmaceutical industries.[23,24]

Likewise, for a DC case,[11] the crystallization of VEC in the presence of alternating (AC) electric fields should facilitate changes in the crystallization patterns. Some of these aspects were demonstrated by us recently.[25] Interestingly, it was found that the crystallization behavior depends on both the magnitude and the frequency of the applied electric field. With increasing the magnitude of the ac field or lowering the frequency, the crystallization was observed to become faster.

The present study aims to investigate in more detail the crystallization tendency of VEC in the presence of alternating

[a] Institute of Physics, University of Silesia, 75 Pulku Piechoty 1a, 41-500 Chorzow, Poland. E-mail: kadrjano@us.edu.pl

[b] Silesian Center for Education and Interdisciplinary Research (SMCEBI), 75 Pulku Piechoty 1, 41-500 Chorzow, Poland

[c] School of Molecular Sciences, Arizona State University, Tempe, Arizona 85287, USA

58

(AC) electric fields and compare obtained results with that observed when using dc-fields. In order to facilitate such comparison, we have followed the same experimental protocols, which allow us to get insight into various aspects of the field-assisted crystallization. Our results point to the electric field promoting the formation of polar crystallites, whose concentration in the final material can be controlled by the frequency and the amplitude of the electric field. At low frequencies and high electric fields (ac), the crystallization behavior of VEC turns out to coincide with that observed in the presence of static fields (dc). Therefore, this work shows that both electrical fields (ac and dc) provide an interesting strategy to obtain novel materials and control the crystallization outcome for numerous molecular systems. The clear advantage of ac-fields is the reduction or elimination of space charge buildup and its impact on the crystallization outcome, which is inevitable when applying static fields for extended periods of time.
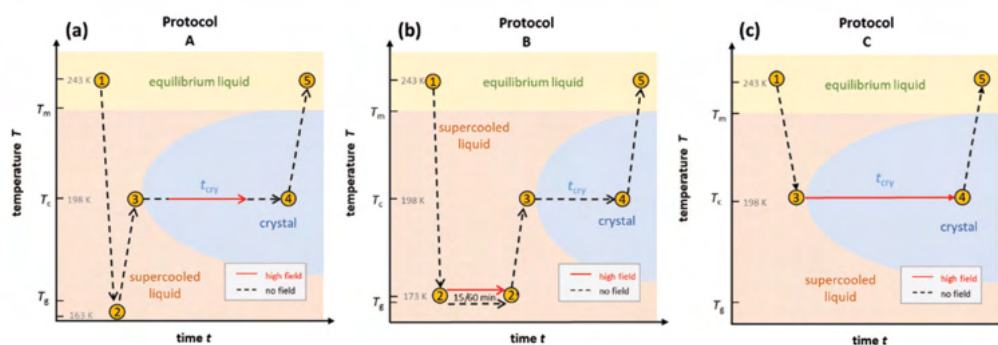
Experimental

The sample material, 4-vinyl-1,3-dioxolan-2-one or vinyl ethylene carbonate (VEC, 99% purity, CAS number 4427-96-7), was purchased from Sigma-Aldrich and used as received. VEC is a vinyl derivative of the model glass-forming liquid propylene carbonate (PC),[26] which is a highly polar and low-molecular-weight van der Waals liquid with a large dipole moment ($\mu = 4.76$ D).[27] It has been referred to as 'vinyl-PC'. The sample was loaded into a high-field capacitor cell described in detail in previous publications.[11,25,28,29] Parallel discs of stainless-steel (SS) or titanium (Ti) served as electrodes, with the disc pair being separated by a Teflon ring of 25 or 50 µm thickness. The active inner electrode surface area is of 7 mm radius. For the $d = 25$ µm, the geometric capacitance is $C_{geo} = \varepsilon_0 \pi r^2/d = 54.5$ pF. By comparing the observed permittivity, $\varepsilon = \varepsilon' - i\varepsilon''$, with reference

data, the actual electrode separations were determined to be 20 and 53 µm. In order to assess possible electrode surface effects, some experiments were done using highly polished stainless-steel electrodes, while others were done using titanium electrodes with a somewhat rougher surface texture. Varying the gap between the electrodes helps to gauge the effect of electrode polarization. A Novocontrol Quatro system was used to control the temperature of the sample cell.

Large ac electric fields were achieved by using a Trek PZD-700 high-voltage amplifier that boosts the output voltage of a Solartron SI-1260 gain-phase analyzer by a factor of 200. The current was determined from the voltage drop across a calibrated RC-shunt connected to the analyzer via a buffer amplifier that supports voltages up to 500 V_p. The role of this buffer amplifier is to protect the equipment from sample failure. In this configuration, the dielectric response of the sample can be measured within the frequency range from 30 mHz to 200 kHz at low fields and between 30 mHz to 120 kHz for fields up to 240 kV cm^{-1}. All voltage and field amplitudes are reported as root-mean-square (RMS) values. More information about the system can be found elsewhere.[29] All fields intended to affect the crystallization of VEC were around (and above) $E \approx 80$ kV cm^{-1}, while the amplitudes of the alternating fields used to measure dielectric permittivity only were kept below 16 kV cm^{-1}, which is a factor of 25 lower in terms of nonlinear ($\sim E^2$) effects. Fields much below 80 kV cm^{-1} that are used only to measure the permittivity (without affecting the crystallization) are notified in the following parts also as $E \approx 0$ kV cm^{-1}, regardless of their actual value.

Results and discussion

To gain a detailed understanding of the effect of the ac-field on the crystallization, we have performed sets of experiments by following three different protocols. They are schematically shown in Fig. 1. Note that they are identical to the protocols

Fig. 1 Overview of the experimental protocols used to study the effect of frequency and magnitude of the ac field on the crystallization behavior of VEC. Protocols 'A' and 'B' were used to evaluate the ac field effect on the ongoing crystallization and nucleation rate. Protocol 'C' was followed to favor the formation of only the high-field polymorph as the optimal temperature range for nucleation of the low-field polymorph is located close to T_g. Each experiment starts at the equilibrium liquid state (1) at $T = 243$ K $\approx T_m + 15$ K, and takes the sample to point (3), where the temperature is held at $T_c = 198$ K. Protocols 'A' and 'B' insert cooling to point (2) at $T = 163$ K ($T_g - 8$ K), or either $T = 173$ K ($T_g + 1$ K). In contrast, the temperature in protocol 'C' is never lower than $T_c = 198$ K. Crystallization occurs during the time interval t_{cry}, step 3 → 4. Finally, the melting behavior is recorded during heating from $T_c = 198$ K back to $T = 243$ K, step 4 → 5.

polymorph. Thus, our present finding is in line with the effects seen when a dc-bias instead of an ac field was used to induce changes in the crystallization behavior.[11]

B. High field timing

To further illustrate how an ac-field promotes crystallization of VEC, we have also switched it on/off at different stages of the ongoing crystallization process, as can be seen in Fig. 4. Note that the field magnitude ($E = 80$ kV cm^{-1}) and its frequency ($\nu = 5.62$ Hz) are the same in each case. For the case in which spontaneous crystallization had formed already about 20% of the ordinary crystal, turning on the electric field has no considerable effect on the ongoing crystallization (see diamonds in Fig. 4a). On the other hand, applying the ac field during the induction period (the time prior to the onset of crystallization) activates crystallization immediately. The same effect is observed when the sample is exposed to the ac field just after reaching $T_c = 198$ K (see squares in Fig. 4a). Subsequent heating of the crystalline material obtained in this way gives back two melting events, as illustrated in Fig. 4b. The melting point detected at a lower temperature ($T_{m2} = 208.5$ K) corresponds to polymorphic form '2' generated only in the presence of an ac field, while ($T_{m1} = 227$ K) refers to the ordinary zero-field crystal. The melting curves presented in Fig. 4b suggest a near 100% volume fraction of the low-temperature polymorph for the crystals obtained in the course of the crystallization shown in Fig. 4a. Melting at T_{m2} recovers practically the static permittivity, $\varepsilon' = \varepsilon_s$, the value characteristic for the pure liquid state as indicated by the dashed gray line. This may be the expected outcome when the ac field is applied during the (low field) induction period. Interestingly, however, this holds even for the case where the field had been applied only after a considerable amount of the ordinary polymorph '1' had already been formed

(see diamonds in Fig. 4a). Therefore, under these conditions, the ac field is capable of converting the more stable polymorph '1' into the field-induced polymorph '2'.

The decrease of the ε' values above T_{m2} signifies the recrystallization of the sample, which leads to the formation of ordinary, low-field crystals. From a previous study,[11] we know that following this protocol and in the absence of any high field, only the high-temperature polymorph is generated, i.e., the ordinary crystal structure that melts at $T_{m1} = 227$ K (see crosses in Fig. 4b). The recrystallization observed for $T > T_{m2}$ is only possible because nuclei of the ordinary polymorph are already present, as their nucleation rate at $T > 198$ K is negligible. Their volume fraction has to be too small to be detected in terms of $\varepsilon' < \varepsilon_s$ at $T = T_{m2}$, but sufficiently large to allow for effective crystal growth for $T_{m2} < T < T_{m1}$.

It is interesting to note that the melting curves of Fig. 4b are virtually identical, regardless of when the ac field has been applied during the (field-free) induction time or crystallization process. We conclude that not only does the ac field open a very effective pathway to forming the field-induced polymorph melting at T_{m2}, but this polymorph '2' is also formed at the expense of the polymorph '1' volume fraction. Field amplitude and frequency will be decisive factors in such experiments.

C. Effect on nucleation

In the next step, we have studied the effect of the ac-field on the nucleation process at temperatures where crystal growth is exceedingly slow. To this end, we applied the protocol 'B', as outlined in Fig. 1b. Based on the previous investigations,[11,25] we know that the optimal temperature region for nucleation of the ordinary VEC crystals is located in the vicinity of the glass transition temperature, T_g. On the other hand, the crystal growth is favored around 30 K above T_g. Therefore, in this experiment, the sample was cooled down to 173 K (= T_g + 2 K). At this temperature, it was subjected to an alternating electric field operating with different amplitudes and frequencies, for either 1 hour or 15 minutes. Then, the temperature was increased up to $T_c = 198$ K, and the crystallization progress was followed using dielectric spectroscopy, that is, by analyzing the drop of the dielectric permittivity ε' at 10 kHz with time.

The crystallization behavior of VEC at T_c is presented in Fig. 5 for those cases when the ac-field was applied for 1 hour at $T = 173$ K. As a reference, we also show the results for the sample annealed at 1 hour in the absence of an ac-field. As can be seen, when the nucleation process was carried out at the ac-field of 130 kV cm^{-1} with $\nu = 30$ mHz, there is a slight difference in the crystallization curves compared to the low-field case. The increase of the field amplitude from 130 kV cm^{-1} up to 180 kV cm^{-1} also has very little effect on the crystallization rate. However, the effect of the high field at $E = 130$ kV cm^{-1} becomes more pronounced when decreasing the frequency of the ac field from 30 mHz to 10 mHz. To understand the frequency effect, we consider the position of the 10 and 30 mHz cases relative to the loss peak frequency (ν_{max}) of the structural α-relaxation. The inset of Fig. 5 shows that at $T = 173$ K, the structural relaxation process has a peak maximum located at $\nu_{max} = 60$ mHz. It looks that the field-effect on the crystallization
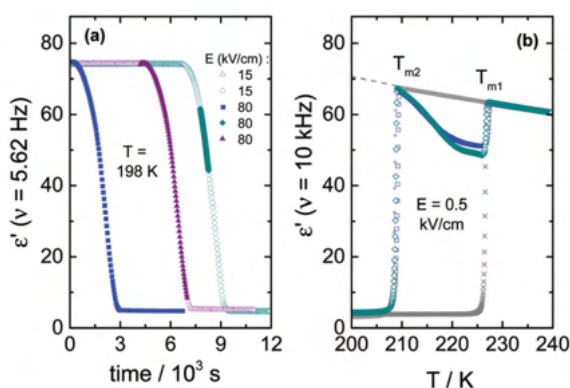

Fig. 4 (a) Isothermal crystallization of VEC at $T_c = 198$ K exposed to an ac field of $E = 80$ kV cm^{-1} at a frequency of $\nu = 5.62$ Hz switched on at the different stages of the crystallization process, as indicated by solid symbols; (b) evolution of the dielectric permittivity at $\nu = 10$ kHz as a function of temperature measured on heating of the crystalline material obtained in the preceding step. At the same conditions, in the absence of a high field, only the ordinary form of VEC is obtained, see crosses. Melting curves were measured at very low fields ($E = 0.5$ kV cm^{-1}) and at a fixed frequency of $\nu = 10$ kHz.
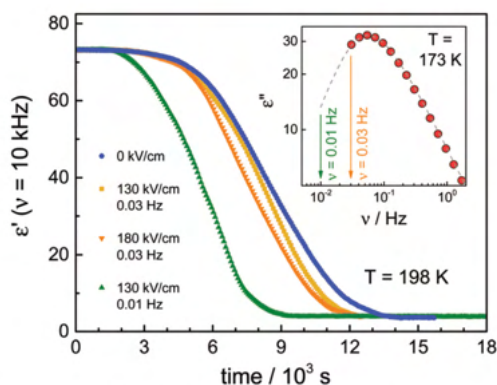
Fig. 5 Time-dependent changes in the dielectric permittivity ε' at frequency $\nu = 10$ kHz recorded upon crystallization of VEC at $T_c = 198$ K. Prior to these measurements, samples were annealed at $T = 173$ K in the presence of an ac field: $E = 130$ kV cm^{-1} ($\nu = 0.03$ Hz and $\nu = 0.01$ Hz), $E = 180$ kV cm^{-1} ($\nu = 0.03$ Hz) and $E = 0$ kV cm^{-1}. The inset shows the α-loss maximum at $T = 173$ K measured within the linear response regime. The arrows identify the frequencies used for high-field experiments.
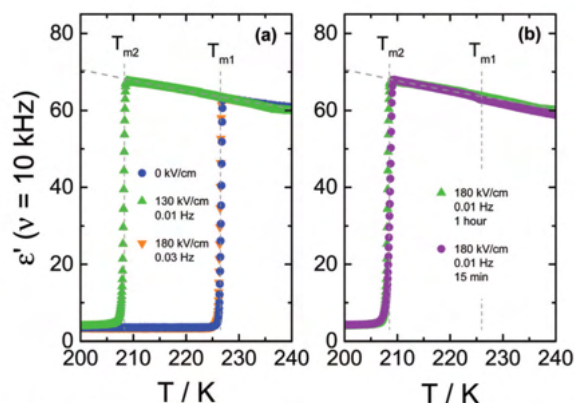

Fig. 6 Temperature dependence of the dielectric permittivity ε' (at $\nu = 10$ kHz) recorded upon heating of VEC crystals generated at $T_c = 198$ K by following protocol B; (a) melting curves recorded for samples nucleated for 1 hour at $T = 173$ K in the presence of an ac field: $E = 130$ kV cm^{-1} ($\nu = 0.03$ Hz and $\nu = 0.01$ Hz), $E = 180$ kV cm^{-1} ($\nu = 0.03$ Hz) and $E = 0$ kV cm^{-1}; (b) melting curves recorded for samples nucleated at $T = 173$ K with a fixed ac-field of $E = 180$ kV cm^{-1} and frequency $\nu = 10$ mHz for either 15 minutes or 1 hour. Data were measured in the linear response regime, at a heating rate of 1 K min^{-1}.

progress is more effective when decreasing the frequency of the ac-field much below ν_{max}. Thus, the onset frequency below which the crystallization rate at $T_c = 198$ K is systematically affected by the ac field is expected to be orders of magnitude below that characterizing molecular reorientation in polar liquids. Indeed, it was found to match with the time scale of the reorientation of much bigger structures like the crystal nuclei.[25] Therefore, the crystallization behavior of such polar molecular systems can be affected by a high ac field only below a certain frequency $\nu \ll \nu_{max}$. Provided this frequency condition is met, the increase of the ac field amplitude can accelerate the crystallization rate.

After complete crystallization, the melting behavior of the materials obtained in the course of the curves of Fig. 5 was identified *via* scanning T from 198 K to 245 K with a constant heating rate of 1 K min^{-1} (step 4 → 5, protocol 'B' shown in Fig. 1b). The corresponding dielectric results are presented in Fig. 6. We observe that the frequency of the ac-field affects not only the rate of crystallization but also the final crystallization product. For the nucleation carried out at $T = 173$ K in the presence of $E = 130$ kV cm^{-1} at $\nu = 10$ mHz, only the high-field polymorph is formed, with no signatures of the recrystallization to the ordinary, zero-field crystals. We obtained the same result earlier when the sample was exposed to a dc-bias field.[11] On the other hand, with $E = 130$ kV cm^{-1} and $\nu = 30$ mHz, it appears impossible to nucleate the high-field form at 173 K and, therefore, only the ordinary (low-field) VEC crystals are formed.

Up to this point, only cases associated with 1 hour annealing time at 173 K have been discussed. Now, we wish to assess if the time of applying high-field close to T_g affects the crystallization outcome. The curves in Fig. 6b compare the melting curves of the final products obtained using protocol 'B' after 15 and 60 minutes annealing at $T = 173$ K in the presence of 180 kV cm^{-1} at $\nu = 10$ mHz. The pure low-field polymorph was obtained in both situations and, by observation of the melting curves, there are no

significant differences in the final product. Consequently, durations beyond 15 minutes of applying the ac-field close to T_g do not have an impact concerning the crystal structure.

From these experiments based on protocol 'B', it is obvious that an alternating electric field can guide the nucleation process away from forming the ordinary crystal structure '1' and towards the new field-induced polymorph '2'. Given the right field conditions, *i.e.*, high amplitude and sufficiently low frequency, the preference for nucleating the low-melting polymorph '2' is extremely high, as no recrystallization is observed after melting at $T_{m2} = 208.5$ K. Again, the field not only produced the polymorph '2' nuclei but also prevent the nucleation of polymorph '1', which does occur in the absence of a field. The very-low-frequency case of 10 mHz yields results consistent with analogous experiments using a dc field.[11]

D. Frequency dependence

For the comparison of ac and dc type fields, it is important to realize that there is a marked frequency dependence for the effects obtained with ac fields. To emphasize this, we show the crystallization kinetics as a function of the frequency for a fixed amplitude of the ac-field using data obtained *via* protocol 'C'. In this case, the liquid sample was cooled down to the selected crystallization temperature, $T_c = 198$ K, which is about 27 K above T_g. At this temperature, the time scale of structural relaxation reaches $\tau_\alpha \approx 10^{-6}$ s. Then, the ac field was applied to induce the crystallization, following the protocol depicted in Fig. 1c. By keeping the field magnitude constant at $E = 80$ kV cm^{-1}, we investigated the frequency dependence of the ac field on the crystallization kinetics of the liquid under test, VEC. We have analyzed the evolution of the dielectric permittivity with time at various frequencies. The raw dielectric data presented in Fig. 7a
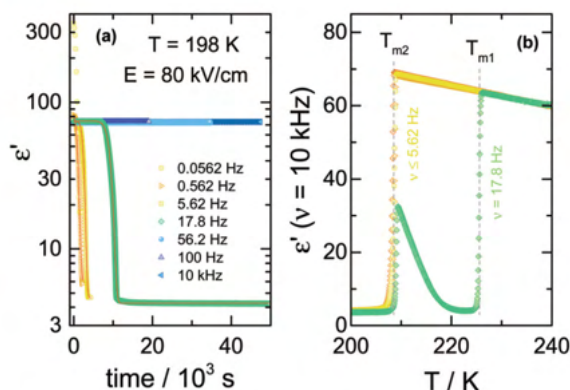
502 | *Phys. Chem. Chem. Phys.*, 2021, **23**, 498–505

This journal is © the Owner Societies 2021

61

Fig. 7 (a) Time evolution of dielectric permittivity ε' at $T_c = 198$ K upon time-dependent measurements of VEC with the ac electric field of $E = 80$ kV cm^{-1} at different frequencies: 56.2, 562 mHz, 5.62, 17.8, 56.2, 100 Hz and 10 kHz. Solid lines refer to data fitting to the stretched exponential function; (b) variation of ε', at $\nu = 10$ kHz, recorded on heating (with a rate of 1 K min^{-1}) of the crystalline material obtained in the preceding step, measured in the absence of a high ac field.

demonstrates that the crystallization speeds up as the ac field frequency decreases. The impact of the frequency is very amazing because after crossing a certain and very sharp threshold, the crystallization will not occur even after a few days waiting. We have pointed out this issue in our recent paper,[25] here changes in the dielectric response of the sample due to crystallization are reported as the volume fraction of crystalline material, V_{cry}/V_{total}.

After crystallization, the heating scan from $T = 198$ K to 245 K was performed to verify the composition of the crystalline material generated in the presence of ac-field. The corresponding melting curves are presented in Fig. 7b. In the low-frequency range, applying an ac-field of 80 kV cm^{-1} induces the formation of the low-temperature polymorph of VEC. The use of dc fields will also generate the high-field polymorph that melts at a temperature of about 20 K below that of the ordinary crystal.[11] However, as the frequency of the ac-field approaches the characteristic threshold of $\nu = 17.8$ Hz at $T = 198$ K, the final product is a mixture of the low-melting polymorph and the standard form. It is worth to note that the frequency of approximately $\nu \approx 18$ Hz corresponds to that associated with the alignment of the small crystal nuclei in electric fields.[25]

As with the nucleation results at $T = 173$ K discussed in Section C, we see again at $T_c = 198$ K that only below a certain frequency threshold can the ac-field alter the crystallization behavior of this polar molecular liquid. As a result, only frequencies below that threshold will be expected to compare with the dc results. It is not the absolute frequency that is relevant, but its value relative to the loss peak frequency, ν_{max}, that characterizes the structural relaxation time and viscosity at a given temperature. Also analogous to the nucleation at a low temperature of $T = 173$ K, field-induced nucleation at $T_c = 198$ K can lead to the low-melting crystal structure with high polymorph purity, as indicated by the lack of recrystallization above T_{m2} for the $\nu \leq 5.62$ Hz cases in Fig. 7b.

E. Crystallization kinetics

Two key parameters than can describe the crystallization kinetics are the characteristic crystallization time τ_{cry} and the Avrami parameter n. The latter provides information about the dimensionality and geometry of the growing crystals.[30] We determine both from the fitting of the crystallization curves with the use of the Avrami equation

$$V_{cry}/V_{total} = 1 - \exp\left[-\left(t/\tau_{cry}\right)^n\right] \quad (2)$$

Here, the time axis origin at $t = 0$ begins with the onset of crystallization and thus does not include the induction period.

The resulting dependencies of τ_{cry} on frequency ν and the field amplitude E at $T_c = 198$ K are collected for the tested compound in Fig. 8a and b, respectively. The evolution of the Avrami parameter n plotted as a function of frequency and amplitude of the ac-electric field is given in Fig. 9a and b, respectively. From the results compiled in Fig. 8, it is clear that the $\tau_{cry}(\nu)$ dependence has a sigmoidal curve with the two plateaus located at the high and low-frequency limits. When the ac field magnitude is fixed, the most pronounced changes are observed at the frequency range around 20–50 Hz. This is at least five orders of magnitude lower than the ν_{max} corresponding to the loss peak of the α-process, which characterizes molecular reorientation in liquids. When using an ac-field frequency, which is above the transition frequency region, the crystallization times are very long. Instead, for frequencies that are located below this transition, the crystallization rate eventually saturates and approaches the value characteristic for the static dc-field ($\nu = 0$ Hz). The use of different electrode materials, which in the present case are more rough titanium and highly polished stainless-steel, results in almost the same crystallization times. The characteristic frequency dependence is also seen when increasing the sample volume achieved by
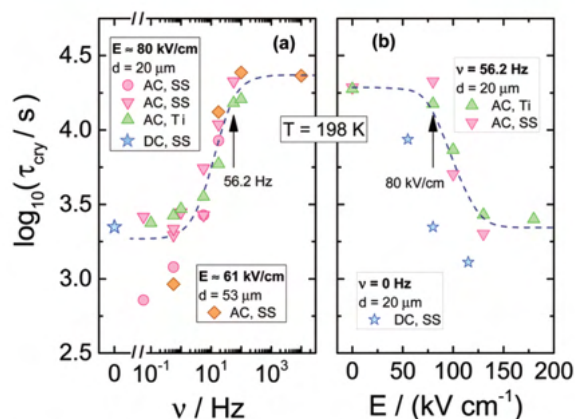

Fig. 8 The characteristic time of crystallization for VEC plotted as a function of (a) frequency at $E = 80$ kV cm^{-1} and $E = 61$ kV cm^{-1}; (b) amplitude of the ac-field at fixed frequency $\nu = 56.2$ Hz. Different electrode materials (SS vs. Ti) and different spacings d between the electrodes were used to discriminate possible electrode effects. The corresponding DC data were added for comparison.
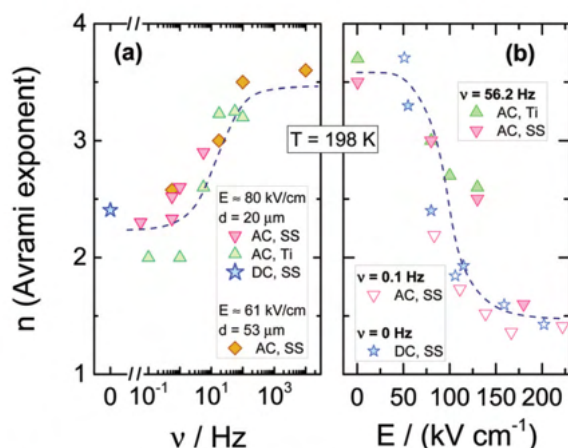
Fig. 9 Dependence of the Avrami parameter n for VEC as a function of (a) frequency at E = 80 kV cm^{-1} and E = 61 kV cm^{-1}; (b) amplitude of the ac-field at fixed frequency ν = 56.2 Hz and ν = 0.1 Hz. Different electrode materials (SS vs. Ti) and different spacings d between the electrodes were used to discriminate possible electrode effects. The corresponding DC data were added for comparison.

changing the electrode separation from 20 to 53 μm. The data of Fig. 8b show that increasing the field magnitude enhances the rate of crystallization, just like decreasing the field frequency. This ease of crystallization at higher amplitudes it due to the alteration of the potential energy of the molecules after them align with the electric field, contributing to form small nuclei that will facilitate effective crystal growth.

In order to observe the distinct changes in crystallization when the sample is exposed to high fields of varying magnitude, its frequency should be taken from the characteristic frequency transition region, as presented in Fig. 8a. When the frequency of the ac-field is remote from that corresponding to the reorientation frequency of the polar crystal nuclei, the effect of the ac field on crystallization is strongly diminished. For 56.2 Hz, the two limiting values of τ_{cry} are at E = 0 kV cm^{-1} and above E = 150 kV cm^{-1}, see Fig. 8b. At this magnitude of the field, the crystallization of VEC is accelerated by a factor of ten compared with the zero-field case. The discrepancy between τ_{cry} values seen in Fig. 8b for ac and dc experiments is only due to the high frequency (ν = 56.2 Hz) of the ac-field relative to the low-frequency limit established in Fig. 8a only for $\nu \leq 5.62$ Hz. Apart from this offset between ac and dc field data, the slope with which $\log(\tau_{cry})$ changes with field magnitude is very similar for the ac and dc cases.

Using high fields, one can influence not only the crystallization time but also how the molecular systems are arranged in the crystalline structure. The Avrami parameter n can capture such features. However, one should remember that the electric field forces a particular orientation of the crystallites, on the condition that the crystal nuclei suspended in the liquid are polar. The evolution of the Avrami parameter n as a function of frequency and field amplitude is presented in Fig. 9a and b, respectively. The results indicate that the morphology of growing

crystals is very sensitive to both parameters. Found at either low fields or high frequencies, the value $n \approx 3.6$ signifies a spherical growth of the crystallites with sporadic nucleation events. In contrast, with decreasing the frequency or increasing the field magnitude, the Avrami parameter drops down to approximately $n \approx 1.5$, which suggests that the crystallites adopt a more rod-like morphology and grow from instantaneously formed nuclei. For comparison, we also show the dependence of the Avrami parameter n on the dc bias field. Amazingly, they both fall onto the same pattern of behavior.

Conclusions

In this work, we have explored the effect of an ac electric field on the crystallization behavior of the polar molecular liquid, VEC. We have applied three experimental protocols that aim to focus on different aspects of the crystallization process. From the results, we deduce that a high electric field favors the formation of the new polymorph with lower melting temperature while at the same time impede the growth of the ordinary zero-field form. Supportive of this effect are a high field amplitude and a frequency of the ac field that allows for the reorientation of crystallites so that their free energy can be lowered by the field. Moreover, varying the field amplitude and frequency facilitates control over the crystallization time and the morphology of the growing crystals. Both parameters of the Avrami equation, the crystallization time (τ_{cry}) and the exponent (n) depend on frequency and field magnitude in a sigmoidal fashion, indicating limiting behavior for high amplitudes/low frequencies and for low amplitudes/high frequencies.

Interestingly, the low-frequency/high-field limiting values of τ_{cry} and n were found to be consistent with those obtained from the dc-bias experiments (ν = 0 Hz). Thus, both ac and dc electric fields can be used to tune and control the crystallization behavior of such materials. The field-induced changes in crystallization outcome will occur only for polar molecular systems that form crystal nuclei with lowered free energy due to the presence of the electrical field. With this condition fulfilled, sufficiently high field amplitudes can modify the crystallization kinetics and favor the formation of the new polymorphs. With the right protocol and field parameters, crystalline materials with very high polymorph purity could be obtained.

The knowledge of how to control the crystallization behavior is of great importance in material engineering and pharmaceutical applications, as different crystal structures will change the final product properties. Thus, the use of high ac-fields provides a new approach to modify the crystallization patterns and even promote or suppress specific polymorphs. This study outlines the potential routes to explore and the key parameters that should be considered to take advantage of the field effects on crystallization. Unfortunately, we are not able to carry out further studies of VEC's unique high-field polymorph due to its low melting point, which prevents ex situ structure studies at room temperature.

63

Conflicts of interest

There are no conflicts to declare.

Acknowledgements

References

1 A. Lendlein and S. Kelch, *Angew. Chem., Int. Ed.*, 2002, **41**, 2034.

2 J. Haleblian and W. McCrone, *J. Pharm. Sci.*, 1969, **58**, 911–929.

3 G. J. Evans, *Mater. Lett.*, 1984, **2**, 420–423.

4 M. Taleb, C. Didierjean, C. Jelsch, J. Mangeot, B. Capelle and A. Aubry, *J. Cryst. Growth*, 1999, **200**, 575–582.

5 C. N. Nanev and A. Penkova, *J. Cryst. Growth*, 2001, **232**, 285–293.

6 C. N. Nanev and A. Penkova, *Colloids Surf., A*, 2002, **209**, 139–145.

7 A. Moreno and G. Sazaki, *J. Cryst. Growth*, 2004, **264**, 438–444.

8 H. Koizumi, K. Fujiwara and S. Uda, *Cryst. Growth Des.*, 2009, **9**, 2420–2424.

9 T. K. Walter, C. F. da G. Ferreira, J. Iulek and E. M. Benelli, *ACS Omega*, 2018, **3**, 8683–8690.

10 G. Sazaki, A. Moreno and K. Nakajima, *J. Cryst. Growth*, 2004, **262**, 499–502.

11 K. Adrjanowicz, M. Paluch and R. Richert, *Phys. Chem. Chem. Phys.*, 2018, **20**, 925–931.

12 H. Koizumi, Y. Tomita, S. Uda, K. Fujiwara and J. Nozawa, *J. Cryst. Growth*, 2012, **352**, 155–157.

13 M. I. Al-haq, E. Lebrasseur, H. Tsuchiya and T. Torii, *Crystallogr. Rev.*, 2007, **13**, 29–64.

14 G. Di Profio, M. T. Reijonen, R. Caliandro, A. Guagliardi, E. Curcio and E. Drioli, *Phys. Chem. Chem. Phys.*, 2013, **15**, 9271.

15 J. E. Aber, S. Arnold, B. A. Garetz and A. S. Myerson, *Phys. Rev. Lett.*, 2005, **94**, 145503.

16 C. Parks, A. Koswara, H.-H. Tung, N. Nere, S. Bordawekar, Z. K. Nagy and D. Ramkrishna, *Cryst. Growth Des.*, 2017, **17**, 3751–3765.

17 K. Kotsuki, S. Obata and K. Saiki, *Langmuir*, 2014, **30**, 14286–14291.

18 E. Gattef and Y. Dimitriev, *Philos. Mag. B*, 1979, **40**, 233–242.

19 E. Gattef and Y. Dimitriev, *Philos. Mag. B*, 1981, **43**, 333–343.

20 D. Kashchiev, *J. Cryst. Growth*, 1972, **13–14**, 128–130.

21 D. Kashchiev, *Philos. Mag.*, 1972, **25**, 459–470.

22 J. O. Isard, *Philos. Mag.*, 1977, **35**, 817–819.

23 A. Y. Lee, D. Erdemir and A. S. Myerson, *Annu. Rev. Chem. Biomol. Eng.*, 2011, **2**, 259–280.

24 J. Bauer, S. Spanton, R. Henry, J. Quick, W. Dziki, W. Porter and J. Morris, *Pharm. Res.*, 2001, **18**, 859–866.

25 D. M. Duarte, R. Richert and K. Adrjanowicz, *J. Phys. Chem. Lett.*, 2020, **11**, 3975–3979.

26 A. Jedrzejowska, K. L. Ngai and M. Paluch, *J. Phys. Chem. A*, 2016, **120**, 8781–8785.

27 A. Jedrzejowska, Z. Wojnarowska, K. Adrjanowicz, K. L. Ngai and M. Paluch, *J. Chem. Phys.*, 2017, **146**, 094512.

28 S. Roy and R. Richert, *Biochim. Biophys. Acta, Proteins Proteomics*, 1844, **2014**, 323–329.

29 U. Pathak and R. Richert, *Colloid Polym. Sci.*, 2014, **292**, 1905–1911.

30 M. Avrami, *J. Chem. Phys.*, 1940, **8**, 212–224.
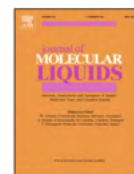
This journal is © the Owner Societies 2021

Phys. Chem. Chem. Phys., 2021, **23**, 498–505 | **505**

64

Bimodal crystallization rate curves of a molecular liquid with Field-Induced polymorphism

D.M. Duarte [a,b,*], R. Richert [c], K. Adrjanowicz [a,b,*]

[a] Institute of Physics, University of Silesia, 75 Pulku Piechoty 1, Chorzow 41-500, Poland
[b] Silesian Center for Education and Interdisciplinary Research (SMCEBI), 75 Pulku Piechoty 1, Chorzow 41-500, Poland
[c] School of Molecular Sciences, Arizona State University, Tempe, AZ 85287, USA

ARTICLE INFO

ABSTRACT

In this study, we use dielectric spectroscopy to explore how frequency and amplitude of an applied strong electric field affect the overall crystallization kinetics over a range of temperatures, focusing on a molecular system with field-induced polymorphism: vinyl ethylene carbonate (VEC). The volume fraction of the field-induced polymorph can be controlled by the parameters of the high-electric field, i.e., frequency and amplitude. We find that the crystallization rate maximum of the field induced polymorph is located at lower temperatures relative to the that of the regular polymorph. The temperature of the highest crystallization rate for the regular polymorph was found to be unaffected by the electric field, but the overall rates increase with increasing field amplitude. The dimensionality of crystal growth is also analyzed via the Avrami parameter and is frequency invariant but affected by the field amplitude. Our results demonstrate that a detailed knowledge of the influence of high fields on crystallization facilitates control over the crystallization behavior and the final product outcome of molecular systems, providing new opportunities for material engineering and improving pharmaceuticals.

1. Introduction

If a liquid is supercooled to a sufficiently low temperature and rapidly enough, it can avoid crystallization and reach a glassy state. In this regime, the system is far from thermodynamic equilibrium and tends to rearrange itself in the well-defined array of atoms/molecules of a crystal structure. A complete understanding of the crystallization process is a fundamental goal since the numerous properties of the final product depend on the degree of crystallinity, polymorphism, grain size, or crystal quality.[1–3]

Different factors can affect crystallization. An elementary guide to the crystal formation and description of its relation to the glassy state comes from the classical theories of nucleation and growth. [4,5] In a classical view, the crystallization process involves forming an embryonic nucleus and its subsequent growth. The rates of nucleation, $J(T)$, and crystal growth, $u(T)$, are subject to distinct temperature profiles, but each process typically reaches its maximum at some temperature between glass transition at T_g and the melting point at T_m. The temperature of the highest crystal growth rate (u) is usually above that of the nucleation rate (J). The temperature zone in which $u(T)$ and $J(T)$ curves overlap considerably leads to ideal conditions for fast crystallization, especially on cooling the melt.[6,7]

Several experimental, as well as theoretical studies, have revealed that sufficiently high electric fields affect crystallization. [5,8–17] However, predicting how the electric field will affect the crystallization is not fully established. In a classical view, the electric field affects both nucleation (J) and crystal growth (u):[18,19]

$$J \propto D \exp\left(-\Delta G_c(E)/k_B T\right) \qquad (1)$$

$$u \propto D[1 - \exp\left(-\Delta \mu(E)/k_B T\right)] \qquad (2)$$

where D is a diffusion constant, ΔG_C is the Gibbs free energy, and $\Delta \mu$ is the difference in chemical potentials between melt and crystal phase. Both ΔG_C and $\Delta \mu$ will be affected by the electric field, also making J and u dependent on the electric field. Still, the information needed to predict the magnitude of the field on the crystallization is generally not available. In the case of polar liquids, the modifications of thermodynamic potentials[20–22], free energy and entropy, and the field-induced orientation[23,24] induced by high electric fields can have an enormous impact due to the possibility of leading the final product into a different polymorph.[17,18]

A single component glass-forming liquid with a relatively large value of the permanent dipole moment[25], vinyl ethylene carbonate (VEC), a vinyl derivative of propylene carbonate (PC), has been studied recently under high electric fields. [9,17,18,26] It was

---

* Corresponding authors.
  E-mail addresses: daniel.duarte@smcebi.edu.pl, dduarte@us.edu.pl (D.M. Duarte).

shown that the crystallization time is shortened and/or a completely new polymorphic form can be obtained when a high electric field is applied. Additionally, it was found that these electric field effects are influenced by the frequency and magnitude of the applied electric field.

Despite the research previously done, there is no predictive theory or experimental evidence that addressed how the high-electric field influences the crystallization rate curves. This work steps forward on resolving this question by exploring how the electric field affects the crystallization behavior of VEC for different temperatures and for different volume fractions of the field-induced polymorph after crystallization has been completed. For a wide range of crystallization temperatures, T_c, VEC is subjected to different magnitudes and frequencies of alternating (AC) or static (DC) high fields. We analyze the Avrami parameters (rate k, exponent n) of the crystallization kinetics and subsequently record the melting profiles of the final crystallized product. This facilitates disentangling the crystallization curves $k(T_c)$ for the two polymorphs, the regular and the field-induced ones, in a more wide temperature range. The results presented in this work yield valuable information about the effects of the electric field on the crystallization rate curve, completing a study on the influence of the electric field on the crystallization of the VEC.

2. Experimental

The compound 4-vinyl-1,3-dioxolan-2-one or vinyl ethylene carbonate (VEC, purity 99%) was obtained from Sigma-Aldrich and used as received. The liquid was loaded into two parallel polished stainless-steel electrodes separated by a Teflon ring of $d = 25$ μm nominal thickness, leaving an active inner electrode surface area of $r = 7$ mm radius. The resulting geometric capacitance is $C_{geo} = \varepsilon_0 \pi r^2 / d = 54.5$ pF. By comparing the observed permittivity with reference data, the actual electrode separation was determined to be closer to 20 μm. A Novocontrol Quatro temperature control system was responsible for regulating the temperature of the sample cell with stability better than 0.1 K.

The dielectric measurements were carried out in the frequency range from 10^{-1} to 10^4 Hz using a Novocontrol Alpha Analyzer. The high voltage unit HVB1000 from Novocontrol was used to achieve the high electric fields. This extension test interface boosts the voltages of the Alpha Analyzer from 40 V_{peak} to 500 V_{peak}. All voltage and field amplitudes are reported as root-mean-square (RMS) values. All fields intended to affect crystallization were around $E \approx 80$ kV cm^{-1}, while amplitudes of the alternating fields used to measure dielectric permittivity, ε, in the linear regime were kept below 16 kV cm^{-1}, which is a factor of ≈ 25 lower in terms of nonlinear ($\sim E^2$) effects.

3. Results and discussion

To identify the influence of the magnitude and frequency of the electric field on the crystallization of VEC at different temperatures, we have followed the thermal protocol shown in Fig. 1. This experiment starts at the temperature $T = 243$ K, which is 15 K above the melting temperature of the low-field polymorph and thus ensures an equilibrated state. In the next step, the sample is cooled down to $T = 173$ K ($= T_g + 2$ K) with a rate of approximately 10 K min^{-1}. The sample is exposed to the desired high field, DC or AC, for 1 h at this temperature. For reference, experiments at zero field were also performed. Thereupon, the temperature of the sample is increased to the crystallization temperature, located between 193 K and 223 K, at a rate of approximately 5 K min^{-1}. The progress of the crystallization is followed using dielectric spectroscopy, that is, by analyzing the drop of the dielectric permittiv-
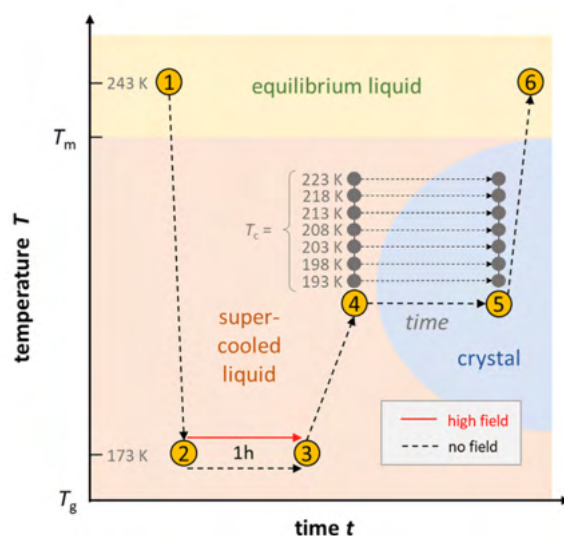

Fig. 1. Overview of the experimental protocol used to study the effect of the magnitude and frequency of the field on the crystallization of VEC at different crystallization temperatures, T_c.

ity at 10 kHz with time. After crystallization, the sample was heated at a constant rate of 1 K min^{-1} to $T = 245$ K, and the melting behavior is followed by measuring the dielectric permittivity at 10 kHz during this heating ramp. Due to the high conductivity of the sample at elevated temperatures and the resulting risk of sample failure, it is not possible to follow a different experimental procedure where high fields are applied during crystallization.

After increasing the temperature from $T = 173$ K to the desired crystallization temperature in the absence of a field, the crystallization progress can be monitored by analyzing the changes in the real part of dielectric permittivity using dielectric spectroscopy. In polar liquids, the dielectric constant is dominated by polarization due to rotational motion of permanent dipoles. However, these motions are suppressed when the sample is crystallized, making it possible to follow the crystallization process using dielectric techniques. Therefore, as a good approximation, ε' measures the fraction of crystal (V_{cry}/V_{total}) through[18,27,28]

$$V_{cry}/V_{total} = (\varepsilon_s - \varepsilon')/(\varepsilon_s - \varepsilon_\infty) \tag{3}$$

where ε_s is the dielectric constant of the liquid and ε_∞ is considered the permittivity of the crystalline state and of the liquid in the high frequency limit, in which orientational contributions from permanent dipoles are absent. The volume fraction can be related to the rate of crystallization, k, and the Avrami parameter, n, which represents the dimensionality and geometry of the crystal growth through the Avrami relation [29,30]

where t is the time after the onset of crystallization, i.e., excluding the incubation time of the process. In cases where both crystal types are formed, the superposition of two Avrami curves may be expected to be required to fit the crystallization behavior. Instead, we observe, as previously, [9,17,18,26] that a single Avrami fit provides a good representation of the data. If the two crystal types lead to distinct Avrami curves, their difference cannot be resolved on the basis of the present data.

3.1. Crystallization rates

In Fig. 2a, we present the temperature dependence of k as measured between $T_c = 193$ K and 223 K using an AC field
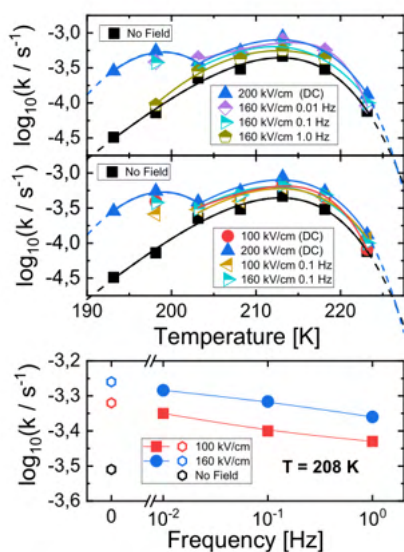
Fig. 2. The characteristic time of crystallization for VEC plotted as a function of crystallization temperature using different field magnitudes (a) E = 200 kV cm^{-1} for a DC field and E = 160 kV cm^{-1} for an AC field with different frequencies; (b) E = 200 and 100 kV cm^{-1} for a DC field and E = 160 and 100 kV cm^{-1} for an AC field at fixed frequency, f = 10^{-1} Hz. Solid lines are fits to the experimental data with the use of an exponential function plus a linear term. Panel (c) shows the frequency dependence of the crystallization rate when using AC fields. The values obtained in the absence of high-field and for DC case were added as a reference.

(E = 160 kV cm^{-1}) of different frequencies. For the crystallization experiments where no field was applied, the logarithmic crystallization rate increases from -4.49 at 193 K to -3.33 at 213 K and then decreases again at higher temperatures. In this way, the most favorable temperature region for crystallization is within the 210–220 K range, as indicated by the maximum of the crystallization rate curve. For the highest field frequency that we use, i.e., 1 Hz, we do not observe any changes in the overall crystallization rate curve position, but a uniform increment in the crystallization rate can be observed if compared to the zero field case.

The crystallization rate behavior, $k(T_c)$, for the case where we use the same field amplitude, 160 kV cm^{-1}, but at a lower frequency, f = 0.1 Hz, shows a qualitative difference compared with the f = 1 Hz situation. At T_c = 198 K and below, instead of the value of k further decreasing, the rate increases and gives rise to another crystallization maximum located at lower temperatures. This new maximum is due to the field-induced polymorph generated for frequencies below a specific threshold and with sufficient magnitude of the field.[9,26] For higher temperatures, $T_c \geq 203$ K, the same field parameters result only in an increase of the magnitude of the crystallization rate. For an even lower frequency, f = 10^{-2} Hz, we also observe two crystallization rate maxima, see Fig. 2a, but with a somewhat higher rate k at low temperatures relative to the f = 0.1 Hz cases. Likewise, for the crystallization curve associated with higher temperatures, the rates also increase with lowering the frequency, while its maximum position is largely maintained. The DC- field, f = 0, promotes the optimal formation rate of the new polymorph, consistent with the frequency dependence discussed above.

The dependence of k with the magnitude of the electric field is presented in Fig. 2b. For the case of the AC field, the chosen fixed frequency was f = 0.1 Hz. At this frequency, it is possible to generate the field-induced polymorph. For both field magnitudes, 100 and 160 kV cm^{-1}, it is possible to observe two crystallization rate

maxima, associated with the field-induced and ordinary polymorphs, at low and higher temperatures, respectively. The magnitude of the crystallization rate increases with higher field amplitudes; however, the temperature position of the maximum remains unchanged. Likewise, for DC values, with field magnitudes of 100 and 200 kV cm^{-1}, it is possible to observe the crystallization maxima associated with both polymorphs. Comparing both curves, we observe that the maximum of the crystallization curve remains unchanged; however, the rates increase with increasing the field magnitude. A closer look at the influence of the magnitude and frequency of the high electric field on crystallization rate k is presented in Fig. 2c. At the selected temperature, T_c = 208 K, we can observe that with increasing the field magnitude the crystallization rate for both AC and DC fields increases. Moreover, in the AC case, the frequency also has an essential role in controlling the crystallization rate. For lower frequencies, the values of k are higher and approach the levels observed with DC fields.

Overall, the position of the crystallization rate maximum is independent of the magnitude and frequency of the applied field. However, these factors can promote crystallization progress. For example, increasing the amplitude of the applied field, or in AC case, decreasing the frequency of the applied field can increase the crystallization rate. Moreover, at lower temperatures (i.e., closer to the glass transition), it is possible to generate a new polymorph when using sufficiently low frequencies or higher field amplitudes. The crystallization rate, also in this case, will depend on the amplitude and frequency of the applied field. As for the separation of these crystallization curves associated with the two polymorphs, the contribution of the ordinary polymorph with a higher maximum position is expected to reflect $u(T)$, as previous studies have shown the absence of nucleation for $T \geq 198$ K.[26] The lower temperature contribution associated with the field-induced polymorph will reflect a mix of $J(T)$ and $u(T)$, since that polymorph can be nucleated at high fields around T = 198 K.

3.2. Avrami analysis

Applying a high-electric field not only affects the crystallization time but also influences the dimensionality of growing crystals. These changes can be tracked using the Avrami parameter, n, see Eq. (4). The evolution of n as a function of temperature is plotted in Fig. 3a and 3b for different field frequencies and amplitudes, respectively. As can be seen, the Avrami parameter increases with increasing the temperature, changing from $n \approx 2$ at lower temperatures to $n \approx 3.5$ at higher temperatures in the case of zero field. When using 200 kV cm^{-1} (DC), the n value at T_c = 193 K is similar to the zero field case, while with increasing the temperature it increases to $n \approx 4$. This suggests that the crystallites adopt a rod-like morphology and grow from instantaneously formed nuclei at lower temperatures, while at higher temperatures, its growth progresses in a spherical way with a sporadic nucleation event. It is observed that increasing the field magnitude will affect the Avrami parameter. The n values are higher when increasing the magnitude of the electric field, both AC and DC. Interestingly, as we observe in Fig. 3b, the frequency of the AC field does not influence the dimensionality of growing crystals in the present temperature range.

In Fig. 3c, we can observe in more detail, for a selected temperature, T_c = 213 K, that the Avrami parameter depends on the magnitude of the applied electric field. Specifically, it increases as the amplitude of the field increases, whereas it does not change significantly when the field frequency is changed. The field frequency should affect more the crystallization rate, as observed in a previous paper.[26] However, in the present experimental protocol, the field is applied at a low temperature, T = 173 K, and the crystallization progresses in the absence of a strong field. Herewith, the particles are not forced to be oriented due to the presence of the field,
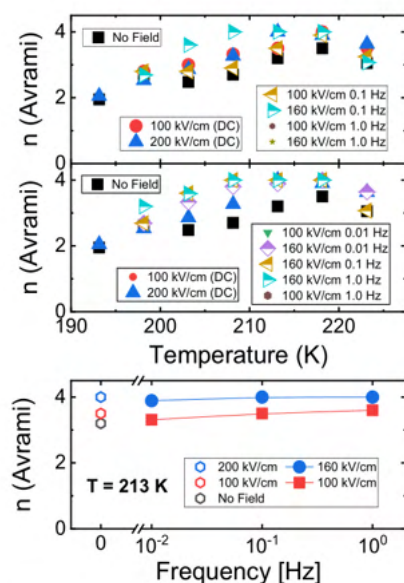
Fig. 3. The Avrami parameter for VEC plotted as a function of crystallization temperature at (a) E = 200 kV cm^{-1} for DC field and E = 160 kV cm^{-1} for AC field with different frequencies; (b) E = 200 kV cm^{-1} for DC field and E = 160 and 100 kV cm^{-1} for AC field at 10^{-1} Hz; Panel (c) shows the evolution of crystallization rate as a function of the frequency of the used AC field. The values obtained in the absence of high-field and for DC case were added for reference. Error bars for n are no included, as they do not exceed the symbol size in this graph.

contrary to what happens when there is a high field applied with the crystallization ongoing.

It is highly desirable to come to a more molecular understanding of the interplay between the effect of the external field and crystallization temperature. The frequency dependence pointed toward the field-induces crystal nuclei being macroscopically polarized but a crystal structure analysis in needed in order to gain a better understanding, which is not available because ex-situ studies are not easily possible with sub-ambient melting temperatures.

3.3. Melting behavior

After the crystallization is completed, the melting process was followed in the absence of a high electric field to verify the final product. The melting curves measured at f = 10 kHz, at a rate of ΔT = 1 K min^{-1}, are shown in Fig. 4, for all crystallization temperatures of this study. In the case when no high electric field was applied, we can observe only the formation of one polymorph with melting temperature $T_{m1} \approx$ 227 K. Similar to the non-field case, when the AC field is applied with f = 1 Hz and magnitude of 100 or 160 kV cm^{-1}, only one melting event is detected, associated with the regular polymorph. However, for a crystallization temperature of T_c = 198 K, with the frequency of the AC field decreased to f = 10^{-1} or 10^{-2} Hz, we observe an additional melting event at $T_{m2} \approx$ 208 K, associated with the field-induced polymorph. Intuitively, melting at T_{m2} is associated with the crystallization event taking place at lower temperatures, as observed in Fig. 2a and 2b. The transition at 208 K is identified as melting of the high-field crystal, as the process recovers the orientational degrees of freedom characteristic of the liquid state. The process is thus incompatible with a solid–solid transition, which would not be associated with
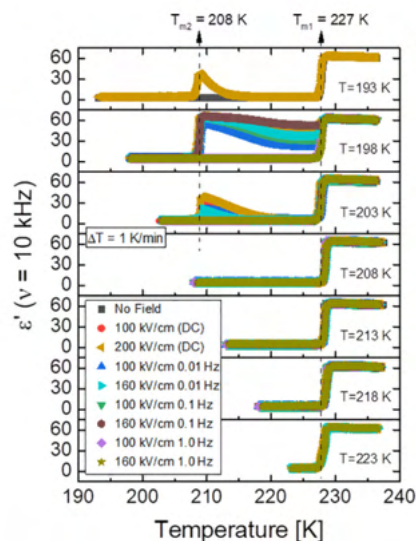
Fig. 4. Melting curves of previously crystallized VEC analyzed in terms of the permittivity ε' measured at a frequency ν = 10 kHz upon scanning temperature from the crystallization temperature to 245 K at a rate of 1 K min^{-1}. Crystallization has been field-induced using different magnitudes and frequencies of the field, as indicated in the legends. The zero field crystallization counterpart is added for reference.

recovering the static dielectric constant of the pure liquid state. The subsequent crystallization above 208 K is the result of residual nuclei of the stable type I crystals, and the melting event at 208 K also occurs in the absence of recrystallization (see for more details [17]). The intensity of the ε' peak near T_{m2}, which can be associated with the volume fraction of the metastable polymorph, increases when using the AC field frequency of f = 10^{-2} Hz compared with f = 10^{-1} Hz. At T_c = 203 K, only the frequency f = 10^{-2} Hz can produce the field-induced polymorph, while in the case of f = 10^{-1} Hz, there are no traces associated with the high-field polymorph melting recorded in the dielectric temperature scans. All other melting curves associated with crystallization temperatures between 208 K and 223 K follow the same behavior as the no-field case, showing only the ordinary polymorph which melts at T_{m1}.

The influence of the magnitude of the high electric field on the final product composition can be observed in the melting events. For example, in Fig. 4, at T_c = 198 K, for frequencies f = 10^{-1} Hz and f = 10^{-2} Hz, we observe that the intensity of dielectric permittivity is higher when using 160 kV cm^{-1} in comparison with 100 kV cm^{-1}. The same can be observed at T_c = 203 K, for f = 10^{-2} Hz, the melting event is more intense when the field magnitude increases. A higher value of the dielectric permittivity at T_{m2} indicates that the fraction of the high-field polymorph obtained in the crystallized material was greater in such cases. Likewise, when the DC field is used, we observe two melting events for crystallization temperatures between T_c = 193 K and T_c = 203 K, while for the remaining temperatures, only one melting event at T_{m1} is observed. Similar to the AC field, the magnitude of the DC high-field affects the quantity of formed polymorph. At T_c = 198 K and T_c = 203 K, when the magnitude of the field was 200 kV cm^{-1} in comparison to when the field magnitude used was 100 kV cm^{-1} shows a higher intensity of the ε' in comparison to when the field magnitude used was 100 kV cm^{-1}. All the remaining temperatures, between T_c = 208 K to T_c = 223 K, show the same behavior as the zero field case.

4

4. Conclusions

In this work, the effect of the high-electric field on the crystallization of polar molecular liquid was explored, with focus on the crystallization rate in a wide temperature range. First, the electric field was only applied close to T_g, and then the sample was heated up to the desired crystallization temperature, T_c. We have shown that the frequency and amplitude of the applied AC high-field allow forming at lower temperatures one additional crystallization curve maximum, related to the formation of the field-induced polymorph with distinct melting temperature. Moreover, increasing the magnitude or decreasing the frequency of the applied field will increase the crystallization rate of this polymorph. Likewise, a high DC field influences the crystallization in the same manner as an AC field of very low frequency. However, these factors do not affect the position of the crystallization rate maxima. Additionally, the melting curves show that the quantity of the field-induced polymorph in the final crystalline material can be controlled by changing the magnitude or frequency of the field. Finally, the Avrami parameter n was found to be affected by the magnitude of both DC and AC electric fields or by the temperature at which crystallization occurs, while it seems to be independent of the frequency of the applied AC field.

This work sums up the study of how AC and DC fields can influence the crystallization behavior of VEC using dielectric spectroscopy. Together with previous reports,[9,17,18,26] it provides a complete picture of how to control or suppress specific polymorphs by using the frequency or amplitude of the applied field, potentially useful in materials engineering or the pharmaceutical industry. Unfortunately, it is not possible to study the final crystallization product of VEC in more detail due to its low melting point, which limits the options of in-situ studies of the structure. The sub-ambient melting point (-35 °C) of the crystals prevent a direct characterization of their crystal structure and molecular properties. This is especially true for the field-induced polymorph. We aim to conduct such studies for a field induced polymorph for which the melting point is above room temperature. However, our results collected for VEC still provide an essential experimental guide that can be used for more advanced future studies, aimed at applying a high electric field to control the crystallization behavior of molecular materials.

Declaration of Competing Interest

The authors declare that they have no known competing financial interests or personal relationships that could have appeared to influence the work reported in this paper.

Acknowledgment

References

[1] J. Haleblian, W. McCrone, Pharmaceutical Applications of Polymorphism, J. Pharm. Sci. 58 (8) (1969) 911–929, https://doi.org/10.1002/jps.2600580802.
[2] N. Rodríguez-hornedo, D. Murphy, Significance of Controlling Crystallization Mechanisms and Kinetics in Pharmaceutical Systems, *J Pharmaceutical Sci.* Am Chem Soc July 1 88 (7) (1999) 651–660, https://doi.org/10.1021/js980490h.
[3] A. Lendlein, S. Kelch, Shape-Memory Polymers. *Angew. Chemie Int. Ed.* 41 (12) (2002) 2034, https://doi.org/10.1002/1521-3773(20020617)41:12<2034::AID-ANIE2034>3.0.CO;2-M.
[4] R. Becker, W. Döring, Kinetische Behandlung Der Keimbildung in Übersättigten Dämpfen, Ann. Phys. 416 (8) (1935) 719–752, https://doi.org/10.1002/(ISSN)1521-388910.1002/andp.v416:810.1002/andp.19354160806.

[5] I.S. Gutzow, J.W.P. Schmelzer (Eds.), The Vitreous State, Springer Berlin Heidelberg, Berlin, 2013.
[6] J.A. Baird, B. Van Eerdenbrugh, L.S. Taylor, A Classification System to Assess the Crystallization Tendency of Organic Molecules from Undercooled Melts, J. Pharm. Sci. 99 (9) (2010) 3787–3806, https://doi.org/10.1002/jps.22197.
[7] N.S. Trasi, L.S. Taylor, Effect of Polymers on Nucleation and Crystal Growth of Amorphous Acetaminophen, CrystEngComm 14 (16) (2012) 5188, https://doi.org/10.1039/c2ce25374g.
[8] G.J. Evans, Crystal Growth in Electric Fields, Mater. Lett. 2 (5) (1984) 420–423, https://doi.org/10.1016/0167-577X(84)90153-8.
[9] D.M. Duarte, R. Richert, K. Adrjanowicz, Frequency of the AC Electric Field Determines How a Molecular Liquid Crystallizes, J. Phys. Chem. Lett. 11 (10) (2020) 3975–3979, https://doi.org/10.1021/acs.jpclett.0c01002.
[10] K. Kotsuki, S. Obata, K. Saiki, Electric-Field-Assisted Position and Orientation Control of Organic Single Crystals, Langmuir 30 (47) (2014) 14286–14291, https://doi.org/10.1021/la503286y.
[11] C. Parks, A. Koswara, H.-H. Tung, N. Nere, S. Bordawekar, Z.K. Nagy, D. Ramkrishna, Molecular Dynamics Electric Field Crystallization Simulations of Paracetamol Produce a New Polymorph, Cryst. Growth Des. 17 (7) (2017) 3751–3765, https://doi.org/10.1021/acs.cgd.7b0035610.1021/acs.cgd.7b00356.s001.
[12] M. Taleb, C. Didierjean, C. Jelsch, J. Mangeot, B. Capelle, A. Aubry, Crystallization of Proteins under an External Electric Field, J. Cryst. Growth 200 (3–4) (1999) 575–582, https://doi.org/10.1016/S0022-0248(98)01409-2.
[13] Z. Hammadi, S. Veesler, New Approaches on Crystallization under Electric Fields, Prog. Biophys. Mol. Biol. 101 (1–3) (2009) 38–44, https://doi.org/10.1016/j.pbiomolbio.2009.12.005.
[14] C.N. Nanev, A. Penkova, Nucleation of Lysozyme Crystals under External Electric and Ultrasonic Fields, J. Cryst. Growth 232 (1–4) (2001) 285–293, https://doi.org/10.1016/S0022-0248(01)01169-1.
[15] J.E. Aber, S. Arnold, B.A. Garetz, A.S. Myerson, Strong Dc Electric Field Applied to Supersaturated Aqueous Glycine Solution Induces Nucleation of the γ Polymorph, Phys. Rev. Lett. 94 (14) (2005), https://doi.org/10.1103/PhysRevLett.94.145503 145503.
[16] G. Di Profio, M.T. Reijonen, R. Caliandro, A. Guagliardi, E. Curcio, E. Drioli, Insights into the Polymorphism of Glycine: Membrane Crystallization in an Electric Field, Phys. Chem. Chem. Phys. 15 (23) (2013) 9271, https://doi.org/10.1039/c3cp50664a.
[17] K. Adrjanowicz, M. Paluch, R. Richert, Formation of New Polymorphs and Control of Crystallization in Molecular Glass-Formers by Electric Field, Phys. Chem. Chem. Phys. 20 (2) (2018) 925–931, https://doi.org/10.1039/C7CP07352F.
[18] K. Adrjanowicz, R. Richert, Control of Crystallization Pathways by Electric Fields. In *Dielectrics and crystallization*, Springer (2020) 149–167, https://doi.org/10.1007/978-3-030-56186-4_6.
[19] J.W.P. Schmelzer, Crystal Nucleation and Growth in Glass-Forming Melts: Experiment and Theory, J. Non. Cryst. Solids 354 (2–9) (2008) 269–278, https://doi.org/10.1016/j.jnoncrysol.2007.06.103.
[20] D. Kashchiev, Nucleation in External Electric Field, J. Cryst. Growth 13–14 (C) (1972) 128–130, https://doi.org/10.1016/0022-0248(72)90074-7.
[21] D. Kashchiev, On the Influence of the Electric Field on Nucleation Kinetics, Philos. Mag. 25 (2) (1972) 459–470, https://doi.org/10.1080/14786437208226816.
[22] J.O. Isard, Calculation of the Influence of an Electric Field on the Free Energy of Formation of a Nucleus, Philos. Mag. 35 (3) (1977) 817–819, https://doi.org/10.1080/14786437708236010.
[23] E. Gattef, Y. Dimitriev, Reversible Monopolar Switching in Vanadium-Tellurite Glass Threshold Devices, Philos. Mag. B 40 (3) (1979) 233–242, https://doi.org/10.1080/13642817908246373.
[24] E. Gattef, Y. Dimitriev, Nucleation Theory of Threshold Switching in Vanadate-Glass Devices, Philos. Mag. B 43 (2) (1981) 333–343, https://doi.org/10.1080/13642818108221903.
[25] A. Jedrzejowska, Z. Wojnarowska, K. Adrjanowicz, K.L. Ngai, M. Paluch, Toward a Better Understanding of Dielectric Responses of van Der Waals Liquids: The Role of Chemical Structures, J. Chem. Phys. 146 (9) (2017) 094512, https://doi.org/10.1063/1.4977736.
[26] D.M. Duarte, R. Richert, K. Adrjanowicz, AC versus DC Field Effects on the Crystallization Behavior of a Molecular Liquid, Vinyl Ethylene Carbonate (VEC), Phys. Chem. Chem. Phys. 23 (1) (2021) 498–505, https://doi.org/10.1039/D0CP05290F.
[27] J. Mijovic, J.-W. Sy, T.K. Kwei, Reorientational Dynamics of Dipoles in Poly (Vinylidene Fluoride)/Poly(Methyl Methacrylate) (PVDF/PMMA) Blends by Dielectric Spectroscopy, Macromolecules 30 (10) (1997) 3042–3050, https://doi.org/10.1021/ma961774w.
[28] M.H. Jensen, C. Alba-Simionesco, K. Niss, T. Hecksher, A Systematic Study of the Isothermal Crystallization of the Mono-Alcohol n-Butanol Monitored by Dielectric Spectroscopy, J. Chem. Phys. 143 (13) (2015) 134501, https://doi.org/10.1063/1.4931807.
[29] M. Avrami, Kinetics of Phase Change, I General Theory. *J. Chem. Phys.* 7 (12) (1939) 1103–1112, https://doi.org/10.1063/1.1750380.
[30] M. Avrami, Kinetics of Phase Change. II Transformation-Time Relations for Random Distribution of Nuclei, J. Chem. Phys. 8 (2) (1940) 212–224, https://doi.org/10.1063/1.1750631.

5

STATEMENTS OF THE AUTHOR AND CO-AUTHORS

Chorzów, 13.09.2021

Daniel Duarte
Institute of Physics
University of Silesia in Katowice
75 Pułku Piechoty 1A,
41-500 Chorzów, Poland

Declaration

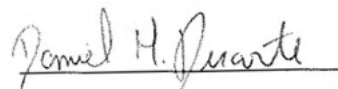**I declare that I contribute to the following works**

Daniel M. Duarte, Ranko Richert, and Karolina Adrjanowicz, *Frequency of the AC Electric Field Determines How a Molecular Liquid Crystallizes*, J. Phys. Chem. Lett. 2020, 11, 10, 3975–3979

Daniel M. Duarte, Ranko Richert, and Karolina Adrjanowicz, *Watching the Polymorphic Transition from a Field-Induced to a Stable Crystal by Dielectric Techniques*, Cryst. Growth Des. 2020, 20, 5406-5412

Daniel M. Duarte, Ranko Richert, and Karolina Adrjanowicz, *AC versus DC field effects on the crystallization behavior of a molecular liquid, vinyl ethylene carbonate (VEC)*, Phys. Chem Chem. Phys., 2021, 23, 498

Daniel M. Duarte, Ranko Richert, and Karolina Adrjanowicz, *Bimodal Crystallization Rate Curves of a Molecular Liquid with Field-Induced Polymorphism*, J. Molecular Liquids, 2021, 342, 117419

In the following way: I acquire, analyse and interpreted the data and draft the manuscripts.

Daniel M. Duarte

Daniel Duarte

Chorzów, 13.09.2021

dr hab. Karolina Adrjanowicz
Institute of Physics
University of Silesia in Katowice
75 Pułku Piechoty 1A,
41-500 Chorzów, Poland

Declaration

I declare that I contribute to the following works

Daniel M. Duarte, Ranko Richert, and Karolina Adrjanowicz, *Frequency of the AC Electric Field Determines How a Molecular Liquid Crystallizes*, J. Phys. Chem. Lett. 2020, 11, 10, 3975–3979

Daniel M. Duarte, Ranko Richert, and Karolina Adrjanowicz, *Watching the Polymorphic Transition from a Field-Induced to a Stable Crystal by Dielectric Techniques*, Cryst. Growth Des. 2020, 20, 5406-5412

Daniel M. Duarte, Ranko Richert, and Karolina Adrjanowicz, *AC versus DC field effects on the crystallization behavior of a molecular liquid, vinyl ethylene carbonate (VEC)*, Phys. Chem Chem. Phys., 2021, 23, 498

Daniel M. Duarte, Ranko Richert, and Karolina Adrjanowicz, *Bimodal Crystallization Rate Curves of a Molecular Liquid with Field-Induced Polymorphism*, J. Molecular Liquids, 2021, 342, 117419

In the following way: I supervised the whole study and revised the manuscripts.

_____
Karolina Adrjanowicz

Tempe, 13.09.2021

Dr. hab. Ranko Richert
School of Molecular Sciences
Arizona State University
551 E University Dr,
Tempe, Arizona 85287-1604
United States

Declaration

I declare that I contribute to the following works

Daniel M. Duarte, Ranko Richert, and Karolina Adrjanowicz, *Frequency of the AC Electric Field Determines How a Molecular Liquid Crystallizes*, J. Phys. Chem. Lett. 2020, 11, 10, 3975–3979

Daniel M. Duarte, Ranko Richert, and Karolina Adrjanowicz, *Watching the Polymorphic Transition from a Field-Induced to a Stable Crystal by Dielectric Techniques*, Cryst. Growth Des. 2020,20, 5406-5412

Daniel M. Duarte, Ranko Richert, and Karolina Adrjanowicz, *AC versus DC field effects on the crystallization behavior of a molecular liquid, vinyl ethylene carbonate (VEC),* Phys. Chem. Chem. Phys., 2021, 23, 498

Daniel M. Duarte, Ranko Richert, and Karolina Adrjanowicz, *Bimodal Crystallization Rate Curves of a Molecular Liquid with Field-Induced Polymorphism*, J. Molecular Liquids, 2021, 342, 117419

In the following way: I discussed the results and reviewed the manuscripts.

Ranko Richert